Maintaining neuroplasticity in a sex-dependent manner during healthy aging: critical role of Neuropeptide Y

Dissertation

zur Erlangung des akademischen Grades

doctor rerum naturalium (Dr. rer. nat.)

genehmigt durch die Fakultät für Naturwissenschaften
der Otto-von-Guericke-Universität Magdeburg

M.Sc. Katharina Klinger

Geb. am 01. November 1989 in Bergisch Gladbach

Gutachter: Prof. Dr. sc. nat. habil. Oliver Stork
Prof. Dr. rer. nat. habil. Roland A. Bender

„Aging seems to be the only available way to live a long life.”
Kitty O’Neil Collins

Abstract

M.Sc. Katharina Klinger

Maintaining neuroplasticity in a sex-dependent manner during healthy aging: critical role of Neuropeptide Y

Aging-related cognitive decline is associated with a reduced number of neuropeptide Y (NPY)-expressing interneurons and a loss of cholinergic function in the hippocampus. Furthermore, NPY-expressing local interneurons in the dorsal DG (dDG) are modulated by the cholinergic system and are critically involved in memory formation and storage in male mice. Moreover, sex differences have been shown in synaptic plasticity and neurotransmission. Apart from its direct effects on neuronal functions and plasticity, the sex hormone estrogen interacts with other neuromodulatory systems and alters the use of cognitive resources via the regulation of circuit plasticity and excitability. Two key neuromodulatory systems substantially affected by estrogen are the NPYergic and cholinergic systems. In the current study, I, therefore, investigated with extracellular field potential recordings the effect of NPYergic neurotransmission on MPP-dDG plasticity and its changes during healthy aging, under intact inhibitory neurotransmission, in male and female mice separately. The data of this thesis show that post-synaptic excitability is increased and that theta-burst stimulation-induced long-term potentiation (LTP) at the MPP-dDG synapse in aged male mice is dependent on cholinergic and NPYergic neurotransmission, whereby MPP-dDG LTP depends in aged anestrus females only on the NPYergic neurotransmission. This is indicated by a loss of LTP in aged male mice, which could be restored by increasing the cholinergic activity through physostigmine. Strikingly, this cholinergic effect strictly depends on NPY and could be blocked by a Y1 receptor antagonist, BIBP3226. Moreover, the MPP-dDG LTP deficit could be restored by the NPY application. In contrast, in aged anestrus female mice, post-synaptic excitability is unaltered compared to young low estrus females. LTP is not abolished during healthy aging but is dependent on NPYergic neurotransmission. Interestingly, LTP is independent of Y1-R blockade under moderate cholinergic activation, whereby the cholinergic system does not mediate NPY release in aged and low estrus females. Moreover, the sex differences displayed in post-synaptic excitability and MPP-dDG LTP are also abundant in NPY concentrations and ERK1/2 phosphorylation in the dDG. This is demonstrated by the reduction of NPY concentration but an increase of ERK1/2 phosphorylation in naive-aged male mice. NPY concentrations and ERK1/2 phosphorylation are unaltered upon aging in females. These observations together suggest that NPYergic neurotransmission becomes critical for maintaining and recovering synaptic plasticity in the dDG during healthy aging.

Zusammenfassung

M.Sc. Katharina Klinger

Maintaining neuroplasticity in a sex-dependent manner during healthy aging: critical role of Neuropeptide Y

Der altersbedingte kognitive Verfall wird mit einer verringerten Anzahl von Neuropeptid Y (NPY)-exprimierenden Interneuronen und einem Verlust der cholinergen Funktion im Hippocampus in Verbindung gebracht. NPY-exprimierende lokale Interneurone werden im dorsalen Gyrus Dentatus (dDG) durch das cholinerge System moduliert und sind bei männlichen Mäusen entscheidend an der Gedächtnisbildung und -speicherung beteiligt. Darüber hinaus wurden Geschlechtsunterschiede bei der synaptischen Plastizität und der Neurotransmission nachgewiesen. Abgesehen von seinen direkten Auswirkungen auf die neuronalen Funktionen und die Plastizität interagiert das Sexualhormon Östrogen mit anderen neuromodulatorischen Systemen und verändert die Nutzung kognitiver Ressourcen durch die Regulierung der Plastizität und Erregbarkeit von Schaltkreisen. Zwei wichtige neuromodulatorische Systeme, die von Östrogen wesentlich beeinflusst werden, sind das NPY-erge und das cholinerge System. In der vorliegenden Studie untersuchte ich daher mit extrazellulären Feldpotentialableitungen die Wirkung der NPY-ergen Neurotransmission auf die MPP-dDG-Plastizität und deren Veränderungen während des gesunden Alterns bei intakter inhibitorischer Neurotransmission in männlichen und weiblichen Mäusen. Die Daten dieser Arbeit zeigen, dass die postsynaptische Erregbarkeit erhöht ist und die durch Theta-Burst-Stimulation induzierte Langzeitpotenzierung (LTP) an der MPP-dDG-Synapse bei gealterten männlichen Mäusen von der cholinergen und NPY-ergen Neurotransmission abhängt, während das MPP-dDG-LTP bei gealterten Weibchen im Anöstrus nur von der NPY-ergen Neurotransmission abhängt. Dies wird durch einen Verlust des LTPs bei gealterten männlichen Mäusen deutlich, welches durch eine Erhöhung der cholinergen Aktivität durch Physostigmin wiederhergestellt werden kann. Bemerkenswerterweise ist dieser cholinerge Effekt strikt von NPY abhängig und kann durch einen Y1-Rezeptor-Antagonisten, BIBP3226, blockiert werden. Außerdem kann das MPP-dDG-LTP-Defizit durch die NPY-Applikation wiederhergestellt werden. Im Gegensatz dazu ist die postsynaptische Erregbarkeit bei älteren Mäusen im Anöstrus-Stadium im Vergleich zu jungen Mäusen mit niedrigen Östrogenspiegeln unverändert. Das LTP wird während des gesunden Alterns nicht aufgehoben, sondern ist von der NPY-ergen Neurotransmission abhängig. Interessanterweise ist MPP-dDG LTP bei moderater cholinerger Aktivierung unabhängig von der Y1-R-Blockade, wobei das cholinerge System bei weiblichen Mäusen nicht die NPY-Freisetzung vermittelt. Die

geschlechtsspezifischen Unterschiede in der postsynaptischen Erregbarkeit und des MPP-dDG-LTP sind auch in den NPY-Konzentrationen und der ERK1/2-Phosphorylierung im dDG deutlich zu erkennen. Dies wird durch die Verringerung der NPY-Konzentration, aber einen Anstieg der ERK1/2-Phosphorylierung bei naiven männlichen Mäusen im Alter belegt. Die NPY-Konzentration und die ERK1/2-Phosphorylierung bleiben bei weiblichen Mäusen im Alter unverändert. Diese Beobachtungen deuten zusammengenommen darauf hin, dass die NPY-erge Neurotransmission für die Aufrechterhaltung und Wiederherstellung der synaptischen Plastizität im dDG während des gesunden Alterns entscheidend ist.

Table of Contents

1. Introduction

1.1. Aging

Harman defined aging as “the progressive accumulation of changes with time associated with or responsible for the ever-increasing susceptibility to disease and death which accompanies advancing age. This process may be common to all living things, for the phenomenon of aging and death is universal.” People over 80 are expected to triple between 2020 and 2050 (https://www.who.int/news-room/fact-sheets/detail/ageing-and-health), so it is crucial to investigate the cause of increased susceptibility. Changes during aging are manifold, they can be evident, like grey hair and more wrinkles, but they can also be observed on molecular, physiological, and psychological levels (reviewed in da Costa et al., 2016). One common hallmark of aging is cognitive decline, primarily associated with Alzheimer’s Disease (AD). For that, it is essential to state that cognitive decline can occur during healthy aging without pathological neurodegeneration. The mechanisms contributing to and preventing cognitive decline without pathological alterations are far from being understood.

Understanding these mechanisms would set the stage for identifying novel targets for clinical interventions and improving mental aging, quality of life, and lifespan. When investigating the mechanism that prevents cognitive decline, one must consider that in some neurodegenerative diseases, sex differences in prevalence or steepness are reported. For example, the cases of dementia have more than doubled from 1990 to 2016, with a higher prevalence in women (Nichols et al., 2019). A steeper cognitive decline in AD for women has been reported (Irvine et al., 2012; Mielke et al., 2014), and the beneficial effect of standard pharmacological treatment in AD, namely acetylcholine esterase inhibitor treatment, is controversially discussed for women (reviewed in Canevelli et al., 2017; Giacobini & Pepeu, 2018; https://www.nia.nih.gov/health/how-alzheimers-disease-treated). The higher life expectancy and the discussed differential effect of a pharmacological treatment point to different aging processes in men and women.

The most noticeable cognitive decline during aging is the reduction of memory, whereby episodic memory is impaired chiefly. Episodic memory encodes and retrieves the spatiotemporal context of previous personally relevant events (Light, 1991; Nyberg & Tulving, 1996; Tulving & Markowitsch, 1998). Specifically, preserved hippocampal activity is correlated with maintaining episodic memory during aging (Persson et al., 2012).

In humans, activity changes can hardly be investigated with invasive techniques and, as such, are measured through neuroimaging (metabolism) or electroencephalogram (EEG)

recordings (Rosen et al., 2002). A typical measurement of brain activity is the event-related brain potential (ERP) which is highly precise in the temporal but not spatial resolution. Importantly, ERP has also been used to assess episodic and working memory. Yet, concluding from scalp potentials to intracerebral potentials, especially in deeper brain areas, is difficult (Friedman, 2003, 2013). Thus, this thesis aims to investigate physiological plasticity changes in the hippocampus and its mechanistic alterations that govern cognitive decline in the absence of pathological markers. This needs a high temporal resolution and specific modulation and measurement of synaptic plasticity in the hippocampus, which invasive methods can only approach. Hence, a suitable animal model is of crucial importance.

1.1.1. Natural aging mouse as a model for human aging

For aging studies, the same quality criteria as for every other model account, which are face validity (similarity of the phenotype), predictive validity (similarity of drug effects), and construct validity (accuracy of the intended measurements) (Willner, 1966)

Numerous animal models have been established over the last decades, like *Caenorhabditis elegans*, *Drosophila melanogaster*, fish, birds, cats, dogs, and primates. All of them display characteristics of aging, but lack homology of structure, homology of complex behavior, inappropriate lifespans, or have high ethical restrictions (Mitchell et al., 2015), which makes them unsuitable for this study. The group of animal models with similar homology and complex behavior to humans and a reasonable timespan with accessible ethic regulations are rodents. Especially mice are very well-established as animal models. For aging, the Mouse Phenomena Project performed by the Jackson laboratories characterized 31 genetically diverse inbred mouse strains by collecting information about development, reproduction, physiology, behavior, and genetics (Ackert-Bicknell et al., 2010, 2015; Lutz & Osborne, 2014; Yuan et al., 2011). Altogether, these studies show enormous similarities in age-related changes between mice and humans; of particular interest is episodic memory's occurring impairment (Ackert-Bicknell et al., 2015; Davis et al., 2013). That could be translated to humans based on the lifespan equivalence (Fig. 1). The life phases of mice are typically discriminated into mature adulthood (3-6 months), middle age (10-14 months), and old age (18-24 months) corresponding to 20-30 years, 38-47 years, and 56-69 years in humans, respectively. These life phases resemble the following criteria: 1) fully developed but not yet affected by senescence (3-6 months), 2) some senescent changes can be already observed (10-14 months), and 3) senescent

changes can be detected in all animals at almost all levels (18-24 months) (Jackson Laboratories www.jax.org).

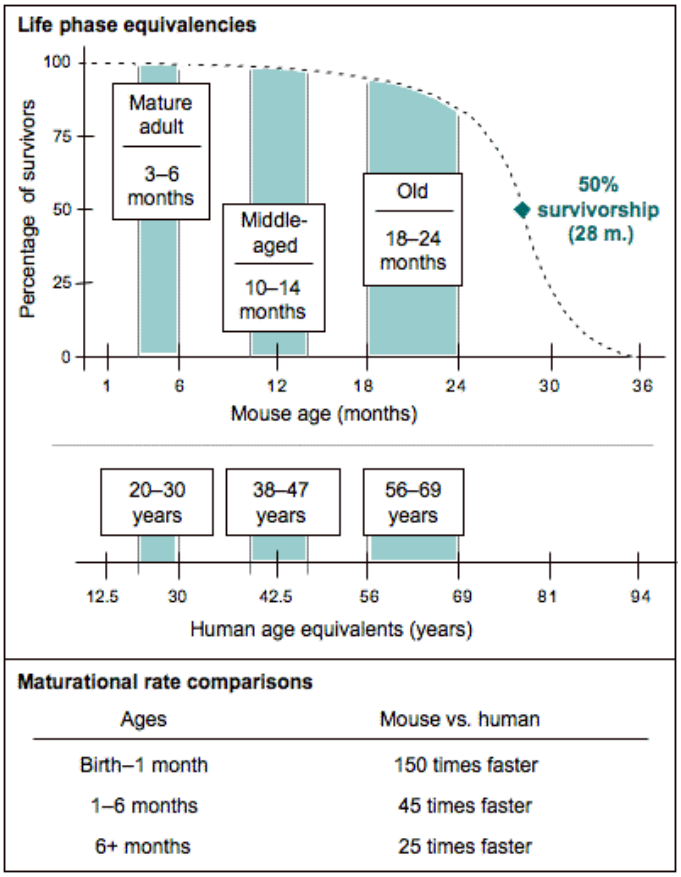

Figure 1: Life phase equivalents of C57BL/6J mice and humans. Mature adults: reference group. Mice are fully developed but not yet affected by senescence. Middle age: some senescent changes can already be observed but not all. Old: senescent changes can be detected in all animals at almost all levels. (www.jax.org).

The downside of the mouse models to study neurodegenerative diseases might be the lack of naturally occurring neurodegenerative diseases in mice (Lutz & Osborne, 2014). However, this, on the other hand, allows studying healthy aging to its full extent. Furthermore, using mice allows investigation of the role of sex hormones during aging. Female mice show an estrus cycle, even though it is much shorter than humans and not a menstrual cycle. The estrus cycle contains four cycle stages, each lasting approximately one day, and comprises a hormonal fluctuation like in the human menstrual cycle: proestrus (Fig. 2A), estrus (Fig. 2B), metestrus (also called diestrus I) (Fig. 2C), and diestrus stages (also called diestrus II; Fig. 2D) (Allen, 1922; Byers et al., 2012). The stages can be investigated by defining the cytology of vaginal smear as described in (Byers et al., 2012) (Fig. 2). Similar to female humans, the cycle of female mice becomes irregular during aging (i.e., between 10-15 months in the mice), and

acyclic at 16-20 months of age, depending on the strain (Nelson et al., 1981). Indeed, expecting a lifespan of 24 months in a mouse, acyclicity occurs in mice comparatively much later than in humans, but still, differences coming from cycle depletion can be measured (Bimonte-Nelson et al., 2021; Koebele & Bimonte-Nelson, 2016). Sixty-seventy percent of the old mice that stop cycling stay in a polyfollicular anovulatory state called permanent estrus, where plasma-estradiol levels remain high and progesterone levels are low (Koebele & Bimonte-Nelson, 2016). Only 30-40% end up in an anestrus phase with low levels of ovarian steroids as well as a decline in follicles, but not fully depleted (Bimonte-Nelson et al., 2021; Huang et al., 1978; Koebele & Bimonte-Nelson, 2016). While this does not reflect the hormonal changes of humans during aging to its full extent, mouse models provide a valuable tool to study the role of sex hormones in aging processes.

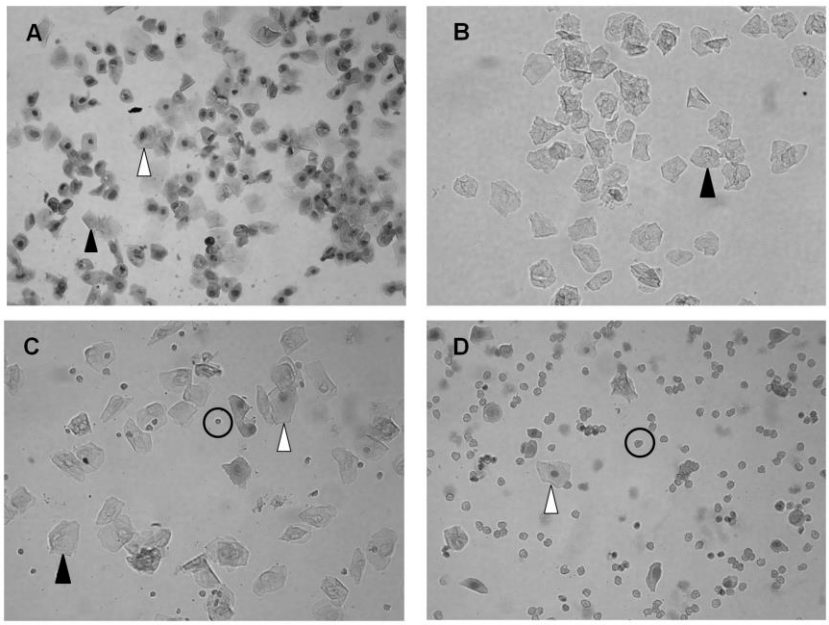

Figure 2: Cytology of vaginal smear of each cycle stage. Each cycle stage contains three cell types, and the predominant cell type defines the cycle stage. The three different cell types are leukocytes (circle), cornified epithelial cells (black arrow), and nucleated epithelial cells (white arrow). **A:** proestrus with mainly nucleated epithelial cells, **B:** estrus with mainly cornified epithelial cells, **C:** metestrus with all three cell types almost evenly distributed, and D: diestrus with primary leukocytes. (Byers et al., 2012).

1.1.2. Memory performance during aging

When talking about reduced memory performance or memory loss during aging, the declarative part of long-term memory is usually affected, defined as everything that is learned explicitly, like facts and events (Squire, 2009; Zlotnik & Vansintjan, 2019). Episodic memory belongs to declarative memory and encodes rather personal important events than facts (Tulving, 2001). Episodic memory is one of the first declining systems during aging in humans (Nyberg et al., 2012). Investigation of episodic memory has focused on rodents' spatial memory

as the ‘where’ component of episodic memory (Aggleton & Pearce, 2001; Gaffan, 1991; Zhou & Yu, 2018). Notably, during aging, rodents show an apparent decline in learning, retaining, and reversal in different spatial tasks, among several others, in the Morris water maze (MWM) (Foster et al., 1991; Pawluski et al., 2009) and the Barnes maze (Barnes, 1979; Barnes & Mcnaughton, 1980, 1986). Furthermore, rats' long-term potentiation (LTP) in the dentate gyrus (DG) has been demonstrated to represent impaired learning in the MWM, 8-radial arm maze, and BM (Barnes, 1979; Detoledo-Morrell et al., 1988; Jeffery & Morris, 1993). Excitatory post-synaptic potential (EPSP) recordings of the perforant path (PP)-DG synapse in the rat reveal a higher induction threshold and a faster decay for LTP after Barnes maze training. The higher induction threshold has been interpreted as the electrophysiological resembling of the longer latency to learn the location and the faster decay as the quicker loss of remembering the place (Barnes, 1979; Barnes & McNaughton, 1986), whereby the actual LTP size with the performance in the MWM correlates (Jeffery & Morris, 1993). The abolishment of PP-DG LTP and reduced MWM performance after applying an N-methyl-D-aspartate (NMDA) antagonist supports the view of LTP resembling spatial memory performance *in vivo* (Morris, 1989). Furthermore, MWM performance is impaired after LTP saturation in the PP-DG synapse (Moser, 1998). This selection of studies reveals a clear impact of aging on spatial and episodic memory in rodents and that LTP correlates with spatial performance. Those to investigate cognitive decline LTP recordings are a highly suitable approach. Furthermore, it is well-established that the encoding phase of episodic memory is hippocampus-dependent in humans and mice (Dere et al., 2005; Squire & Zola, 1996; Zola-Morgan, 1996).

1.2. The Hippocampus

As the central area of learning and memory, the hippocampus is of particular interest for investigating cognitive decline during healthy aging. Significantly during normal aging, reduced plasticity, neurogenesis, episodic and memory, as well as cell loss occur in the hippocampus (Barnes et al., 2000; Bettio et al., 2017; Driscoll et al., 2003; Geinisman et al., 1995; McEwen Harold & Milliken, 1999). The hippocampal formation is located in the medial temporal lobe and shows a unique and distinct architecture along its dorsoventral axis (Witter, 2012). It comprises the DG and the hippocampus proper, subdivided into cornu ammonis (CA) 3-CA1, and is ordered in a so-called tri-synaptic circuit (Witter, 2012). The DG receives input from the entorhinal cortex (EC) through the PP, which can be divided into medial PP (MPP) and lateral PP (LPP). The LPP provides non-spatial information to the hippocampus, while the

MPP delivers spatial information from the EC (Hargreaves et al., 2005; Hunsaker et al., 2007). Through mossy fiber synapses, the DG communicates with the CA3, which terminates in the stratum lucidum of the CA3 (Witter, 2012). The output of CA3 is connected to CA2 and CA1 via the Schaffer collaterals (SC). CA2 is relatively tiny, and CA1 is the central output region of the hippocampus and connects the hippocampus back to the EC. Along the dorsoventral axis, the hippocampus is divided anatomically and functionally into the dorsal, medial, and ventral hippocampus (Witter, 2012). Anatomically, the dorsal part differs from the ventral part in the number of neurons and slightly in the dendritic branching of GC (Witter, 2012). Functionally the ventral hippocampus is thought to be involved in emotional memory, anxiety, and depression (Fanselow & Dong, 2010). On the other hand, the dorsal hippocampus is involved in episodic memory, pattern separation, spatial learning, and working memory (Liu & Zhao, 2013; Shapiro, 2001; Tonegawa & McHugh, 2007).

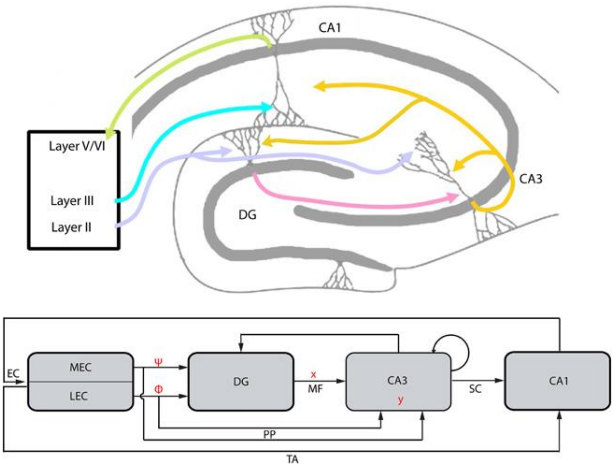

Figure 3: Schematics of the hippocampal formation. The EC projection to DG and CA3 via the perforant path (PP). DG afferents are projecting to CA3 (mossy fibers, MF). CA3 projects to itself via recurrent connections and to CA1 via the Schaffer Collaterals (SC), and the information loop closes by the CA1 feedback to the EC, which also receives the EC input via the Temporoammonic pathway (TA) (adapted from Petrantonakis & Poirazi, 2014).

As mentioned above, the encoding of episodic memory is commonly accepted to happen in the hippocampus, shown by impaired long-term memory after hippocampal lesion in mice, rats, monkeys, and humans (Broadbent et al., 2006; Dillon et al., 2008; Squire & Zola, 1996; Talpos et al., 2008; Zola-Morgan, 1996). In contrast, the area of long-term memory storage is discussed based on the single-system model and the multiple-trace theory. According to the single trace theory, the hippocampus is essential to store and retrieving memory in the beginning. Still, during memory consolidation, the hippocampus' contribution diminishes. Finally, the neocortex exclusively sustains and retrieves memory (Moscovitch, 1995). In this

theory, repeating a particular event strengthens only one memory trace (Hintzman & Block, 1971). The single system model has been underlined by different experiments (Nadel & Moscovitcht, 1997).

Nevertheless, Hintzman and Block (1986) proposed the multi-trace theory (Hintzman, 1986; Hintzman & Block, 1971; Zlotnik & Vansintjan, 2019). Here the concept of initial recognition and encoding is similar to the single-system model. In contrast, the multiple-trace theory postulates that memory strengthens through the number of traces. This leads to a permanent interaction between the neocortex and hippocampus, and the memory does not become independent of the hippocampus (Hintzman & Block, 1971; Moscovitch, 1995; Nadel & Moscovitcht, 1997). With that, the faster decline of recently allocated memories than older memories during aging can be explained: A memory that has already allocated several traces is less vulnerable to the loss of single traces than a memory that is relatively new and assigned with fewer traces (Moscovitch, 1995; Nadel & Moscovitcht, 1997). Indeed, the multiple-trace theory is strengthened by hippocampal lesion studies of monkeys, showing severe long-term memory impairment. By contrast, lesion of the EC leads only to mild impairment of long-term memory, speaking for a crucial role of the hippocampus in memory consolidation and storage (Squire, 2009). Moreover, the research on the neuronal unit of memory, the 'engram', shows that artificial activation of neuronal assemblies in the mouse DG, formed during an exposure, can retrieve the memory in another context. Strikingly, this synthetic activation (through optogenetics) can retrieve memory also when natural cues cannot (Liu et al., 2012; Ramirez et al., 2013) as well as in a mouse model of AD (Perusini et al., 2017; Roy et al., 2016). Additionally, optogenetic silencing of DG granule cells (GC) leads to a loss of memory function. Comparison of silent and activated engrams reveal a reduced synaptic strength for silent engrams (Denny et al., 2015; Lacagnina et al., 2019). Together this suggests that studying the hippocampus is instrumental in understanding fundamental circuit mechanisms of cognitive decline during healthy aging.

1.2.1. The involvement of dDG in aging

With its position as the entry region to the hippocampus, the DG can be considered the gatekeeper in the machinery of hippocampal information processing (Witter, 2012). The dorsal, as well as the ventral DG, comprise three layers. These comprise the molecular layer (ML), with the dendrites of the GC, the 'U' (ventral) or 'V' (dorsal) shaped principal cell or granule layer (GL), packed with the GCs, and the polymorphic layer or hilus/hilar layer, containing a broad range of cell types (Witter, 2012). The molecular layer is mostly cell-free. It harbors

dendrites of mainly GCs and axon terminals from a variety of interneurons and astrocytes (Jinno & Kosaka, 2006; Witter, 2012). The GL and hilus host numerous cells. In the GL, the variety of cells is low. Still, it is closely packed with GCs, which have apical dendritic trees arising from the superficial part of the soma and unmyelinated axons that are projecting to CA3 as well as to mossy cells (MCs). Besides the glutamatergic MC, the hilus contains different types of gamma-aminobutyric acid (GABA) interneurons (Witter, 2012). The GABAergic cells in the hilus are mainly parvalbumin-positive (PV+), cholecystokinin (CCK+), and somatostatin-positive (SST+) interneurons (Freund & Buzsáki, 1996; Witter, 2012). PV+ interneurons are mainly located on the border to the GL and connect directly with the cell bodies or initial axon segments of GCs and deliver a strong feed-forward and feedback inhibition (Freund & Buzsáki, 1996; Houser, 2007; Sambandan et al., 2010). Another group is the CCK-expressing hilar commissural associated path (HICAP) cells. They are located within or below the granule layer and bordering the hilus. HICAP cells get input from the PP and local mossy fibers onto their apical (reaching the inner ML) and basal (reaching the hilus) dendritic tree. Furthermore, they form synaptic contacts with the soma and the distal dendrites of the contralateral GCs and provide perisomatic inhibition to other inhibitory interneurons, mainly PV+ interneurons (Freund & Buzsáki, 1996; Savanthrapadian et al., 2014). The biggest subclass of GABAergic interneurons in the hilus is the SST+ interneurons (Houser, 2007). They can be further divided into so-called hilar-perforant-path-associated interneurons (HIPP) and hilus-associated interneurons (HILs). HIPP cells provide feedback inhibition on distal dendrites of the GCs in the outer molecular layer and onto PV+ interneurons of the hilus (Freund & Buzsáki, 1996; Yuan et al., 2017). Moreover, HIL cells provide potent perisomatic inhibition on other GABAergic interneurons and show long-range projections to the medial septum (MS) (Houser, 2007; Yuan et al., 2017). Besides projecting to the MS through HIL cells, the DG receives input from the MS (Witter, 2012; Yuan et al., 2017) and other subcortical regions. The septal nuclei project mainly to the hilus of the DG and partly to the ML, as evident by acetylcholinesterase-positive projections in the GL (Witter, 2012) that connect to GCs as well as to interneurons (e.g., SST+ interneurons) (Raza et al., 2017; Witter, 2012; Yuan et al., 2017). Besides the cholinergic projections, GABAergic long-range projections are sent from the MS to the DG (Köhler & Eriksson, 1984; Unal et al., 2015; Witter, 2012). Functionally, the dDG has been implicated in the encoding and retrieval of contextual fear memory (Liu et al., 2012), spatial orientation (Morris et al., 2012), and context discrimination (Liu et al., 2012; Tonegawa & McHugh, 2007), as mentioned above. In particular, the DG translates multi-informational patterns from the neocortex into sparse codes for the CA3 (Leutgeb et al., 2007;

Treves & Rolls, 1994), which is only possible with the tight inhibitory control orchestrating the synaptic activity of the DG (Lee et al., 2016; Nitz & McNaughton, 2004). Furthermore, this excitation-inhibition balance (E-I) is essential for spatial performance, signal-to-noise ratio, and sparse GC activation in the DG (Coulter & Carlson, 2007; Lee et al., 2016; Madar et al., 2019). In contrast to the hippocampus proper, the DG does not show spine density or volume loss during aging (Curcio et al., 1983). However, a reduction in cell number has been established for cells in the hilus but not for the GCs. Furthermore, the DG shows reduced synaptic contacts during aging, indicated by the loss of synaptic contacts in the middle ML and inner ML (Geinisman et al., 1992), including a loss of PP connection (Amani et al., 2021; Barnes et al., 2000; Barnes & Mcnaughton, 1980). A reduced magnitude of PP EPSPs and reduced amplitude of the pre-synaptic response underlines the loss of afferent projections. In contrast, GCs of aged rodents exhibit greater synaptic field potentials and a reduced voltage threshold (Barnes, 1979; Barnes & Mcnaughton, 1980). Moreover, *in vivo* studies show that LTP induction, maintenance, and decay are impaired in DG of aged male rodents (Barnes, 1979; Barnes et al., 2000; Barnes & Mcnaughton, 1986; Geinisman et al., 1995). It is noteworthy that faster DG LTP decay is only shown in the late phase of LTP when using low-stimulation protocols (Barnes, 1979; Barnes & McNaughton, 1980). Nevertheless, despite the general impairment of synaptic plasticity (induction, maintenance, decay) in old rodents, subcortical and local neuromodulation of DG plasticity during aging is underinvestigated. Hippocampal interneurons control the plasticity of principal synapses (e.g., MPP to DG) *in vitro* and *in vivo* (Castillo et al., 2011; Freund & Buzsáki, 1996; Kullmann et al., 2012) via restricting excitation and shaping the firing of principal cells (Lee et al., 2016; Liguz-Lecznar et al., 2022). A structural or functional decline in this interneuronal population might have a tremendous effect on the intrinsic hippocampal system and the neuromodulation of principal cells by subcortical cholinergic projections (Palacios-Filardo & Mellor, 2019). Thus, aging research needs to investigate their neuromodulatory impact on dDG plasticity.

1.3. Neuropeptide-Yergic system during aging

Neuropeptide-Y (NPY) belongs to the pancreatic polypeptides class and is phylogenetically highly preserved (Armstrong et al., 1982). NPY is widely distributed in the nervous system, abundantly expressed, and released after depolarization by exocytosis (Armstrong et al., 1982; Tasan et al., 2016). In rodents, most of the hilar SST+ interneurons co-localize with NPY (Freund & Buzsáki, 1996; Houser, 2007; Köhler & Eriksson, 1984; Raza et al., 2017). As the

main neuropeptide in the central nervous system (CNS), it has numerous physiological and pathological functions, like seizure suppression, circadian rhythm, anxiety control, feeding behavior, and learning and memory (Botelho & Cavadas, 2015; Vezzani & Sperk, 2004). Five types of G-protein-coupled receptors mediate these different functions (GPCR), termed Y1-Y5. They all inhibit adenylyl cyclase that decreases cyclic adenosine phosphate (cAMP) levels and intracellular calcium (Ca^{2+}) levels, and activates the mitogen-activated protein kinase (MAPK) (Benarroch, 2009; Colmers et al., 1988). The most abundant receptor subtypes in the DG are Y1 and Y2 (Dumont et al., 1993, 1998; Silva et al., 2005). Y1 receptors (Y1-R) and Y2 receptors (Y2-R) can be found in the same regions. Y2-R are mainly located in the pre-synapses of the GL and hippocampus. Y1-R are located postsynaptically, mainly in the ML on the dendrites of the GL and in some interneurons, and inhibit GC by decreasing glutamate release and reducing intracellular Ca^{2+} (Sperk et al., 2007a; Tasan et al., 2016). Functionally, NPY shows various effects, including differentiation of precursor cells in the DG, preventing status epilepticus (Cardoso et al., 2010; Vezzani & Sperk, 2004), and preventing generalization of fear memory (Besnard & Sahay, 2021; Danielson et al., 2016; McAvoy et al., 2016; Raza et al., 2017). During aging, several studies show a decline in NPY secretion (Gruenewald et al., 1994), NPY mRNA (Gruenewald et al., 1994; Ramos et al., 2006), Y1-R and NPY immunoreactivity (Hattiangady et al., 2005; Matsuoka et al., 1995; Sawano et al., 2015), which is related with memory impairment (Spiegel et al., 2013). NPY modulates hippocampus-dependent learning and memory, neuroprotection, and antiepileptic effects through the Y2-R (Botelho & Cavadas, 2015; Redrobe et al., 2004; Silva et al., 2005). The beneficial effect of Y2-R activation is underlined by cognitive impairment of a Y2-R knockdown mouse model (Redrobe et al., 2004), while the neuroprotective effect is strengthened through a longer lifespan of NPY overexpressing rats (Michalkiewicz et al., 2003). In contrast, NPY modulation through Y1-R is known to be involved in neuroprotection, anxiolytic and antidepressant effects (Botelho & Cavadas, 2015; Redrobe et al., 2004). Nevertheless, a study from our laboratory showed that antagonizing Y1-R in the DG leads to generalized fear in a background fear paradigm (Raza et al., 2017) and proved the role of Y1-R in learning and memory. Moreover, studies from overexpressing Y1-R models show cognitive impairment at a young age ameliorated during aging (Carvajal, 2007). Furthermore, in an AD rat model, agonizing Y1-R increases learning in the MWM test, whereby a selective Y1-R antagonist attenuates the positive effect of the Y1-R activation (Rangani et al., 2012). So far, it has been shown that NPY decreases LTP evoked on the LPP-DG synapses while not affecting neurotransmission of the PP-DG synapse of young mice (Baratta et al., 2002; Klapstein & Colmers, 1993; Raza

et al., 2017)t al., 2002; Klapstein & Colmers, 1993; Raza et al., 2017). This NPY-mediated decrease in DG LTP is due to a reduction in dendritic calcium (Ca^{2+}) (Baratta et al., 2002). Moreover, McQuiston and colleagues demonstrated unchanged GC resting potential and dendrite Ca^{2+} levels but decreased depolarization-induced Ca^{2+} influx through N-type voltage-gated calcium channels (VDCC) after NPY application dependent on Y1-R activation in DG GCs of adult rats (McQuiston et al., 1996). Given the modulation of HIPP cells through the cholinergic system and the relationship between cognitive impairment and interneuron decline during aging, it is thus essential to investigate the effect of the direct peptidergic modulation as well as the indirect modulation through the cholinergic system in the dDG.

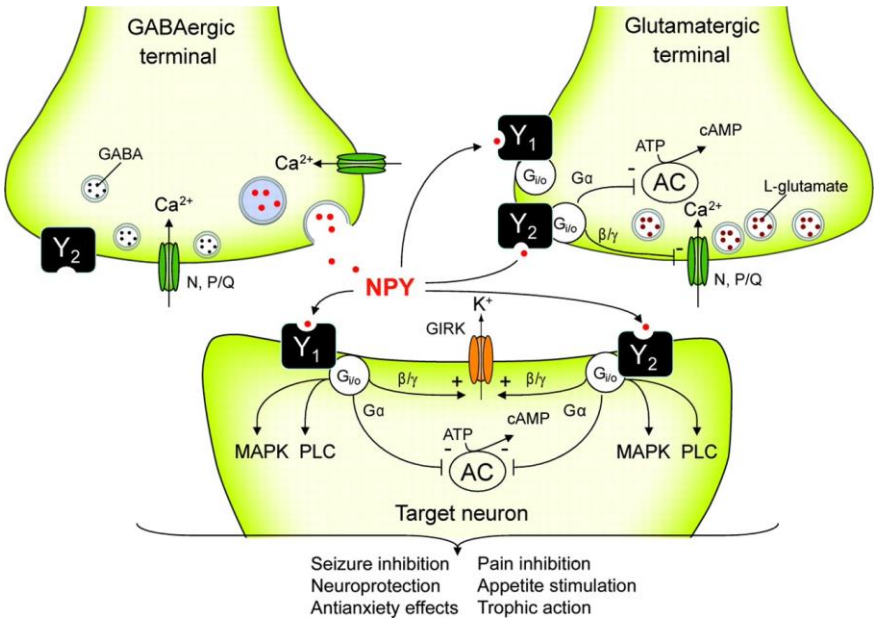

Figure 4: Neuromodulatory effects of NPY. Neuropeptide Y (NPY) is present in interneurons synthesizing γ-aminobutyric acid (GABA). NPY is a potent neuromodulator that acts via G protein-coupled receptors. The most abundant receptors are Y1-R, located mainly postsynaptically, and Y2-R, both presynaptically and postsynaptically. Y1- and Y2-R inhibit adenylyl cyclase (AC) and pre-synaptic N and P/Q-type Ca^{2+} channels. Furthermore, they are involved in releasing glutamate and other neurotransmitters. Postsynaptically, these receptors activate G-protein-coupled, inwardly rectifying potassium (K^+) currents (GIRKs). Other transduction cascades include the activation of mitogen-activated protein kinase (MAPK) and phospholipase C (PLC). cAMP = cyclic adenosyl monophosphate (Benarroch, 2009).

1.4. The cholinergic system and its involvement in aging

Hippocampal acetylcholine (ACh) levels are strongly associated with learning during arousal, and primary reinforced cues (Palacios-Filardo & Mellor, 2019; Teles-Grilo Ruivo et al., 2017). The main source of endogenous ACh release in the hippocampus is the MS/diagonal band of Broca (Mesulam et al., 1983). They are part of the basal forebrain, located close to the medial and ventral surface of the cerebral hemisphere (Zaborszky et al., 2012). ACh acts

through nicotinic ionotropic (in the hippocampus principally α4β2, α3β4, and α7) and muscarinic (M1-M4) GPCRs and facilitates LTP and LTD (reviewed in Palacios-Filardo & Mellor, 2019). Specifically, in the DG, the α7-, M1-, and M2-type receptors (-R) appear to be the most abundant (reviewed by Prince et al., 2016).

Furthermore, ACh can enhance post-synaptic excitability through M1 receptors (the major muscarinic receptor) and acts on the synapse in multiple ways, either depressing or activating NMDA-R (reviewed in (Palacios-Filardo & Mellor, 2019). Specifically, in the DG, previous work from our group showed that endogenous ACh release mildly increases the excitability, evidenced by the increase in the area of population spikes (Raza et al., 2017). This may also involve decreased spike threshold and increased propensity of action potential generation upon stimulation of cholinergic afferents (Martinello et al., 2015; Prince et al., 2016). Furthermore, ACh promotes an increased response of mature GCs to afferent stimulation upon cholinergic modulation by perisomatic disinhibition of PV+ interneurons through activation of SST+ interneurons (Ogando et al., 2021). It is thus striking that the cholinergic agonist carbachol reduces LTP in mature granule cells under the blockade of $GABA_A$-receptor ($GABA_A$-R). The same protocol increases LTP in immature GCs after blocking $GABA_A$-R with bicuculline (Zhang et al., 2010). This discrepancy points to a distinct cholinergic regulation of DG circuitry and activation of distinct cholinergic receptors depending on the level of cholinergic stimulation. In addition to controlling principal neuron activity, ACh profoundly modulates inhibitory interneurons. This leads to an altered configuration of the local circuit output by transiently increasing spontaneous GABA release indicating that ACh plays a crucial role in the functional modulation of inhibitory synapses (Palacios-Filardo & Mellor, 2019). Significantly, the activation of HIPP cells mediated by the cholinergic system through M1-R leads to distinct memory retrieval during cued fear conditioning in adult male mice (Raza et al., 2017).

Furthermore, evidence suggests that cholinergic neurons of MS co-transmit GABA and acetylcholine (Takács et al., 2018a). Indeed, local disturbances in the hippocampal circuit function and structure are accompanied by distorted functional or structural alterations in the long-range projections to the hippocampus in AD and during healthy aging (Ballinger et al., 2016). The loss of cholinergic function can be observed in the early stages of AD and in patients with mild cognitive impairment (MCI). In contrast, degeneration of the whole cholinergic system is demonstrated in the later stages of AD (Schliebs & Arendt, 2011). Besides that, implications of the cholinergic system during aging are given by cholinergic lesions as a model for aging (Berger-Sweeney et al., 2001; Kesner et al., 1986; Nicolle et al., 1997) and

acetylcholine esterase inhibitors as standard pharmacological treatment during aging (Yiannopoulou & Papageorgiou, 2020). In line with that, muscarinic agonist increases LTP at the MPP-DG synapse in aged rats (Pang et al., 1993). Thus, studying the cholinergic system in the context of aging is particularly crucial due to its vulnerability to neurodegeneration during aging and a possible change in the cholinergic modulation of DG interneurons.

1.5. Plasticity as a cellular correlate for learning

In 1949, Donald Hebb postulated the basis of plasticity in his book 'The Organization of Behavior', known as the 'neurophysiological postulate'. He described that repetitively activated neurons are more likely to be connected, leading to activity facilitation of both cells even if (only) one is activated. Strengthening happens through transmitter release, which depolarizes through receptor binding the post-synapse and is considered the basis of learning but also the storage of memory (Abraham et al., 2019).

1.5.1. Hebbian plasticity

One form of Hebbian plasticity is called long-term potentiation (LTP) and was first described by Bliss and Lomo in 1973. They stimulated the PP with extracellular micro-electrodes and observed the simultaneously recorded GC signal potentiation in anesthetized rabbits (Bliss & Lomo, 1973). In general, the term LTP describes an increase in efficiency of synaptic transmission and excitability of a post-synaptic cell mediated by a short train of stimulations at the pre-synapse, shown by changes in latency and amplitude of the cell signal, that persist for at least 30 min (Bliss & Lomo, 1973). Importantly, LTP shows the so-called 'input specificity', meaning that only the stimulated post-synapse elicits LTP and the cooperativity, which ensures that only a strong input leads to LTP (Nicoll, 2017). Since then, LTP has been shown for several species and different synapses (Douglas & Goddard, 1975; Racine et al., 1983; Schwartzkroin & Wester, 1975). LTP can be divided into three phases based on the terminology of Racine and colleagues as well as Park and colleagues. Depending on the author, the basis for the discrimination is the origin of plasticity or the cellular-induced steps. For both definitions, the third phase of LTP is expected to persist over days and include protein synthesis or even gene transcription. The other two phases either strengthen only one of the synapses or do not include gene transcription. Both are not leading to long-lasting changes (Park et al., 2014; Racine et al., 1983).

LTP can be induced with electrical, chemical, or optogenetic stimulation of specific synapses *in vivo* and in *ex vivo* slice recordings. The commonly used and the most intensively studied electrical stimulations to induce LTP are high-frequency (tetanic) and patterned electrical stimulation for *in vivo* and anesthetized DG stimulations, containing 100Hz or 15Hz trains for 3-4 sec or 15-20 sec, respectively (Bliss & Lomo, 1973; Raymond, 2007). The simulations used can differ depending on the synapse. Besides the train stimulation, time-dependent spike plasticity (STDP) protocols that rely on pre- and post-synapse co-activation are commonly used to induce LTP reliably. The STDP varies the timing between pre- and post-synaptic firing by stimulation and causes a combination of Hebbian and anti-Hebbian plasticity (reviewed in Bliss et al., 2014).

The induction of dDG LTP under physiological conditions is restricted with the HFS due to solid feed-forward inhibition. For that reason, LTP studies *in vitro* are rarely done in the dDG (Wigström & Gustafsson, 1983), and if done, are performed under the blockade of $GABA_A$-R (by using bicuculline or picrotoxin) to reduce the inhibitory tonus (Hanse & Gustafsson, 1992; Zhang et al., 2015). Nevertheless, STDP TBS protocols induce LTP *in vitro* in the dDG (Lopez-Rojas et al., 2016).

Besides LTP, other forms of plasticity are the short-term facilitation or depression caused by paired-pulse stimulation (Zucker & Regehr, 2002), homeostatic plasticity (Turrigiano & Nelson, 2004) occurring after persistent activity change, and metaplasticity (Abraham & Bear, 1996) describing possible alterations of the ability to induce plasticity (reviewed in Citri & Malenka, 2008). As mentioned, LTP induction and maintenance are reduced in the DG of aged rodents. Possible mechanisms are mostly explored in the CA1. For CA1, an increase in pre-synaptic calcium resting level and signaling following stimulation has been shown (Pereda et al., 2019). This might also occur in the DG, underlined by the increased ratio of pre-synaptic fiber volley and post-synaptic fEPSP in the DG of aged rats compared to young rats (Barnes, 1979; Barnes & McNaughton, 1980). The increased E-I balance in the DG correlates with reduced cognitive performance in aged rats and is mediated by reduced inhibitory recruitment after LPP stimulation (Tran et al., 2019). So, inducing LTP at the MPP-DG synapse in vitro is an excellent approach to investigating plasticity changes during aging in a highly controlled and adjustable environment.

1.5.2. Molecular components of long-term potentiation in the dentate gyrus

Regardless of the different forms of LTP, all LTP types follow the same structure: induction, expression, and maintenance (Rosenblum et al., 1996). Notably, the molecular key

players can differ in these three phases. Since the pre-synaptic LTP is rarely expressed in the dDG, the central aspect of this research project will focus on postsynaptically-mediated LTP, as the main form observed in the DG (Hanse & Gustafsson, 1992; Rosenblum et al., 1996).
Induction of LTP causes an increase in extracellular glutamate release, leading to an NMDA-R-dependent LTP, shown by DG recordings of anesthetized rats and *in vivo* recordings (Errington et al., 2003; Morris, 1989). As a result of this, the magnesium (Mg^{2+}) blockade of the NMDA-R is removed through post-synaptic depolarization, causing an influx of Ca^{2+} (Bliss & Collingridge, 1993; Errington et al., 2003; Morris, 1989). That causes an enhancement of α-amino-3-hydroxy-5-methyl-4-isoxazole propionic acid receptor (AMPA-R) trafficking and insertion in the synapse membrane in a long-lasting manner. In contrast to induction, the molecules involved in the expression and maintenance are not identified to their full extent. It is known that the phosphorylation of the D-aspartate receptor subtype 2B (NR2B) subunit of NMDA-R is crucial for LTP induction since it mediates Ca^{2+} influx (Chen et al., 2007; Rosenblum et al., 1996). For the AMPA-R GluA1 subunit, it has been shown that mice lacking the ability to phosphorylate the GluA1 subunit exhibit deficits in spatial learning, LTP, and LTD (Lee et al., 2003). Moreover, GluA1 subunit levels are increased after high-frequency stimulation of the DG at PP (Kennard & Woodruff-Pak, 2011). Interestingly, increased GluA1 expression is also involved in adaptive forgetting (Fraize et al., 2017). NR2B and GluA1 show several phosphorylation sites. Specifically, the phosphorylation sites tyrosine1472 (Y1472) and serine1480 (S1480) of NR2B, as well as the serine831 (S831) and serine845 (S845) of GluA1, are of particular interest for plasticity. Y1472 is the leading phosphorylation site of NR2B. It is essential for surface expression and activation (Waters et al., 2019), whereas phosphorylation on S1480 reduces the surface expression of NR2B (Chen & Roche, 2007). GluA1 phosphorylation of S845 is involved in membrane insertion, mediating homeostatic plasticity and increasing the opening probability of the channel (Diering & Huganir, 2018). Furthermore, S831 phosphorylation increases channel conductance and lowers the LTP induction threshold, indicated by abolished LTP in mice with abolished phosphorylation at S831 and lowered LTP induction threshold in knock-in mice mimicking phosphorylation (Lee et al., 2003; Makino et al., 2011). The most-investigated player for phosphorylation of the subunits to maintain LTP in the DG is calcium/calmodulin-dependent protein kinase II (CaMKII) (Jiang et al., 2015; Wu et al., 2006). Protein kinase A (PKA) is also vital for DG LTP through abolishing late LTP after applying a PKA inhibitor and after co-inhibiting with CaMKII (Nguyen & Kandel, 1997; Wu et al., 2006). Besides CaMKII and PKA, the extracellular signal-regulated kinase/MAP (ERK/MAP) pathway is essential for LTP induction

as well as for LTP maintenance in the hippocampus and is indispensable for TBS-mediated LTP induction in the CA1 subregion (Citri & Malenka, 2008; Coogan et al., 1996; English & David Sweatt, 1997; Thomas & Huganir, 2004). Furthermore, ERK is critically involved in DG LTP, as shown by the brain-derived neurotrophic factor (BDNF)-induced LTP in young anesthetized rats (Gooney et al., 2002, 2004) and by abolished LTP in the DG after co-application of MAP and CaMKII inhibitors (Wu et al., 2006). ERK is activated by PP-DG tetanic stimulation and is modulated through MRs in a phosphoinositide 3-kinase (PI_3K)-dependent manner (Rosenblum et al., 2000). All three kinases can phosphorylate cAMP element-binding protein (CREB), which seems intimately linked to DG LTP maintenance (Schulz et al., 1999). The phosphorylation of CREB would activate immediate early genes like c-fos or zif268, which have been shown to lead to learning and memory processes (Citri & Malenka, 2008; Thomas & Huganir, 2004; Tischmeyer & Grimm, 1999). Notably, the ERK/MAP phosphorylates CREB and mediates glutamate release, shown by reduced glutamate release after MAP inhibition *in vitro* (Mcgahon et al., 1999). Indeed, S845 of GluA1 is phosphorylated by PKA (upstream of ERK) and S831 by CaMKII, Y1472 of NR2B by Fyn (upstream of MAPK), and S1480 by CaMKII (Chen & Roche, 2007; Diering & Huganir, 2018; Hayashi, 2022; Waters et al., 2019).

Besides others, the importance during aging has been shown for NR2B, GluA1, and ERK. NR2B depletion mimics reduced LTP in CA1 and spatial impairments in rats, as during aging (Clayton et al., 2002). Furthermore, NR2B declines during aging in the DG (Newton et al., 2008). The beneficial effect of spatial training on memory performance has been shown to increase spine generation, GluA1, and NR2B levels through increased CaMKII activity in the DG (Jiang et al., 2015). For ERK opposing results have been shown in the literature. ERK activity is reduced in the hippocampus of aged rats and aged depressed mice, while overall ERK levels are unaltered during aging (Li et al., 2017; Mo et al., 2005). In line with that, increased ERK phosphorylation enhances cognition in AD models (Ibrahim et al., 2020; Zhang et al., 2015). Moreover, defective LTP and impaired memory formation are related to ERK1/2 inhibition (English & David Sweatt, 1997; Ying et al., 2002). In contrast, inhibition of the ERK pathway leads to recovery of Aβ-induced cellular changes and memory deficits in a mouse model of AD (Chang et al., 2020; Feld et al., 2014; Lee et al., 2009; Wang et al., 2019). Furthermore, elevated ERK1/2 phosphorylation is associated with long-term memory deficits in a mouse model for autism (Seese et al., 2014). Due to the involvement of these factors in LTP and aging- or AD-related processes, it is important to investigate possible alterations of activation levels of these molecules during healthy aging in the dDG of both sexes.

1.6. Sex differences in aging

Sex differences are generally abundant on a morphological, cellular, and physiological level in healthy developing mammals. There are morphological differences in GCs and PCs between the sexes and the cycle stages of females in the hippocampus. Some examples include the dendritic intersection of granular cells (higher in males than females) and alterations in the CA1 apical spine density, the cell number of GCs or hilar neurons (males having higher numbers than females; cell types not further specified) (Azcoitia et al., 2005; Yagi & Galea, 2019). Differences do not only exist on a morphological level but also on a molecular level. For example, endogenous estrogen levels lead to tonic phosphorylation of ERK/MAPK in the brain of natural cycling females mediated by estrogen fluctuations (Bi et al., 2000). Additionally, exogenous β-estradiol infusion mediates the enhancement of object memory consolidation by ERK1/2 activation in the dorsal hippocampus (Fernandez et al., 2008).

Furthermore, hippocampus-dependent behavioral performance varies over the estrous cycle. Estrogen improves the performance of novel object recognition tasks but worsens the performance of spatial memory tasks in females (Sheppard et al., 2019). Moreover, physiological sex differences are also occurring, for example, the requirement of membrane estrogen receptor-α (ERα) to promote LTP induction and a higher LTP magnitude during the proestrus phase of natural cycling females in the CA1 (Warren et al., 1995). Furthermore, female rodents display an increased threshold for LTP induction in the CA1 and DG compared to male rodents (Bi et al., 2000; Maren, 1995; Maren et al., 1994; Wang et al., 2018; Yang et al., 2004). Besides the already-mentioned sex differences, the differences in the NPYergic and the cholinergic systems are highly relevant to this study. It has been shown that NPY levels differ between sexes in several brain regions. Specifically, in the hippocampus (under baseline conditions), females have lower NPY levels than males (reviewed in Nahvi & Sabban, 2020). Immunoreactivity, release, and NPY gene expression can be augmented by ER α and β in the female DG (Corvino et al., 2015; Hilke et al., 2009; Ledoux et al., 2009; Velíšková et al., 2015; Velíšková & Velíšek, 2007). Besides the NPYergic system, the cholinergic system also shows remarkable sex differences. Even though the number and size of cholinergic cells are similar in young males and females, the spontaneous release of ACh is higher in males than in female rats during the night cycle in the dorsal hippocampus. The number of cholinergic neurons is similar in male and female rodents in the MS (Masuda et al., 2005; Miettinen et al., 2002; Mitsushima et al., 2003, 2009a). Moreover, ovariectomy (OVX) rats displayed increased acetyltransferase activity after estrogen treatment in the hippocampus (Gibbs, 2000).

Furthermore, estrogen can mediate ACh release through Erα, located in the MS, and at cholinergic projections (Miettinen et al., 2002; Mufson et al., 1999).

Sex-specific alterations can also be observed during aging and AD. Generally, females suffer earlier from AD and have a steeper memory decline than males (Irvine et al., 2012). In aging, a sex-dependent area-specific decrease in neuronal density has been shown; for males in the CA3 and females in the CA1 (Yagi & Galea, 2019), whereby hilar neuron decline can be observed to a similar degree in aged male than female rats (cell types are not further specified) (Azcoitia et al., 2005). Studies on muscarinic receptors indicate that the cholinergic system declines during pathological aging and healthy aging in the hippocampus of females and males (Gibbs, 1998; Granholm et al., 2003.; Lukoyanov et al., 1999; Pilch & Miller, 1988). Nevertheless, density reduction of the cholinergic fibers targeting the DG is significantly larger in aged male rats than in aged females (Lukoyanov et al., 1999). In contrast, cholinergic cell sizes remain stable during aging in both sexes (Gibbs, 1998). In the case of the NPYergic system, some evidence from other areas hints at reduced Y1-R levels in females, which might be counterbalanced with higher Y1-R affinity (reviewed in Nahvi & Sabban, 2020). Interestingly, human studies show that NPY-like immunoreactivity in plasma increases in aged females, and postmenopausal women develop higher NPY plasma levels than cycling females at any stage of the cycle (Khoury & Mathé, 2004; Kluess et al., 2019). Notably, most NPYergic and cholinergic system studies were done in OVX mice, which is a model for menopause and might also account for aging. Here, it is also essential to mention the lack of research on the interaction of the cholinergic and the NPYergic systems in aged males and females, as shown for young male mice in our laboratory (Raza et al., 2017). Given the known sex differences in plasticity, brain structure, and memory performance in spatial tasks (reviewed in, e.g., Hyer et al., 2018; Yagi & Galea, 2019), it is crucial also to investigate sex differences in aging. Therefore, this study evaluates the neurotransmission and plasticity in the MPP-dDG pathway of aged anestrus females.

1.6.1. Ovariectomy in mice as a model for human menopause

As mentioned in section 1.1.1., female mice undergo an estrus cycle change during aging. The follicular decline rather than depletion, the relatively short lifetime of animals with reduced sex steroids, and the extended waiting time to reach an anestrus state have prompted most researchers to study ovariectomized female rodents (Bimonte-Nelson et al., 2021; Koebele & Bimonte-Nelson, 2016). For example, the augmented inhibition through the increase of NPY immunoreactivity and release of NPY by ERα and ERβ has been shown in the DG and

hippocampus of ovariectomized rats (Corvino et al., 2015; Ledoux et al., 2009; Velíšková et al., 2015; Velíšková & Velíšek, 2007). Additionally, a decline in cell number has been shown in the MS of OVX female rats for the cholinergic system. This and its maladaptive effect (reduced spontaneous release) can be reversed by estrogen treatment (Gibbs, 1998; Mufson et al., 1999). Moreover, estrogen can mediate plasticity indirectly by NPY and cholinergic activation through G protein-coupled receptor for estrogen (GPR30) and ERα (Gibbs, 1998; Gibbs et al., 2014; Luine, 1985; Marriott & Korol, 2003; Nakamura et al., 2002) or in a direct way through ERα and ERβ (Baudry et al., 2013; Ooishi et al., 2012; Smith et al., 2009; Waters et al., 2019). All these critical insights into estrogen modulation are highly important, but the use of OVX also has limitations. Firstly, OVX causes premature aging of the nervous system (Baeza et al., 2010). A reduced cholinergic cell number in the MS has been shown for OVX rats but not for natural aging rats (Gibbs, 1998). Moreover, the length of OVX but not natural aging abolished LTP in the CA1, shown by an LTP comparison of females with OVX for 19 months and aged-matched females with OVX for 1 month (Smith et al., 2010). Thus, uncommon phenomena during this premature aging cannot be ruled out. Furthermore, the results of ovariectomy on acetylcholine esterase activity are inconsistent. Therefore, investigating the cholinergic substitution in ovariectomized female mice might give artificial results on the effects of ACh on memory. Studies from humans show contradictory effects of the protective effect of estrogen after menopause, and the theory of a time-window-dependent beneficial effect of estrogen treatment has been established (Bean et al., 2015; Russell et al., 2019). In this light, ovariectomy is a very nice tool to investigate the effect of estrogen on a distinct time point. However, its value in addressing age-mediated changes in electrophysiological properties needs clarification. Intriguingly, most studies focus on the impact of estrogen on different circuits in ovariectomized females. Therefore, the effect of the cholinergic and NPYergic system on MPP-dDG plasticity will be evaluated in young OVX females to assess the possibility of using OVX as an aging model for MPP-dDG plasticity.

2. Aims

The cholinergic system has been shown to degenerate during aging (Schliebs & Arendt, 2011), and acetylcholine esterase inhibitor is one of the most efficient pharmacological interventions in AD (Nichols et al., 2019; Yiannopoulou & Papageorgiou, 2020), but still, this treatment does not prevent the cholinergic decline – they counterbalance the neurotransmitter imbalance (Hasselmo, 2006; Yiannopoulou & Papageorgiou, 2020). Critically, women seem to have a steeper cognitive decline when suffering from AD (Irvine et al., 2012b Mielke et al., 2014). Furthermore, the literature on the effect of acetylcholine esterase treatment in women is controversial (reviewed by Canevelli et al., 2017; Giacobini & Pepeu, 2018). Therefore, the first main aim of this study was to investigate the sex dependence of cholinergic maintenance of plasticity in the aging rodent. The dentate gyrus was chosen for the subsequent investigations due to its key role in the information flow. The LTP was investigated in slice preparation as the cellular correlate of memory.

Moreover, a decline in the NPYergic system has also been shown during aging (Hattiangady et al., 2005; Matsuoka et al., 1995; Sawano et al., 2015). Adding to this, chronic chemogenetic inactivation of hilar SST+ interneurons has recently been shown to cause cognitive impairment (Lyu et al., 2022). Importantly, the ACh-mediated release of NPY is crucial for proper memory retrieval in young male mice from our laboratory (Raza et al., 2017). Therefore, the second main aim of my study was to investigate the interaction of cholinergic and NPYergic transmission during healthy aging in a slice preparation of the dorsal hippocampus containing the dDG in both sexes.

To this end, I defined the following specific objectives:

- Establishing a TBS protocol for induction of LTP in the MPP-dDG synapse under intact inhibition (in the absence of GABAergic antagonists)
- Measuring the change of MPP-dDG LTP during aging in both sexes
- Investigating the effect of acetylcholine esterase inhibition on MPP-dDG LTP in aged animals of both sexes
- Determining the involvement of the local NPYergic system in the aging-induced plasticity changes and the recovery by acetylcholine esterase inhibition
- Evaluating the role of hormonal depletion on plasticity and the contribution of ACh and NPY in young female mice

Investigating plasticity and mechanistic changes during healthy aging in a sex-dependent manner would help determine the factors involved in preserving and impairing memory. This could ultimately lead to new targets and the evaluation of new sex-specific treatments to increase the life quality during aging.

3. Material and Methods

3.1. Animals

The mice used in these studies were housed and bred in the animal facility of the Department of Genetics and Molecular Neurobiology, Institute of Biology, Otto von Guericke University Magdeburg under standard laboratory conditions or purchased from Jackson Laboratories (Bar Harbor, Maine, USA) and housed for at least four weeks before performing experiments. The animals were kept in groups of two to five individuals in Macrolon cages (36.2 cm x 16 cm x 14.3 cm; Ebeco, Castrop-Rauxel, Germany) with standard bedding (Lignocel BK8/15, J. Rettenmaier & Söhne, Rosenberg, Germany) in an inverse 12 h light/ dark cycle (lights on from 7 PM – 7 AM with a 30 min dawn phase). They had access to food (Ssniff R/M-H V-1534, Ssniff Spezialdiäten, Soest, Germany) and water *ad libitum*. The room temperature and moisture were constantly monitored and kept at 21°C and 50-55 % air humidity. All preparations for the experiments were conducted during the animals' dark (active) phase, between 8 AM and 3 PM.

3.1.1. Animal welfare

Animal housing and experiments in these studies were conducted in accordance with the European and German regulations for animal experiments. The organ harvesting was performed on C57BL/6 mice whose breeding was approved by the Landesverwaltungsamt Saxony-Anhalt (AZ 2-1628).

3.1.2. Mouse lines

3.1.2.1. C57BL/6 mice

C57BL/6 BomTac mice used in the different studies were obtained from breeding in the Department of Genetics and Molecular Neurobiology animal facility. Initially, the breeding pairs were purchased from Taconic (M&B Taconic, Berlin, Germany). The breeding schema is one male mated with two females. The offspring were weaned at the age of four weeks and group-housed (2-5 animals separated by sex) until assignment for the different experiments.
Furthermore, due to the lack of aged male C57BL/6 mice, 12- and 18-month-old male C57BL/6J were purchased from Janvier Labs (Le Genest-Saint-Isle, France) and Charles River (Wilmington, Massachusetts, USA). The purchased animals were aged in the animal facility of the department until they reached at least 20 months of age. Group-caged animals were used for the experiments at 2-5 months or >20 months for both sexes.

Another set of experiments was performed with OVX female C57BL/6J mice. These animals were purchased from Janvier Labs (Le Genest-Saint-Isle, France) at the age of 10 weeks (Janvier labs performed surgical intervention at the age of 8 weeks) and were assigned to two different groups. One group was fed standard food while the other group received a low-phytoestrogen diet, called phyto-free food (see section 3.1.3; Ssniff R/M-H V-1554, Ssniff Spezialdiäten, Soest, Germany). Meanwhile, the animals were allowed to habituate to the animal facility and the inverse light/dark cycle in groups of 2-5 animals. Female OVX mice were used at 4-8 months of age, earliest 8 weeks after OVX.

3.1.3. Low phytoestrogen diet

To evaluate the impact of external estrogen sources, a part of the experiments was conducted with female OVX mice under a low phytoestrogen-containing diet (phyto-free; ssniff R/M-H, 10 mm, low phytoestrogens, V1554, Ssniff Spezialdiäten, Soest, Germany) that was composed of cereals (wheat products, barley), corn gluten, and potato protein. It contained 19.1% crude protein, 3.4% crude fat, 4.6% crude fiber, and 6.0% crude ash. In contrast to the standard food, the phyto-free food is low in the phytoestrogens genistein (<10mg/kg), daidzein (~10mg/kg), and coumestrol (<1mg/kg) and does not contain soybean or alfalfa products. The mice were purchased from Janvier Labs (Le Genest-Saint-Isle, France) and put on phyto-free food and water *ad libitum* six weeks before the experiments were conducted following our lab's previous work (Çalışkan et al., 2019).

3.1.4. Determination of the cycle stage in female mice

Investigation of the cycle stage in female mice was performed to correlate possible changes in neurotransmission and plasticity under various modulations or during aging and to determine when aged female mice transitioned to anestrus (closest hormonal status to menopause in natural aging female mice). In young females, the so-called swabbing was done right after decapitating the animals for slice recordings to correlate hormonal status directly with the electrophysiological data. In the case of the aged female mice, the swabbing was done for 15 days consecutively to determine a possible transition to anestrus in aged female mice, starting at the age of 18 months and repeated every two months in the case of cycling females. Females in permanent estrous were not used for experiments, and anestrus females were not further swabbed. The swab was collected using a 20 µL Eppendorf pipette with a filter tip and distilled water. The filter tip with 20 µL distilled water was carefully inserted into the vaginal opening. Only the tip was inserted to avoid penetration of the orifice (which could induce

pseudopregnancy). The vaginal opening was flushed by pipetting 3-5 times up and down to collect the cells from the wall of the vagina. To determine the cycle stage, the accumulated fluid was placed on a glass slide (Menzel-Gläser Superfrost; Menzel-Gläser, Braunschweig, Germany) and dried (at room temperature (RT) ~30 min and under the hood ~10 min). After drying the swab, the major cell type in the swab was determined qualitatively under a light microscope with an ocular magnification of 10x/20 combined with an objective magnification of 4x/0.10 (overview) and 10x/0.25 (investigating the shape of the cells). Each cycle stage contains three different cell types, and by defining the predominant cell type, the cycle stage of the animal was qualitatively determined (described in Allen, 1922; Byers et al., 2012; Goldman et al., 2007; McLean et al., 2012; Nelson et al., 1982). The three different cell types were leukocytes, cornified epithelial cells, and nucleated epithelial cells. In the so-called proestrus stage, mainly nucleated epithelial cells were identified (Fig. 5A). In contrast, during estrus, the predominant cells were the cornified epithelia cells (Fig. 5B). At metestrus, all three cell types were almost evenly distributed (Fig. 5C), and in the diestrus stage, mainly leukocytes were observed (Fig. 5D) (see Tab.1; Byers et al., 2012; Nelson et al., 1982).

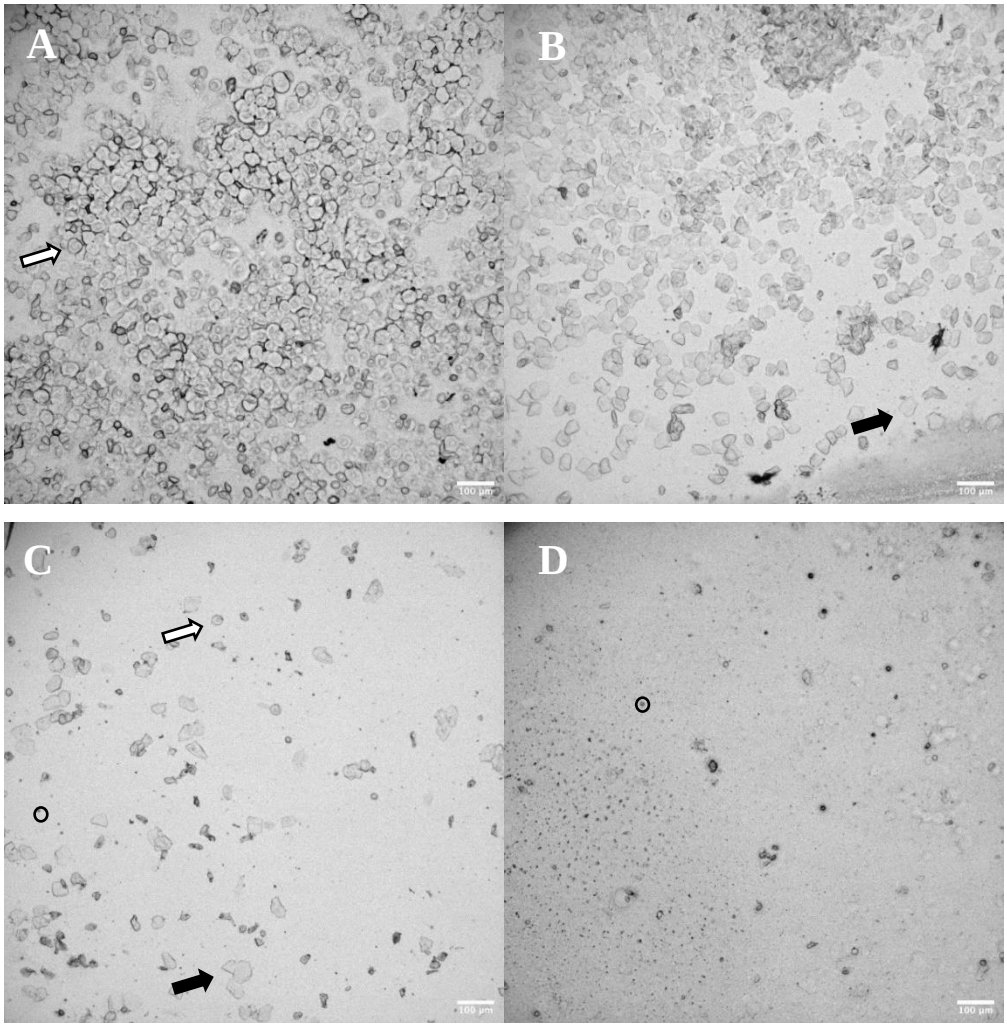

Figure 5: Example pictures of self-evaluated swabs of young C57BL/6 female mice. A: Proestrus phase with mostly nucleated epithelial cells (white arrow points to an example) **B:** Estrus with mainly cornified epithelia cells (black arrow points to an example). **C:** Metestrus with all cells are almost equally apparent**. D:** Diestrus with mainly leucocytes (circle around an example). Scale bar 100µM

Table 1: Classification of the estrous cycle stage by vaginal smear (modified after Nelson et al., 1982).

Cycle stage	nucleated epithelia	cornified epithelia	Leucocytes	smear density
Proestrus	0 to + (often degenerating)	+ to +++ (well-formed and predominant)	0 to +	medium
Estrus	0	0	++ to +++ (relatively small and predominant)	medium to heavy
Metestrus	++ to +++ (predominant)	+ to ++ (often irregularly shaped and vacuolated)	+ to ++	medium to heavy
Diestrus	+ to +++	+ (often irregularly shaped and vacuolated)	0	thin

0 = none, + = few, ++ = moderate, +++ = heavy

3.2. Electrophysiological recordings

To investigate synaptic plasticity and transmission during aging and under different pharmacological conditions, adult and senescent mice of both sexes (C57BL/6BomTac, C57BL/6J) were firstly deeply anesthetized with isoflurane and then decapitated. Brains were rapidly (within 60 s) removed and placed into cold (4–8 °C) carbonated (5% CO_2/95% O_2) artificial cerebrospinal fluid (aCSF) containing (in mM) 129 NaCl, 21 $NaHCO_3$, 3 KCl, 1.6 $CaCl_2$, 1.8 $MgSO_4$, 1.25 NaH_2PO_4, and ten glucose. Parasagittal slices, which contain the dorsal hippocampus, were obtained by cutting the brain at an angle of about 12° on an angled platform. The four most dorsal slices were transferred to an interface chamber perfused with aCSF at 32 ± 0.5 °C (flow rate: 1.8ml ± 0.2 ml per min, pH 7.4, osmolarity ~ 300 mosmol kg^{-1}). After cutting, the slices were left to rest for 1 hour before starting recordings. For dDG electrophysiology, one glass electrode, filled with aCSF (~ 1 MΩ), was placed at 70–100 μm depth into the molecular cell layer to measure the slope of the fEPSP. The stimulation of the MPP was performed with a bipolar tungsten wire electrode, with exposed tips of ~ 20 μm and tip separations of ~ 75 μm (electrode resistance in aCSF: ~ 0.1 MΩ, purchased from world precision instruments; Friedberg, Germany). A second bipolar tungsten electrode (same parameters as in the MPP) was placed into the hilus of the dDG to elicit an antidromic stimulation during LTP induction. Two input-output (I-O) curves were recorded after stabilization of the responses (0.033 Hz, pulse duration: 100 μs) over 20 min. The baseline

excitability and maximal synaptic response were measured by obtaining the I-O curve using pulses with stimulation intensities ranging from 10 to 200 μA. The stimulus intensity that resulted in ~ 50% of the maximum fEPSP amplitude of the ML after orthodromic stimulation was subsequently used for baseline recordings with orthodromic stimulation. While the stimulus intensity that resulted in ~ 70% of the maximum fEPSP amplitude of the ML after antidromic stimulation was used for the antidromic stimulation during LTP induction. The appropriate placement of the orthodromic stimulation was verified through paired-pulse stimulation with different inter-pulse intervals right after obtaining the I-O curve before starting the baseline recording. The characteristic feature of the MPP-DG synapse is the consistent paired-pulse depression at 50 ms interpulse interval (Barnes & Mcnaughton, 1980a; Froc et al., 2003). In all protocols, baseline and post-theta-burst stimulation (TBS) recordings were done with orthodromic stimulation (in the MPP). Exclusively the four repetitions of TBS (4x TBS) were done with a combination of orthodromic and antidromic stimulation (in the hilus of the DG). Using the general construct of a stimulation protocol (I-O curve, paired-pulse inhibition, 20min baseline, MPP-dDG LTP stimulation, 40min LTP recording), the order of the stimulations to induce reliable MPP-dDG LTP was evaluated. First, the antidromic stimulation was placed before the orthodromic stimulation without inducing LTP at the MPP-dDG synapse (see appendix; Fig. A1). The second protocol exchanged the stimulation order, resulting in unchanged fEPSP slopes upon 4x TBS (see appendix; Fig. A1). In the next step, the antidromic stimulation strength was increased, leading to a broader excitement of GCs and a higher possibility that ortho- and antidromic activation are summed up in one GL to overcome the spike threshold. Strikingly, the second increase reliably induced MPP-dDG LTP (see appendix; Fig A1). Here, the stimulation strength of both antidromic and orthodromic stimulations was determined by the size of the field (f)EPSP amplitude in the ML. The following experiments were performed with orthodromic stimulation of the MPP (using 50% of the fEPSP amplitude to perform recordings) followed by the antidromic stimulation during 4x TBS using 70% of the fEPSP amplitude produced through the antidromic stimulation. Signals were pre-amplified using a custom-made or EXT20-F amplifier (npi electronics, Tamm, Germany) and low-pass filtered at 3 kHz. Signals were sampled at a frequency of 10 kHz and stored on a computer hard disc for offline analysis. Twenty to eighty percent of the fEPSP slope size was analyzed offline using self-written MATLAB-based analysis tools (MathWorks, Natick, MA, USA). Slices with epileptic discharge, unstable baseline (variability more than 20%), or post-LTP signal 10% lower than baseline signal were excluded.

3.2.1. Pharmacological intervention during electrophysiological recordings

To investigate the effect of changes in the NPYergic system, cholinergic system, and the change of the sex steroid estradiol on MPP-dDG neurotransmission and plasticity, different drugs for exogenous modulation were applied to the slices obtained from C57BL/6 mice.

3.2.1.1. Exogenous modulation of the NPYergic system

The effect of selective Y1-R blockade on the fEPSP slope at the MPP-dDG synapse during neurotransmission and LTP responses in young and aged males and females, as well as in young OVX females, was evaluated. In these experiments, the selective Y1-R antagonist BIBP3226 (1 µM; Cat.-No. 2707; Tocris, Bristol, UK) was added to the aCSF for 20 min (until TBS) after 20 min baseline recording. In all experiments, the perfusion solution was changed back to aCSF at the timepoint of TBS.

Figure 6: Timeline for exogenous modulation of the NPYergic system through selective Y1-R blockade. aCSF = artificial cerebrospinal fluid, DMSO = dimethlysulfoxide, LTP = long-term potentiation, and TBS = Theta Burst Stimulation.

Furthermore, the effect of increased NPYergic transmission on the fEPSP slopes at the MPP-DG synapse during neurotransmission and LTP responses in aged male mice were tested by applying NPY (1 µM; Cat.-No. 90880-35-6; CaymanChemicals, Ann Arbor, Michigan, USA) for 40 min (until the TBS) 20 min baseline recording. In all experiments, the perfusion solution was changed back to aCSF at the timepoint of TBS.

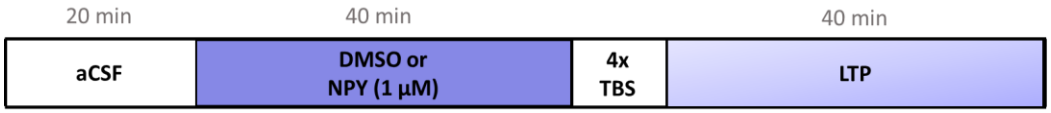

Figure 7: Timeline for an exogenous increase of the NPYergic system through NPY application. aCSF = artificial cerebrospinal fluid, DMSO = dimethlysulfoxide, LTP = long-term potentiation, NPY = Neuropeptide Y, and TBS = theta-burst stimulation.

Additionally, the effect of selectively activating Y1-R through the selective Y1-R agonist [Leu^{31}, Pro^{34}]-Neuropeptide Y (human, rat; 0.5 µM; Cat.-No. 1176; Tocris, Bristol, UK) was investigated on MPP-dDG neurotransmission in young female mice. [Leu^{31}, Pro^{34}]-

Neuropeptide Y (0.4 µM) was applied for 40 min after baseline recording. The combination of [Leu31, Pro34]-Neuropeptide Y with BIBP3226 was also tested in a set of experiments with young female mice. In these sets of experiments, [Leu^{31}, Pro^{34}]-Neuropeptide Y (0.4 µM) was applied for 20 min followed by 20 min BIBP3226 (1 µM) application after 20 min baseline recording.

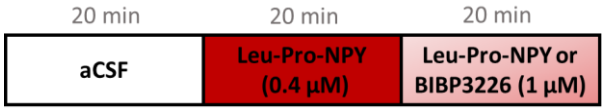

Figure 8: Timeline for an exogenous Y1-R activation through [Leu31Pro34]-NPY application and additional Y1-R blockade through BIBP3226. aCSF = artificial cerebrospinal fluid, NPY = Neuropeptide, and Y1-R = Neuropeptide Y receptor type 1.

3.2.1.2. Exogenous modulation of the cholinergic system

To evaluate the effect of moderate cholinergic activation on the fEPSP slope at the MPP-dDG synapse during neurotransmission and LTP, the acetylcholine esterase inhibitor physostigmine hemisulfate (PHY; 2µM; Cat.-No. sc-203661; Santa Cruz Biotechnology, Dallas, Texas, USA) was applied in young and aged males and females as well as in young OVX females. PHY was applied for 60 min after 20 min baseline recording. In all experiments, the perfusion solution was changed back to aCSF at the timepoint of TBS.

The effect of selective Y1-R blockade under moderate cholinergic activation on MPP-dDG neurotransmission and LTP was investigated in young and aged males and females as well as in young OVX females. PHY (2 µM) was applied for 40 min followed by 20 min BIBP3226 (1 µM) application after an initial 20 min baseline recording. In all experiments, the perfusion solution was changed back to aCSF at the timepoint of TBS.

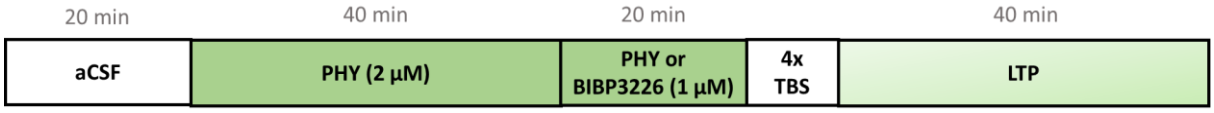

Figure 9: Timeline for exogenous activation of the cholinergic system through an acetylcholine-esterase inhibitor and applying a Y1-R antagonist. aCSF = artificial cerebrospinal fluid, LTP = long-term potentiation, PHY = physostigmine, TBS = theta-burst stimulation, and Y1-R = Neuropeptide Y receptor type 1.

3.2.1.3. Application of the sex steroid estradiol

The effect of exogenously applied β-estradiol on the fEPSP slope at the MPP-DG synapse during neurotransmission was evaluated in a cycle or Y1-R-dependent manner. β-estradiol

(10nM; Cat.-No. sc-204431; Santa Cruz Biotechnology, Dallas, Texas, USA) was applied for 50 min after an initial 20 min baseline recording. In all experiments, the perfusion solution was changed back to aCSF at the timepoint of TBS.

Another set of experiments investigated the effect of β-estradiol (10 nM) under selective Y1-R blockade. BIBP3226 (1 µM) was applied for 20 minutes, followed by 30 minutes of β-estradiol after an initial 20 min baseline recording. In all experiments, the perfusion solution was changed back to aCSF at the timepoint of TBS.

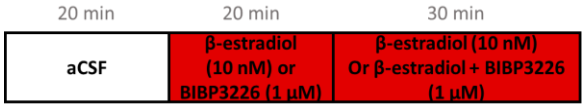

Figure 10: Timeline for exogenous estradiol increase through β-estradiol and additional application of the Y1-R antagonist. aCSF = artificial cerebrospinal fluid, and LTP = long-term potentiation, TBS = theta-burst stimulation, and Y1-R = Neuropeptide Y receptor type 1.

3.3. Protein analysis

Mice were deeply anesthetized with isoflurane and killed by cervical dislocation after reaching the deep surgical anasthesia, verified by the abolishment of the toe-pinch reflex. After cervical dislocation, the mice were decapitated, and the brains were carefully removed from the skull and transferred to ice-cold PBS to minimize protein degradation. For protein analysis, the dDG was dissected manually. To dissect the dDG, the frontal cortex and the cerebellum were removed, followed by the separation of the left and right brain hemispheres along the longitudinal fissure with a blade. The thalamus and hypothalamus were removed to expose the (underlying) hippocampus by pulling them away with forceps. After revealing the hippocampus, the dorsal and ventral parts and the DG and CA area were identified and carefully separated from each other (Hagihara et al., 2009). Samples were snap-frozen with liquid nitrogen and stored at -80°C until usage for Western blot (WB) or Enzyme-linked Immunosorbent Assay (ELISA).

3.3.1. Western Blot analysis

Hippocampal tissue of aged and young males and females were mechanically homogenized on ice in cold LM-buffer containing 1% Laurylmaltoside, 1% NP-40, 1mM Na_3VO_4, 2mM EDTA, 50 mM Tris-HCl pH 8.0, 150 mM NaCl, 0.5% deoxycholate, 1mM NaF 1mM AEBSF protease inhibitor (cat. No. 78431; Thermo Fisher Scientific, Massachusetts, USA), 1 µM Pepstatin A (cat. No. 78436; Thermo Fisher Scientific, Massachusetts, USA), and 1 Tablet

of Pierce protease inhibitor (cat. No. A32963; Thermo Fisher Scientific, Massachusetts, USA) and incubated for 25 min on ice. Afterward, the lysates were centrifuged at 13.000 g (Eppendorf Microcentrifuge 5415; Eppendorf SE, Hamburg, Germany), and the supernatant was collected. The protein concentration was quantified with the RC DC Protein assay Kit II (cat. No. 5000122; Bio-Rad Labortaories Inc, California, USA). After protein concentration assessment, the samples were prepared for immunoblot analysis by adding 4X sample buffer (40% glycerol, 240 mM Tris HCL pH 6.8, 8% SDS, 0.04% Bromophenol blue, and 5% mercaptoethanol) and incubated for 5 min at 95°C. For electrophoretic separation, an SDS Bis-Acrylamide gel was loaded with 20 µg of protein from each sample and a standard marker to define the band length after separation. The proteins were transferred to FL- PVDF membranes (cat. No. IPFL00010; Merck Millipore; Massachusetts, USA). The membranes were incubated with primary antibody solution at 4°C overnight. A near-infrared labeled secondary antibody IRDye 800CW or IRDye680CW (1:10,000; LI-COR Biosciences, Nebraska, USA) was used to detect the primary antibody. Finally, the imaging of the antibodies was performed using the Odyssey Imaging system (LI-COR Biosciences, Nebraska, USA), and the protein signal was quantified in the Image Studio software (LI-COR Biosciences, Nebraska, USA).

Table 2: Used antibodies for WB.

Antibody	concentration	company	catalog number	tissue used	sex	age
ms anti-GluR1	1:1000	Synaptic systems	#182011	dDG	♀/♂	young/aged
rb anti pGluR1 (Ser845)	1:1000	Invitrogen	#10555893	dDG	♀/♂	young/aged
ms anti-ERK1/2	1:1000	Invitrogen	#10221703	dDG	♀/♂	young/aged
rb anti pERK1/2	1:1000	cell signaling	#4370	dDG	♀/♂	young/aged
ms anti-NR2 B	1:1000	BD Bioscience	#610417	dDG	♀/♂	young/aged
rb anti pNR2B (Tyr1472)	1:1000	Invitrogen	#10650654	dDG	♀/♂	young/aged
gt anti M1-R	1:1000	abcam	#ab77098	dDG/CA3	♂	young/aged
ms anti-Y1-R	1:500	Santa Cruz Biotechnology	#sc-393192	dDG	♀/♂	young/aged

3.3.2. ELISA analysis of NPY

dDG tissues (of old and young male and female mice) were mechanically homogenized on ice in a cold LM Buffer. To determine the NPY peptide levels, 50 µl of the protein extract was prepared and analyzed with the ELISA kit for NPY (Product No. CEA879Hu; UOM: 96T; with minimum detectable dose less than 9.44pg/mL) according to manufacturer's instructions (cloude-clone corp., Texas, USA). In short: a 50 µL sample or standard solution (control) was mixed with 50 µL Reagent A and incubated for 1 hour at 37°C (one well per sample and two technical duplicates). After incubation, the mixture was washed three times, 100 µL detection reagent B was added and incubated for 30 min at 37°C. Followed by five wash steps and incubation of 90 µL substrate solution for 10-20 min at 37°C. The reaction was stopped by adding 50 µL stop solution and read at 450 nm immediately.

3.4. Statistics

Electrophysiological data were statistically compared by normalizing the fEPSP slopes to aCSF condition and averaging the normalized fEPSP slopes of the last 6 min during drug application for MPP-dDG neurotransmission evaluation. For plotting the fEPSP slopes after TBS, the fEPSP slope was normalized to the last 10 min before TBS, and the normalized fEPSP slopes of the last 10 min from the LTP recording were averaged. For the MPP-dDG neurotransmission recordings, a group comparison was performed between the average of the last 6 min of each drug. In the case of two drugs, either a two-tailed unpaired t-test (normal distributed) or a two-tailed Mann-Whitney test (non-normal distributed data) was performed. In the case of age and drug comparison, a (repeated) two-way- analysis of variance (ANOVA) with Geisser-Greenhouse correction and the post-hoc Fisher's least significant difference (LSD) test was applied. An in-slice comparison was performed when analyzing the electrophysiological data for successful LTP induction. For that, the averaged raw fEPSP slopes of the last 10 minutes after TBS were compared to the averaged raw fEPSP slope of the last 10 minutes before TBS using a one-tailed paired t-test (for normally distributed data) or the one-tailed Wilcoxon test (non-normal distributed data). Furthermore, to evaluate the LTP strength between groups, a group comparison was additionally performed by applying a two-tailed unpaired t-test or a two-way ANOVA on the normalized, averaged fEPSP slope from the last 10 min after TBS.

ELISA data (NPY concentrations) were normally distributed and, as such, analyzed with an ordinary one-way ANOVA with Fisher’s LSD test as a post-hoc comparison. Furthermore, for WB analysis of the Y1-R expression, the data were normalized to tubulin, and one-way ANOVA with the post-hoc Fisher’s LSD test was performed for normally distributed data. The WB analysis of all other markers was performed with the data normalized to tubulin and additionally to the young male mice. This was done to enable a comparison with samples from different WB blots. The normalized data were analyzed with a two-way ANOVA with Geisser-Greenhouse correction and Fisher’s LSD post-hoc test. Outliers were identified after ROUT, and normality was evaluated with the D’Agostino-Pearson test for all statistical tests, except for two-way ANOVA, where Geisser-Greenhouse correction was applied. Graphs and statistical tests were conducted with GraphPad Prism (version 9.4.1(681); Dotmatics, Boston, Massachusetts, USA).

Note that *n* accounts for the number of slices while *N* accounts for the number of animals.

4. Results

4.1. LTP induction at the MPP-dDG synapse in male mice

Due to a prominent feed-forward inhibition in the dDG, the likelihood of LTP induction at MPP to dDG synapses has been reported to be extremely low (Wigström & Gustafsson, 1983). Thus, LTP induction is mainly performed under the blockade of fast GABAergic transmission using a competitive blocker (e.g., Picrotoxin, 100 µM) of $GABA_A$-R as previously reported (Annamneedi et al., 2018). Therefore, my first goal during the initial phases of my thesis project was to establish an LTP induction protocol at the MPP-DG synapse without blocking the inhibitory GABAergic neurotransmission in slice preparations of the dDG. The establishment of this protocol was crucial for the aim of this thesis - to examine the neuromodulation of inhibitory interneurons in the dDG circuitry during cognitive decline. A standard LTP induction protocol under $GABA_A$-R blockade based on orthodromic stimulations of MPP fibers (Hanse & Gustafsson, 1992; L. Zhang et al., 2015). However, this protocol does not lead to LTP in most slices recorded when the GABAergic tonus is intact. Thus, I adapted a TBS stimulation protocol with a series of pre-and post-synaptic stimulations (Lopez-Rojas et al., 2016) and tested several variations to induce LTP. First, I established the pre-and post-synaptic stimulation order, also named ortho- and antidromic stimulation. This was followed by evaluating the percentage of the fEPSP amplitude to determine the strength of the antidromic stimulus (see appendix; Fig. A1).

Finally, using a series of TBS protocols with orthodromic stimulations (~50% of maximal orthodromic fEPSP amplitude) followed by antidromic stimulations (~70% of maximal antidromic fEPSP amplitude) led to successful LTP in young male mice (Fig. 11). Four repetitions of the TBS train could generate LTP ($t_{(8)}$ =2.056, p=0.0369, paired t-test, one-tailed, *n*=9; Fig. 11D), shown by an increased fEPSP slope.

There is a known general impairment in LTP induction and maintenance in the dDG *in vitro* of middle-aged rodents, as shown by Schreurs and colleagues (2017) using micro-array recordings (Schreurs et al., 2017). Indeed, LTP was abolished in aged male mice ($t_{(9)}$=0.9207, p=0.1906, paired t-test, one-tailed, *n*=10; Fig. 11D), shown by the unchanged fEPSP slope after 4x TBS. Furthermore, circuit changes can be assessed by evaluating post-synaptic and pre-synaptic excitability. The I-O curves revealed an increase in post-synaptic excitability in aged male mice in comparison to young male mice ($F_{(5,\ 270)}$=4.316, p=0.0009, repeated-2-way ANOVA, uncorrected Fisher's LSD, *n*=26 (aged) and n=30 (young); Fig. 11A). While no change was observed in the pre-synaptic fiber volley (FV) amplitude of the aged male mice

($F_{(5, 330)}$=0.7626, p=0.5773, repeated 2-way ANOVA, *n*=43 (aged) and n=15 (young); Fig. 11B). The increased baseline excitability in aged male mice could hint at a possible reduction of the inhibitory tonus in the dDG. Therefore, the impact of NPY-mediated inhibition on MPP-dDG LTP of male mice was tested by applying the selective Y1-R antagonist BIBP3226 (1 µM) before TBS stimulation. The data showed that blockade of Y1-R did not affect MPP-dDG LTP in young males with 4x TBS ($t_{(8)}$=3.080, p=0.0076, paired t-test, one-tailed, *n*=9 Fig. 11C), as shown by the significant increased fEPSP slope. Furthermore, Y1-R blockade did not modulate MPP-dDG LTP in aged animals, as shown by the unchanged fEPSP slope after TBS ($t_{(8)}$=1.044, p=0.3271, paired t-test, one-tailed, *n*=9¸ Fig. 11D). Moreover, the strength is significantly different between the age groups ($F_{(1, 33)}$=8.499, p=0.0063, two-way ANOVA, Fig. 11D), but no interaction between age and treatment could be observed. This experiment revealed increased post-synaptic excitability and a deficit of MPP-dDG LTP in aged male mice.

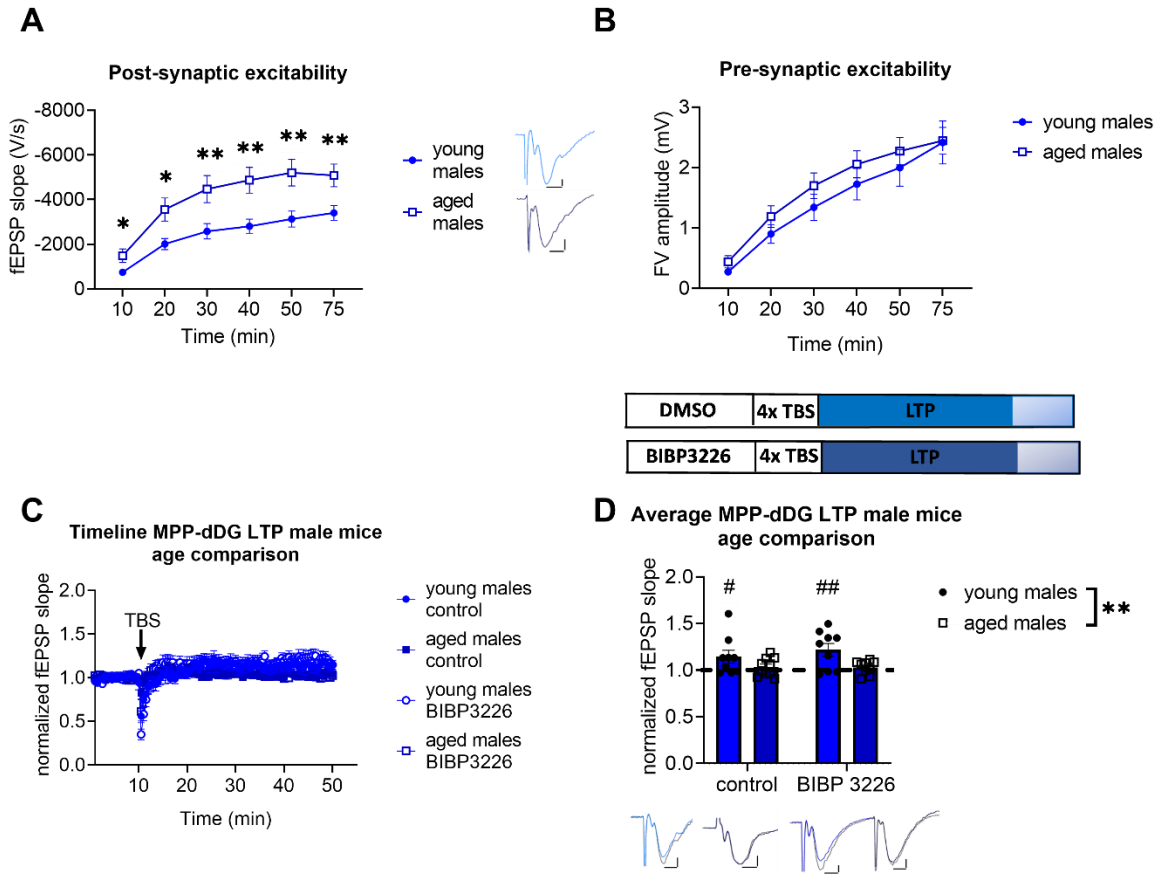

Figure 11: MPP-dDG LTP is abolished in aged male mice, while baseline excitability increases compared to young male mice. A: Post-synaptic excitability is increased in aged male mice (dark blue) compared to young males (blue), measured by the input-output (I-O) curve with stimulation strengths ranging from 10 to 75 μA. Besides the graph, representative fEPSP slope signals were plotted for young and aged mice at 30 μA stimulation strength. Scale bar x-axis2 ms each and scale bar y-axis: 1 mV each. **B:** The pre-synaptic excitability is similar in aged (dark blue) and young males (blue), shown by similar FV amplitude during the I-O curve. **C:** The plotted timeline of MPP-dDG LTP with the average values from young male mice control (blue), young male mice with BIBP3226 (white with blue), aged control (dark blue), and aged male mice with BIB3226 (white with dark blue) starts with the last 10 min of baseline recording (0-10 min), followed by 4x TBS induction at 10 min, and finishes with 40 min of LTP recording (10-50 min). **D:** Scheme of the experimental protocol for Y1-R blockade under control conditions. The normalized data from the last 10 min, indicated by transparent sections in the columns, were used for statistical comparison shown in bar graphs. The average of the last 10 min from the LTP recordings in the bar graph reveals a significant increase in baseline fEPSP slope after TBS in young (blue) and young with BIBP3226 (blue) but not in aged male mice (dark blue) and aged male mice with BIBP3226 (dark blue). Nevertheless, a difference in MPP-dDG LTP strength between young and aged males is demonstrated. Below the graph, representative fEPSP traces are plotted: before TBS (colored) and from the last 10 min of LTP recording (grey). Scale bar x-axis: 2 ms each and y-axis: 1 mV (young males) and 0.4 mV (aged males). dDG = dorsal dentate gyrus, DMSO = dimethylsulfoxid, LTP = long-term potentiation, MPP = medial perforant path, an, TBS = theta-burst stimulation. MPP-dDG LTP strength (group comparison): *, $p< 0.05$, **, $p< 0.01$; MPP-dDG LTP induction (in slice comparison): #, $p < 0.05$, ##, $p < 0.01$

4.2. Neuromodulation of neurotransmission and plasticity at the MPP-dDG synapse in male mice

Neuromodulators like acetylcholine and NPY can modulate MPP-dDG neurotransmission and plasticity by exciting or inhibiting GCs, respectively. An imbalance or change during aging in those systems could drastically disrupt synaptic transmission and plasticity. The literature indicates that the projections from the medial septum, the main source of ACh, decline during aging (Schliebs & Arendt, 2011). The decline leads to synaptic loss and cholinergic axonal degeneration in the dDG (Ypsilanti et al., 2008). Additionally, regarding the NPYergic system, Matsuoka and colleagues demonstrated that the somatostatinergic interneurons decline during aging (Matsuoka et al., 1995; Stanley & Shetty, 2004). Pharmacotherapies targeting the NPYergic system have not been established for AD treatment. However, one standard treatment in AD patients is the increase of the cholinergic tonus through acetylcholine esterase inhibitors, like physostigmine (Yiannopoulou & Papageorgiou, 2020).

Nevertheless, the exact mechanism of the beneficial effect of this treatment has not been fully resolved yet. To investigate the impact of these two declining systems during healthy aging, I applied PHY (an acetylcholine esterase inhibitor), BIBP3226 (a selective Y1-R blocker), or NPY. The effects of these drugs were measured during neurotransmission and plasticity at the MPP-dDG synapse in male mice.

Furthermore, I investigated a possible interaction between these two declining systems. Based on our laboratory's investigation that the ACh-mediated release of NPY is essential for memory retrieval in the dDG of young male mice (Raza et al., 2017), I evaluated the importance of Y1-R activation after moderate cholinergic activation. Furthermore, the impact of NPY on MPP-dDG neurotransmission and plasticity was assessed.

4.2.1. Moderate cholinergic activation leads to elevated Y1-R activation in young but not aged male mice

First, I established the minimal concentration of PHY for my *in vitro* recordings (see appendix Fig. A2), which resembled the decrease of DG neurotransmission after the PHY application shown previously (Colgin et al., 2003). The minimal concentration of 2 µM caused a reduction in MPP-dDG neurotransmission. After establishing the concentration of PHY, the effect of the Y1-R antagonist BIBP3226 (1 µM) on MPP-dDG neurotransmission and MPP-dDG neurotransmission under moderate cholinergic activation (PHY 2µM) was tested. MPP-dDG neurotransmission remained unchanged after selective Y1-R blockade independent of age, shown by the unchanged fEPSP slope ($F_{(1, 72)}$=3.625 p=0.0609, two-way ANOVA, *n*=28 (young males + BIBP3226); *n*=29 (young males control); *n*=9 (aged males + BIBP3226); *n*=10 (aged males control) Fig. 12C). Next, I tested the impact of moderate cholinergic activation on the Y1-R activation. Strikingly, a treatment ($F_{(1, 50)}$=9.116 p=0.0040, two-way ANOVA; Fig. 12F) and age effect ($F_{(1, 50)}$=4.884 p=0.0317, two-way ANOVA; Fig. 12F) was evident. MPP-dDG neurotransmission increased to control levels after additional blockade of the Y1-R in young male mice (post-hoc comparison to young male mice + PHY: p=0.0037, two-way ANOVA, Fisher's LSD test, *n*=16 (young males + PHY + BIBP3226); *n*=14 (young males + PHY); post-hoc comparison to aged male mice + PHY: p=0.0003, two-way ANOVA, Fisher's LSD test, *n*=16 (young males + PHY + BIBP3226); *n*=13 (aged males + PHY); post-hoc comparison to aged male mice + PHY + BIBP3226: p=0.0269, two-way ANOVA, Fisher's LSD test, *n*=16 (young males + PHY + BIBP3226); *n*=11 (aged males + PHY + BIBP3226); Fig. 12F). However, the reversal of MPP-dDG neurotransmission with additional Y1-R blockade was not present in the aged male mice, pictured by the unchanged MPP-dDG neurotransmission (post-hoc comparison to aged males mice + PHY: p=0.1910, two-way ANOVA, Fisher's LSD test, *n*=10 (aged males PHY + BIBP3226); *n*=13 (aged males + PHY); Fig. 12F) and also not compared to young male mice + PHY (post-hoc comparison: p=0.5836, two-way ANOVA, Fisher's LSD test, *n*=11 (aged males PHY + BIBP3226); *n*=14 (young males + PHY); Fig. 12F). Moreover, fEPSP slope remained lower than in young male mice +

PHY + BIBP3226 (post-hoc comparison: p=0.0269, two-way ANOVA, Fisher's LSD test, *n*=11 (aged males PHY + BIBP3226); *n*=16 (young males + PHY + BIBP3226); Fig. 12F). An interaction ($F_{(1,\ 50)}$=1.086 p=0.3024, two-way ANOVA; Fig. 12F) was not evident. Interestingly, a decreased MPP-dDG neurotransmission after increasing the cholinergic tonus was evident in aged male mice, similar to the young male mice marked by the decrease of the normalized fEPSP slope after PHY application (see appendix Fig. A3). Taken together, increased cholinergic tonus mediated a decrease of MPP-dDG neurotransmission in male mice independent of age. In contrast, the reversal of MPP-dDG neurotransmission by Y1-R blockade was age-dependent. In summary, moderate cholinergic activation mediates Y1-R activation in young male mice.

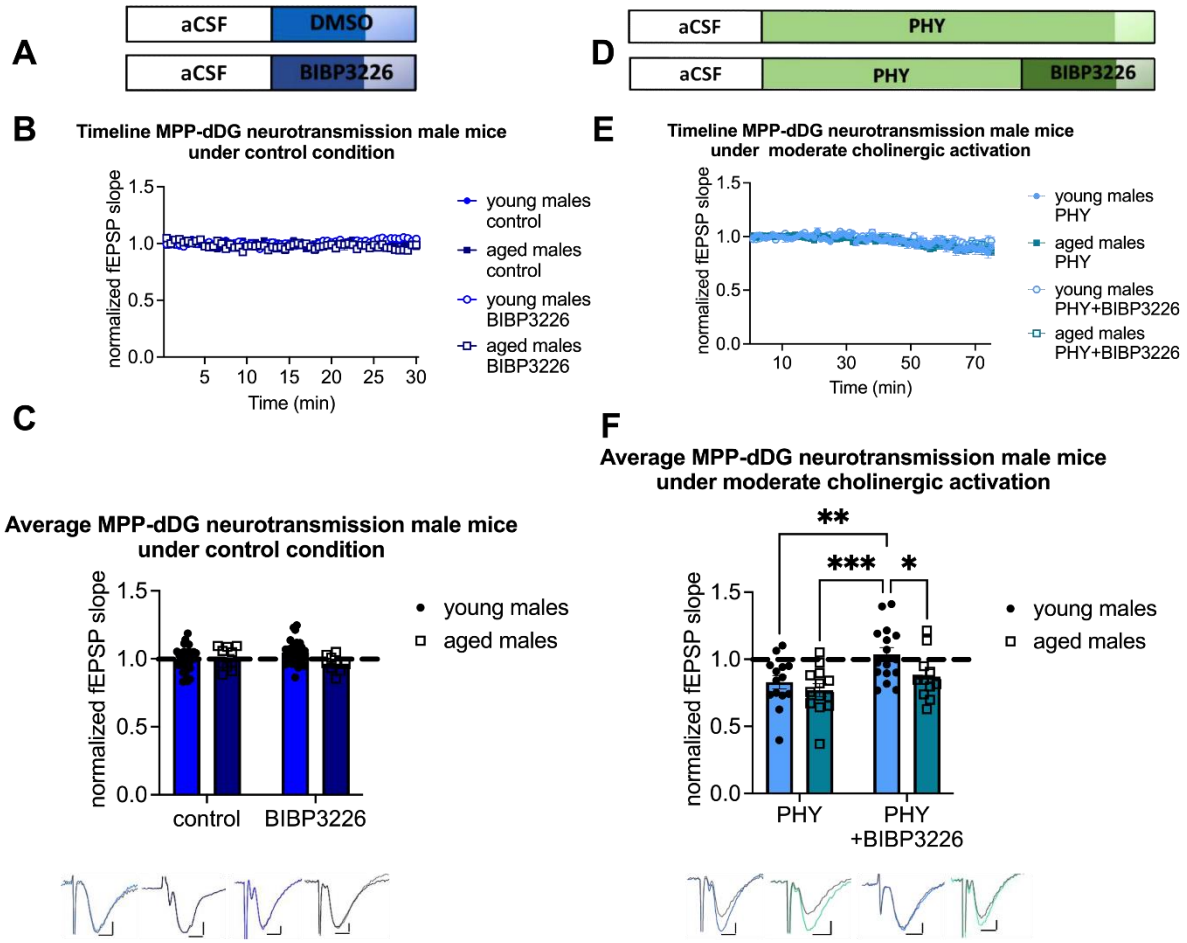

Figure 12: Moderate cholinergic activation mediates Y1-R activation in the MPP-dDG synapse in an age-dependent manner. A: Scheme of the experimental protocol for Y1-R blockade under control conditions. The normalized data from the last 6 min, indicated by transparent sections in the columns, were used for statistical comparison shown in bar graphs. **B:** Timeline of the MPP-dDG neurotransmission recording from young males under control condition (blue), young males with blockade of Y1-R through BIBP3226 (white with blue), aged males under control condition (dark blue), and aged males with Y1-R blockade through BIBP3226 (white with dark blue) starts with 10 min baseline recording (0-10 min) and is followed by 20 min BIBP3226 or DMSO application as control (10-30 min). **C:** The average from the last 6 min of MPP-dDG neurotransmission recording under control conditions and Y1-R blockade reveals an unchanged fEPSP slope in young (blue) and aged male mice (dark blue). Below the graphs, representative fEPSP traces are plotted: in color: the baseline; in grey: after drug application. Scale bar x-axis: 2 ms each and y-axis: 0.4 mV each. **D:** Scheme of the experimental protocol for Y1-R blockade under moderate cholinergic activation. The normalized data from the last 6 min, indicated by transparent sections in the columns, were used for statistical comparison shown in bar graphs. **E:** Timeline of the MPP-dDG neurotransmission recording from young males with moderate cholinergic activation (light blue), young males with moderate cholinergic activation plus Y1-R blockade (white with light blue), aged males under moderate cholinergic activation (petrol), and aged males under moderate cholinergic activation plus Y1-R blockade (white with petrol) starts with 10 min baseline recording (0-10 min) and is followed by 60 min PHY application or 40 min PHY plus 20 min BIBP3226 (10-70 min). **F:** The average from the last 6 min of MPP-dDG neurotransmission recording reveals a Y1-R-dependent increase of MPP-dDG neurotransmission after moderate cholinergic activation in young male mice (light blue) but not in aged male mice (petrol). Below the graph, representative fEPSP traces are plotted: before drug application (colored) and the last 6 min of drug application (grey). Scale bar x-axis: 2 ms each and y-axis: 0.4 mV each. dDG = dorsal dentate gyrus, DMSO = dimethylsulfoxide, MPP = medial perforant path, PHY = physostigmine, and Y1-R = Neuropeptide Y 1 Receptor. Changes in fEPSP slope after Y1-R blockade (group comparison) **, $p < 0.01$, ***, $p < 0.001$

4.2.2. Moderate cholinergic activation in the dH rescues MPP-dDG LTP of aged male mice in a Y1-R-dependent manner

The literature shows that the cholinergic system mediates NPY release in young male mice (Raza et al., 2017). Additionally, this was proved in the experiment above. Furthermore, the beneficial effect of acetylcholine esterase inhibitor for AD treatment and on CA1 LTP in aged rodents is well documented (Fujii & Sumikawa, 2001; Hornick et al., 2011; Yiannopoulou & Papageorgiou, 2020; https://www.nia.nih.gov/health/how-alzheimers-disease-treated) and involvement of Y1-R activation is indicated by Y1-R-dependent beneficial effects of nicotine treatment on MWM memory performance in a rat model of AD (Rangani et al., 2012). Nevertheless, the exact mechanism of the beneficial effect of this treatment on MPP-dDG LTP has not been fully resolved yet. For that reason, the impact of moderate cholinergic activation on MPP-dDG plasticity was investigated by applying the evaluated PHY concentration (2 µM) and the combination of PHY and BIBP3226 (1 µM). Moderate cholinergic activation in the dH led to MPP-dDG LTP in a Y1-R independent manner in young male mice (PHY: $t_{(8)}=2.403$, $p=0.0215$, paired t-test, one-tailed, $n=9$; PHY + BIBP3226: $t_{(9)}=2.265$, $p=0.0249$, paired t-test, one-tailed, $n=10$; Fig. 13). Furthermore, moderate cholinergic activation rescued the MPP-dDG LTP in aged male mice ($t_{(12)}=3.821$, $p=0.0012$, paired t-test, one-tailed, $n=13$; Fig. 13). This

rescue was dependent on the activation of the Y1-R as shown by the abolished MPP-dDG LTP after additional BIBP3226 application ($t_{(10)}$=1.569, p=0.0739, paired t-test, one-tailed, *n*=11; Fig. 13). A treatment effect was depicted ($F_{(1, 38)}$=7.746, p=0.0083, two-way ANOVA; Fig. 13C) for young male mice with PHY (p=0.0067, two-way ANOVA, Fisher's LSD test; Fig. 13C) and aged male mice with PHY compared to PHY with BIBP3226 (p=0.0320, two-way ANOVA, Fisher's LSD test; Fig. 13C). These results indicate a crucial role of Y1-R activation under moderate cholinergic activation in the MPP-dDG LTP of aged male mice.

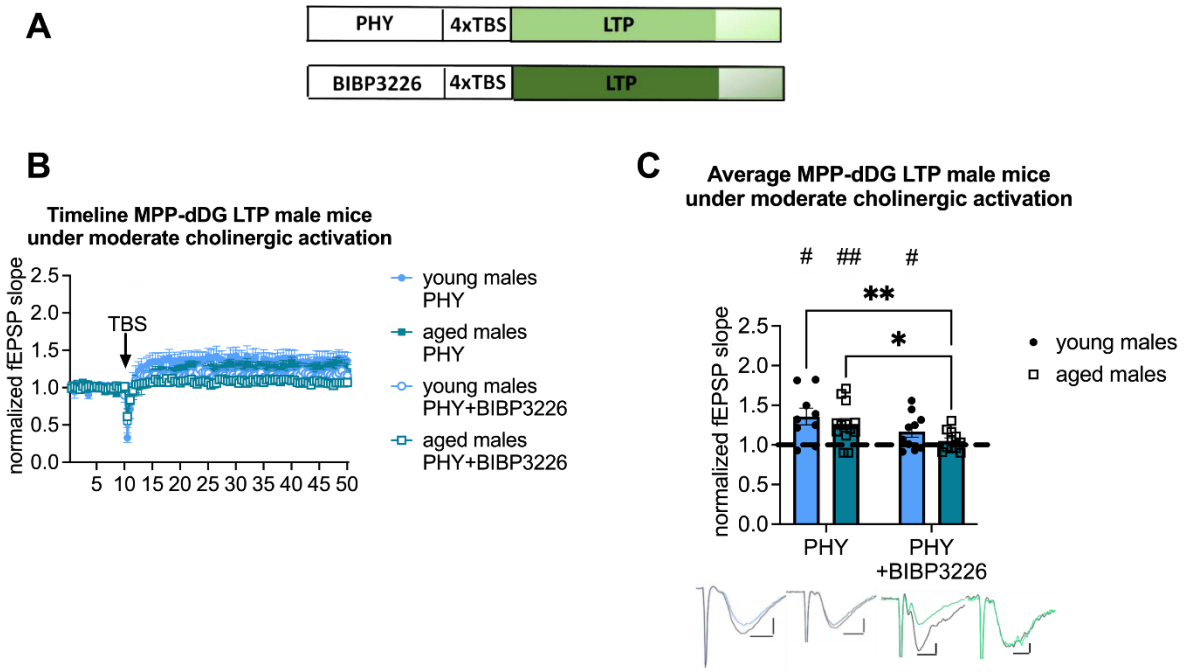

Figure 13: Moderate cholinergic activation rescues MPP-dDG LTP in aged male mice in a Y1-R-dependent manner. A: Scheme of the experimental protocol for Y1-R blockade under moderate cholinergic activation. The normalized data from the last 10 min, indicated by transparent sections in the columns, were used for statistical comparison shown in bar graphs. **B:** The plotted timeline of the average fEPSP slopes from young males with PHY (light blue), young males with PHY + BIBP3226 (white with light blue), aged males with PHY (petrol), and aged male mice with PHY + BIBP3226 (white and petrol) starts with the last 10 min of moderate cholinergic activation or selectively Y1-R blockade recording (0-10 min), followed by 4x TBS induction at 10 min, and finishes with 40 min of LTP recording (10-50 min). **C:** The average of the last 10 min from the MPP-dDG LTP recordings reveals a significant increase of the fEPSP slope under moderate cholinergic activation, which is independent of Y1-R activation in young male mice (light blue) but dependent on Y1-R activation in aged male mice (petrol). MPP-dDG LTP strength is not changed between the groups. Below the graph, representative fEPSP traces are plotted: before TBS (colored) and from the last 10 min of MPP-dDG LTP recording (grey). Scale bar x-axis: 2 ms each and scale bar y-axis: 1 mV (for young males) and 0.4 mV (for aged males). dDG = dorsal dentate gyrus, LTP = long-term potentiation, MPP = medial perforant path, PHY = physostigmine, TBS = theta-burst stimulation, Y1-R = Neuropeptide Y 1 receptor. MPP-dDG LTP induction (in slice comparison): #, $p < 0.05$, ##, $p < 0.01$

4.2.3. Application of NPY rescues MPP- dDG LTP in aged male mice

Previous data from our laboratory showed that NPY release depends on the activation of SST+ interneurons through ACh-mediated M1-R activation (Raza et al., 2017).

Furthermore, Santos and colleagues conducted a beneficial effect of intracerebroventricular NPY infusion on spatial memory in young male mice (dos Santos et al., 2013). Therefore, the potential impact of NPY (1 µM) on MPP-dDG LTP in aged male mice was investigated. Application of NPY rescued MPP-dDG LTP ($t_{(10)}$=3.222, p=0.0046, paired t-test, one-tailed, *n*=11; Fig. 14), shown by the persistent LTP after TBS under NPY. Furthermore, NPY application led to a significantly more robust MPP-dDG LTP (p=0.0087, Mann-Whitney test, two-tailed, *n*=11 (NPY group); *n*=5 (control group); Fig. 14). Whereby MPP-dDG neurotransmission was unchanged after NPY application (see appendix, Fig. A4). This experiment underlines the importance of NPYergic tonus for successful MPP-dDG LTP induction in aged male mice.

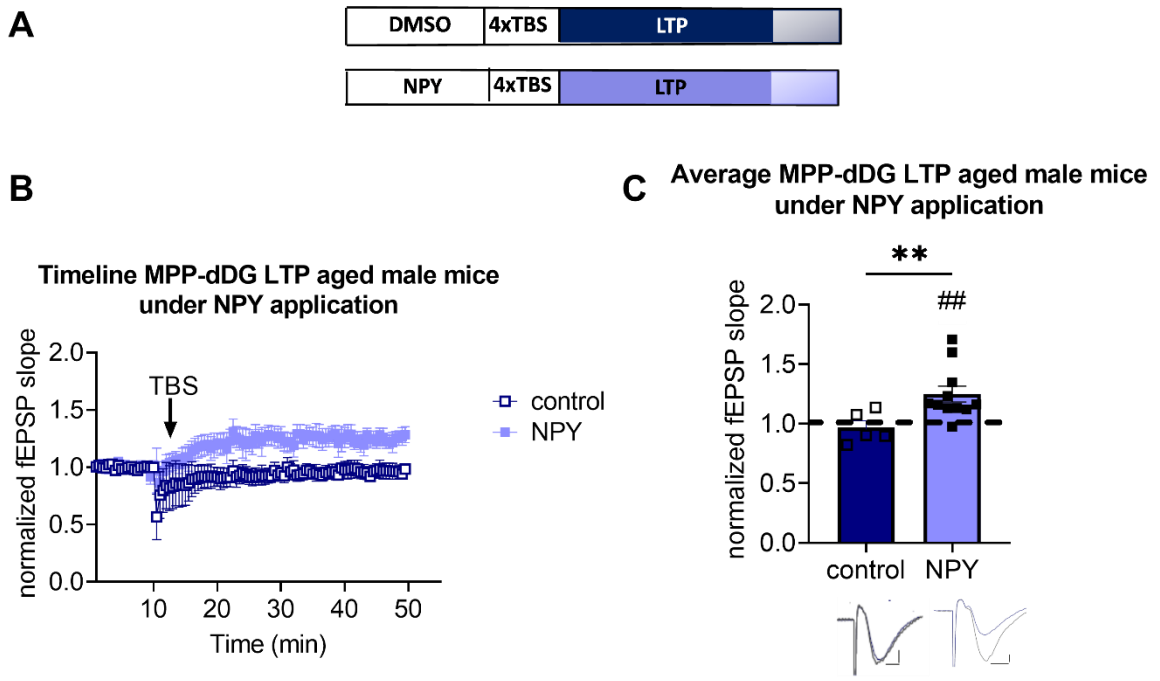

Figure 14: Increased NPYergic neurotransmission rescues MPP-dDG LTP in aged male mice. A: Scheme of the experimental protocol for NPY application under control conditions. The normalized data from the last 10 min, indicated by transparent sections in the columns, were used for statistical comparison shown in bar graphs. **B:** The plotted timeline of MPP-dDG LTP with the average fEPSP slopes from aged male mice with increased NPYergic transmission (light violet) and control (dark blue) starts with the last 10 min of increased NPYergic transmission or control (0-10 min), followed by 4x TBS induction at 10 min, and finishes with 40 min of LTP recording (10-50 min). **C:** The average of the last 10 min of MPP-dDG LTP recording reveals a significant increase of the fEPSP slope after TBS after NPY application (light violet) which also leads to an increased MPP-dDG LTP strength compared to control (dark blue). Below the graph, representative fEPSP traces are plotted: before TBS (colored) and from the last 10 min of MPP-dDG LTP recording (grey). Scale bar x-axis: 2 ms each and scale bar y-axis: 0.4 mV (control) and 1 mV (NPY). dDG = dorsal dentate gyrus, DMSO = dimethylsulfoxide, LTP = long-term potentiation, MPP = medial perforant path, NPY = Neuropeptide Y, and TBS = theta-burst stimulation. MPP-dDG LTP strength (group comparison): **, $p < 0.01$ and MPP-dDG LTP induction (in slice comparison): ##, $p < 0.01$

4.3. LTP induction at the MPP-dDG synapse in hippocampal slices of female mice

The electrophysiological recordings at the MPP-dDG pathway from young female rodents are mainly without taking the estrous cycle into account or from young OVX females, which might only partially depict neuroplasticity properties and modulation. These studies show a more stable LTP at the PP-DG synapse of young anesthetized male rats and a higher PP-DG LTP induction threshold in young anesthetized female rats (Maren, 1995; Maren et al., 1994). Therefore, I took the cycle stage into account and sorted the mice into two groups, namely the high estrous stage females (estrus and proestrus; estradiol, progesterone, FSH, LH high) and the low estrus stage females (metestrus and diestrus; progesterone, estradiol, FSH, LH low) (Huang et al., 1978; Inoue, 2022). I investigated MPP-dDG neurotransmission and plasticity under physiological-like conditions and its modulation through neuromodulators and sex steroids using slice electrophysiology.

4.3.1. MPP-dDG LTP is inducible in aged female mice, whereby pre- and post-synaptic excitability is increased

The same TBS protocol as used for male mice is able to induce MPP-dDG LTP in female mice independent of cycle stage, as shown by the significant increase of the fEPSP slope after 4x TBS in young low estrus females ($t_{(7)}$=2.532, p=0.0196, paired t-test, one-tailed, *n*=8; Fig. 15D) and also in young high estrus female mice ($t_{(10)}$=2.850, p=0.0086, paired t-test, one-tailed, *n*=11; Fig. 15D).

The synaptic plasticity and transmission properties of aged anestrus female mice in the dDG are unknown. Aged anestrus female mice were chosen because they remained in the closest hormonal state to human menopause in naturally aging female mice (Huang, 1978; Koebele & Bimonte-Nelson, 2016). Application of 4x TBS induced LTP successfully at the MPP-dDG synapse of aged female mice ($t_{(9)}$=1.891, p=0.0456, paired t-test, one-tailed, *n*=10; Fig. 15D). Post-synaptic excitability was increased in young low estrus females compared to their high estrus counterparts at 30, 50 and 75 µA ($F_{(10, 555)}$=4.315, p<0.0001, repeated two-way ANOVA; post-hoc comparison at 30µA: p=0.0388, repeated two-way ANOVA, Fisher's LSD test; post hoc comparison at 50 µA: p=0.0436, repeated two-way ANOVA, Fisher's LSD test; post-hoc comparison at 75 µA: p=0.0310, two-way ANOVA, Fisher's LSD test, *n*=34 (young high estrus females); *n*=45 (young low estrus females); Fig. 15A). On the other hand, the post-synaptic excitability of aged anestrus females was substantially increased in

comparison to young high estrus females in all stimulation strength (post-hoc comparison 10 µA: p=0.0478, repeated two-way ANOVA, Fisher's LSD test; post-hoc comparison 20 µA: p=0.0018, repeated two-way ANOVA, Fisher's LSD test; post-hoc comparison 30 µA: p=0.0002, repeated two-way ANOVA, Fisher's LSD test; post-hoc comparison 40 µA: p=0.0001, repeated two-way ANOVA, Fisher's LSD test; post-hoc comparison 50 µA: p=0.0001, repeated two-way ANOVA, Fisher's LSD test; post-hoc comparison 75 µA: p=0.0004, repeated two-way ANOVA, Fisher's LSD test; *n*=45 (young high estrus females); *n*=35 (aged anestrus females); Fig. 15A) but not compared to young low estrus females in none of the stimulation strength (post-hoc comparison at 10 µA: p=0.8758, repeated two-way ANOVA, Fisher's LSD test; post-hoc comparison at 20 µA: p=0.2903, repeated two-way ANOVA, Fisher's LSD test; *n*=45 (young low estrus females); post-hoc comparison at 30 µA: p=0.1435, repeated two-way ANOVA, Fisher's LSD test; post-hoc comparison at 40 µA: p=0.0519, repeated two-way ANOVA, Fisher's LSD test; post-hoc comparison at 50 µA: p=0.1092, repeated two-way ANOVA, Fisher's LSD test; post-hoc comparison at 75 µA: p=0.1404, repeated two-way ANOVA, Fisher's LSD test; *n*=35 (aged females); Fig. 15A). Furthermore, the pre-synaptic excitability was increased in aged anestrus females compared to young high estrus females at a stimulation strength of 20 µA, 30 µA, 40 µA, 50 µA, and 75 µA ($F_{(10,\ 505)}$=2.744, p=0.0027, repeated two-way ANOVA; post-hoc comparison at 20 µA: p=0.0395, repeated two-way ANOVA, Fisher's LSD test; post-hoc comparison at 30 µA: p=0.0257, repeated two-way ANOVA, Fisher's LSD test; post-hoc comparison at 40 µA: p=0.0169, repeated two-way ANOVA, Fisher's LSD test; *n*=34 (young high estrus females); post-hoc comparison at 50 µA: p=0.0139, repeated two-way ANOVA, Fisher's LSD test; post-hoc comparison at 75 µA: p=0.0301, repeated two-way ANOVA, Fisher's LSD test; *n*=31 (aged females); Fig. 15B) but unchanged compared to young low estrus females at all stimulation strength (post-hoc comparison at 10 µA: p=0.8048, repeated two-way ANOVA, Fisher's LSD test; post-hoc comparison at 20 µA: p=0.2517, repeated two-way ANOVA, Fisher's LSD test; post-hoc comparison at 30 µA: p=0.1094, repeated two-way ANOVA, Fisher's LSD test; post-hoc comparison at 40 µA: p=0.0925, repeated two-way ANOVA, Fisher's LSD test; post-hoc comparison at 50 µA: p=0.0888, repeated two-way ANOVA, Fisher's LSD test; post-hoc comparison at 75 µA: p=0.1489, repeated two-way ANOVA, Fisher's LSD test; *n*=31 (aged females); Fig. 15B). Moreover, the pre-synaptic excitability is unchanged between the cycle stages at all stimulation strength (post-hoc comparison at 10 µA: p=0.5487, repeated two-way ANOVA, Fisher's LSD test; post-hoc comparison at 20 µA: p=0.4205, repeated two-way ANOVA, Fisher's LSD test; post-hoc comparison at 30 µA:

p=0.5581, repeated two-way ANOVA, Fisher's LSD test; post-hoc comparison at 40 µA: p=0.4939, repeated two-way ANOVA, Fisher's LSD test; post-hoc comparison at 50 µA: p=0.4551, repeated two-way ANOVA, Fisher's LSD test; post-hoc comparison at 75 µA: p=0.4941, repeated two-way ANOVA, Fisher's LSD test; *n*=34 (young high estrus females); *n*=39 (young low estrus females); Fig. 15B). The enhanced excitability seen in young low estrus females and aged anestrus females as shown by the I-O curve might be due to altered neuromodulation (e.g., NPYergic, cholinergic) throughout the estrus cycle. The aged females had increased post-synaptic excitability compared to their young high estrus counterparts but unaltered compared to young low estrus females. Nevertheless, similar to the experimental protocols in males, the Y1-R antagonist BIBP3226 (1 µM) was applied before TBS stimulation in female mice to investigate possibly NPY-mediated inhibitory alterations in a cycle- and age-dependent manner. At the MPP-dDG synapse of young low estrus stage females, LTP was successfully induced with 4x TBS, under Y1-R blockade ($t_{(9)}$=2.718, p=0.0119, paired t-test, one-tailed, *n*=10; Fig. 15D). Also, the young high estrus stage females displayed MPP-dDG LTP induction after Y1-R blockade with 4x TBS (p=0.0078, Wilcoxon test, one-tailed, *n*=7; Fig. 15D) like under control conditions. Strikingly, MPP-dDG LTP depended on Y1-R activation in aged anestrus females, underlined by the abolished MPP-dDG LTP after selective Y1-R blockade with BIBP3226, applied before 4x TBS (p=0.3477, Wilcoxon test, one-tailed, *n*=10; Fig. 15D). In summary, these experiments demonstrate a Y1-R- and estrus cycle-independent MPP-dDG LTP in young female mice but Y1-R dependent MPP-dDG LTP in aged anestrus females under control conditions. At the same time, pre- and post-synaptic excitability is unchanged compared to young females with low estrogen levels.

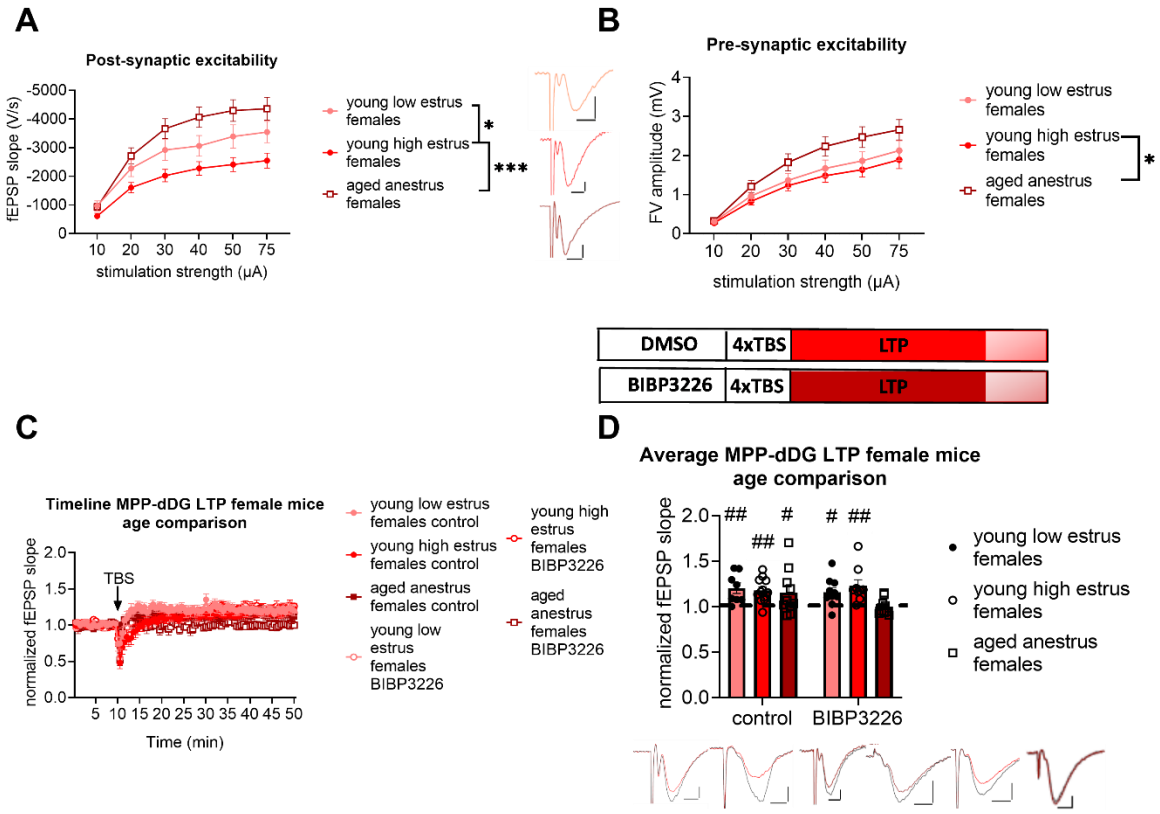

Figure 15: TBS-induced MPP-dDG LTP is Y1-R dependent in aged anestrus female mice. Post-and pre-synaptic excitability increases compared to young high estrus females but not young low estrus females. A: Post-synaptic excitability is increased in low young estrus (light red) and aged anestrus females (white with dark red) in comparison to young high estrus females (red), measured with stimulus strength ranging from 10 µA to 75 µA. Besides the graph, representative fEPSP traces for young and aged animals at 30 µA stimulation strength is shown. Scale bar x-axis: 2 ms each and y-axis: 1 mV (young low and aged anestrus females) and 0.4 mV (young high estrus females). **B:** The pre-synaptic response is similar in aged (white with dark red) and young low estrus females (light red), as well as in young low (light red) and young high estrus females (red). In contrast, pre-synaptic excitability increases in aged anestrus females (white with dark red) compared to young high estrus females (red). **C:** The plotted timeline of MPP-dDG LTP with the average values from young, low estrus female control (light red), young low estrus females with BIBP3226 (light red with white, young high estrus female mice (red), young high estrus females with BIBP3226 (white with red), aged anestrus females control (dark red), and aged anestrus females with BIBP3226 (white with dark red), starts with the last 10 min of drug application (0-10 min), followed by 4x TBS induction at 10 min, and finishes with 40 min of LTP recording (10-50 min). **D:** Scheme of the experimental protocol for Y1-R blockade under control conditions. The normalized data from the last 10 min, indicated by transparent sections in the columns, were used for statistical comparison shown in bar graphs. The average of the last 10 min from the MPP-dDG LTP recordings in the bar graph reveals a significant increase in the baseline fEPSP slope for low young estrus (light red), young high estrus (red), and aged female mice (dark red). Application of BIBP3226 did not affect MPP-dDG LTP in young low (light red) and young high estrus females (red). Interestingly, it abolishes the increase of the fEPSP slope in aged anestrus females (dark red), while MPP-dDG LTP strength is unaltered between the groups. Below the graph, representative fEPSP traces are plotted: before TBS (colored) and of the last 10 min of LTP recording (grey). Scale bar x-axis: 2 ms each and scale bar y-axis: 1 mV (young high estrus females control/BIBP3226 and low estrus females control), 0.4 mV (aged anestrus females control and low estrus females BIBP3226) and 0.2 mV (aged anestrus females BIBP3226). dDG = dorsal dentate gyrus, DMSO = dimethylsulfoxide, LTP = long-term potentiation, MPP = medial perforant path, and TBS = theta-burst stimulation. Change of fEPSP slope (group comparison): *,$p < 0.05$, ***,$p < 0.001$MPP-dDG LTP induction (in slice comparison): #, $p < 0.05$, ##, $p < 0.01$

4.3.2. Moderate cholinergic activation stabilizes MPP-dDG LTP in a Y1-R independent manner in aged anestrus females

The impact of increased cholinergic tonus on MPP-dDG plasticity in aged anestrus female mice is underinvestigated. Moreover, the literature about the beneficial effect of acetylcholine esterase inhibitors in women's studies is controversial. Studies show beneficial, no, or dose-dependent results (reviewed in Canevelli et al., 2017; Giacobini & Pepeu, 2018). Furthermore, a possible interaction between the cholinergic and NPYergic systems is not investigated in naturally aged anestrus female mice. To evaluate the effect of increased cholinergic tonus on the plasticity of the MPP-dDG synapse and its interaction with the NPYergic system, PHY (2 µM) or PHY in combination with BIBP3226 (1 µM) was applied before inducing MPP-dDG LTP in aged anestrus female mice. Interestingly, the application of PHY led to a Y1-R independent MPP-dDG LTP (PHY: $t_{(6)}$=2.290, p=0.0310, paired t-test, one-tailed PHY: $t_{(7)}$=3.388, p=0.0058, paired t-test, one-tailed, *n*=7 (aged anestrus females PHY), *n*=8 (aged anestrus females PHY + BIBP3226); Fig. 16) in aged anestrus female mice, indicated by the persistent increase of the fEPSP slope after the blockade of Y1-R under moderate cholinergic activation. Since the application of PHY in aged anestrus females led to a Y1-R independent MPP-dDG LTP, the question arose if moderate cholinergic activation acts similarly on MPP-dDG LTP in young females. However, the application of PHY and the combination of PHY with BIBP3226 did not affect MPP-dDG LTP of young female mice, neither in the low estrus stage (PHY: $t_{(9)}$=2.072, p=0.0340, paired t-test, one-tailed, *n*=10; PHY + BIBP3226: $t_{(9)}$=2.190, p=0.0281, paired t-test, one-tailed, *n*=10; Fig. 16) nor in the high estrus stage (PHY: $t_{(11)}$=3.493, p=0.0025, paired t-test, one-tailed, *n*=12; PHY + BIBP3226: $t_{(11)}$=3.192, p=0.0043, paired t-test, one-tailed, *n*=12; Fig. 16). Additionally, the extracellular ACh increase led to a similar MPP-dDG LTP strength for all groups ($F_{(2, 52)}$=2.903, p=0.0638, two-way ANOVA; Fig. 16). These results indicated a beneficial effect of PHY on MPP-dDG LTP in aged anestrus females, possibly through increased Y1-R activation.

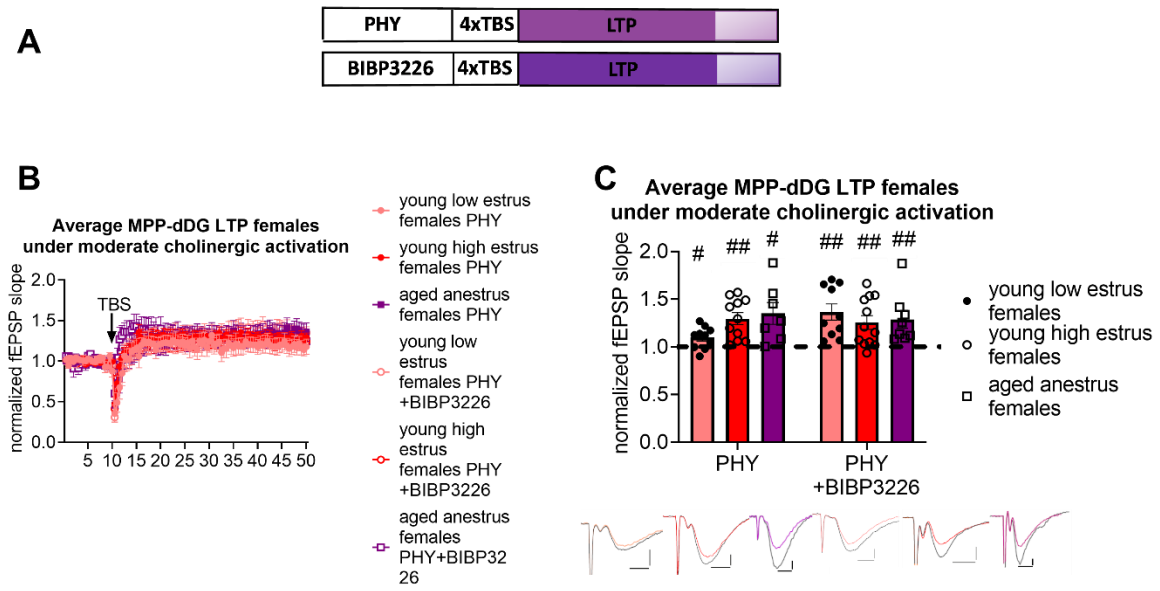

Figure 16: MPP-dDG LTP is stabilized through moderate cholinergic activation in a Y1-R independent manner in aged anestrus females. A: Scheme of the experimental protocol for Y1-R blockade under moderate cholinergic activation. The normalized data from the last 10 min, indicated by transparent sections in the columns, were used for statistical comparison shown in bar graphs. **B:** The plotted timeline of MPP-dDG LTP with the average fEPSP slopes from young low estrus females with PHY (light red), young low estrus females with PHY + BIBP3226 (white with light red), young high estrus females with PHY (red), young high estrus females with PHY + BIBP3226 (white with red), aged female mice with PHY (purple) and aged anestrus females with PHY + BIBP3226 (white with purple) starts with the last 10 min of moderate cholinergic activation or moderate cholinergic activation with Y1-R blockade recording (0-10 min), followed by 4x TBS induction at 10 min, and finishes with 40 min of LTP recording (10-50 min). **C:** The average of the last 10 min from the MPP-dDG LTP recordings in the bar graph reveals a significant increase of fEPSP slope under moderate cholinergic activation in young low estrus females (light red), young high estrus females (red), and aged anestrus females (purple), which also persisted after Y1-R blockade in all groups (Light red/red/purple). Furthermore, MPP-dDG LTP strength is unaltered between the groups. Below the graph, representative fEPSP traces are plotted: before TBS (colored) and from the last 10 min of MPP-dDG LTP (grey). Scale bar x-axis: 2 ms each and scale bar y-axis: 1 mV (young high and low estrus females PHY/PHY + BIBP3226) and 0.4 mV (aged anestrus females PHY/PHY + BIBP3226). dDG = dorsal dentate gyrus, LTP = long-term potentiation, PHY = physostigmine, TBS = theta-burst Stimulation, and Y1-R = Neuropeptide Y 1 Receptor. MPP-dDG LTP induction (in slice comparison): #, $p < 0.05$, ##, $p < 0.01$

4.4. Neuromodulation of MPP-dDG neurotransmission in young female mice

4.4.1. Female mice show increased Y1-R activation during MPP-dDG neurotransmission in a cycle stage- and age-dependent manner

NPY levels are known to be lower in young females than in young males (reviewed in Nahvi & Sabban, 2020). Furthermore, the application of β-estradiol in ovariectomized young female rats increases NPY+ cell number (Corvino et al., 2015; Ledoux et al., 2009; Velíšková et al., 2015; Velíšková & Velíšek, 2007). However, the investigation of Y1-R mediated NPYergic neurotransmission in the dDG of females in a cycle-stage- and age-dependent

manner is still missing. Thus, I investigated possible changes in Y1-R activation on the MPP-dDG neurotransmission of female mice by applying the selective Y1-R antagonist BIBP3226 (1 µM). In low estrus stage females, MPP-dDG neurotransmission was unchanged after BIBP3226 application compared to the control condition ($F_{(2, 123)}$=6.388 p=0.0023, two-way ANOVA; post-hoc comparison to young low estrus control: p=0.8234 two-way ANOVA, Fisher's LSD test, *n*=24 (control); *n*=30 (BIBP3226); Fig. 17C). In contrast, applying BIBP3226 in high estrus females demonstrated an increased MPP-dDG neurotransmission, underlined by the increased fEPSP slope compared to all other groups (post-hoc comparison to young high estrus control: p<0.0001, two-way ANOVA, Fisher's LSD test; post-hoc comparison to low estrus control: p=0.0002, two-way ANOVA, Fisher's LSD test; post-hoc comparison to aged anestrus control: p=0.0006, two-way ANOVA, Fisher's LSD test; post-hoc comparison to low estrus + BIBP3226: p=0.0002, two-way ANOVA, Fisher's LSD test; post-hoc comparison to aged anestrus + BIBP3226: p=0.0003, two-way ANOVA, Fisher's LSD test, *n*=29 (high estrus control); *n*=26 (high estrus + BIBP3226); *n*=24 (low control estrus); *n*=30 (low estrus + BIBP3226);); *n*=10 (aged anestrus females); *n*=10 (aged anestrus females + BIBP3226); Fig. 17C). Additionally, Y-1R blockade under control conditions had no impact on MPP-dDG neurotransmission in aged anestrus female mice (post-hoc comparison to aged anestrus control: p=0.8598, two-way ANOVA, Fisher's LSD test; *n*=10 (aged anestrus females); *n*=10 (aged anestrus females + BIBP3226); Fig. 17C).

The increased NPYergic transmission in young high estrus females raised the question of whether this increase might be mediated by estrogen or increased cholinergic levels. High estrogen levels mediate cholinergic release through ERs at the cholinergic terminals (Miettinen et al., 2002; Mufson et al., 1999) and, as mentioned above, the release of NPY. Moreover, the effect of moderate cholinergic activation on the NPYergic system in the dDG is only investigated in young male mice (Raza et al., 2017), and whether the same mechanism does exist in females is not resolved yet. The effect of a moderate cholinergic activation on MPP-dDG neurotransmission in a cycle stage-dependent manner, as well as the possible interaction with NPY-mediated Y1-R activation, was measured in the same way as in male mice. The investigation of the cholinergic impact on Y1-R activation showed a decreased MPP-dDG neurotransmission after PHY (2 µM) application, independent of cycle stage in young female mice compared to control conditions (see appendix Fig. A5). Interestingly, recovery of baseline transmission after Y1-R blockade under moderate cholinergic activation was not possible in neither of the cycle stages or age compared to PHY condition ($F_{(2, 64)}$=0.4185, p=0.6598, two-way ANOVA, *n*=12 (low estrus females PHY + BIBP3226); *n*=12 (low estrus females PHY);

n=15 (young high estrus females PHY + BIBP3226); *n*=16 (young high estrus females PHY); *n*=8 (aged anestrus females PHY + BIBP3226); *n*=7 (aged anestrus females PHY); Fig. 17F). The rise in MPP-dDG neurotransmission after Y1-R blockade in high estrus females only emphasized the hypothesis that NPY mediated Y1-R activation is altered along the estrus stage in the dDG of naturally cycling young female mice. Additionally, increased MPP-dDG neurotransmission mediated by Y1-R blockade in high estrus females was not mimicked under moderate cholinergic activation.

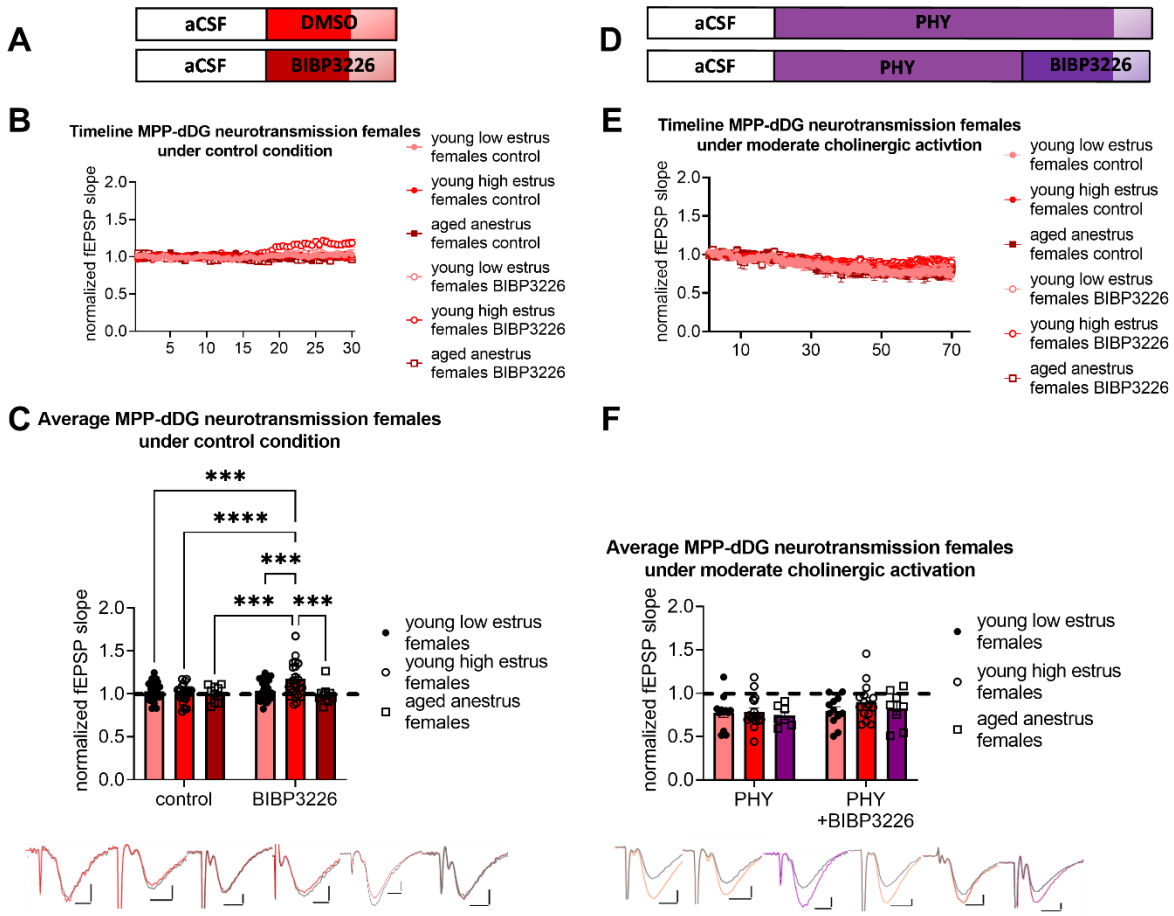

Figure 17: Blockade of Y1-R increases the MPP-dDG neurotransmission of young high estrus female mice. A: Scheme of the experimental protocol for Y1-R blockade under control conditions. The normalized data from the last 6 min, indicated by transparent sections in the columns, were used for statistical comparison shown in bar graphs. **B:** The plotted timeline of MPP-dDG neurotransmission with the average fEPSP slopes of young low estrus females under control condition (light red), young high estrus females under control (red), aged anestrus females control (dark red), Y1-young low estrus females + BIBP3226 (white with light red), young high estrus females with BIBP3226 (white with red), and aged anestrus females with BIBP (white with dark red) starts with the last 10 min baseline recordings (0-10 min) and finishes with a 20 min application of BIBP3226 or DMSO application as control (10-30 min). **C:** In young high estrus female mice, the average of the last 6 min from the MPP-dDG neurotransmission reveals a significant increase of the fEPSP slope after Y1-R blockade (red), which is not present in low estrus (light red) and aged anestrus females (dark red). Furthermore, the Y1-R blockade in young high estrus females increases the fEPSP slope significantly to all other groups. Below the graph, representative fEPSP traces are plotted. Scale bar x-axis: 2 ms each and y-axis: 0.4 mV (young low estrus control/BIBP3226 and aged anestrus females control/BIBP3226) and 0.5 mV (young high estrus control/BIBP3226): before drug application (colored) and from the last 6 min of drug application (grey). **D:** Scheme of the experimental protocol for Y1-R blockade under moderate cholinergic activation. The normalized data from the last 6 min, indicated by transparent sections in the columns, were used for statistical comparison shown in bar graphs. **E:** The plotted timeline of MPP-dDG neurotransmission with the average fEPSP slopes of young low estrus females with PHY (light red), young high estrus females with PHY (red), aged anestrus females with PHY (purple), young low estrus females with PHY + BIBP3226 (white with light red), young high estrus females with PHY+BIBP3226 (white with red), and aged anestrus females with PHY + BIBP3226 (white with purple) starts with the last 10 min baseline recordings (0-10 min) and finishes with a 60 min PHY application or 40 min PHY followed by 20 min BIBP3226 (10-70 min). **F:** The average of the last 6 min from the MPP-dDG neurotransmission reveals an unaltered fEPSP slope after Y1-R is blocked under moderate cholinergic activation in all groups (light red, red and purple). Below the graph, representative fEPSP traces are plotted: before the drug application (colored) and from the last 6 min of drug application (grey). Scale bar x-axis: 2 ms each and y-axis: 0.4 mV (young low estrus PHY + BIBP3226 and aged anestrus females PHY/PHY + BIBP3226) and 0.5 mV (young high estrus PHY/PHY + BIBP3226 and young low estrus females PHY). dDG = dorsal dentate gyrus, DMSO = dimethylsufoxide, PHY = physostigmine, and Y1-R = Neuropeptide Y 1 Receptor. Change in fEPSP slope (group comparison): ***, $p < 0.001$, ****, $p < 0.0001$

4.4.2. Application of M1-R antagonist does not abolish increased MPP-dDG neurotransmission mediated by Y1-R blockade in high estrus females

Raza and colleagues (2017) demonstrated that M1-activation drove the cholinergic-mediated increase of NPY in young male mice (Raza et al., 2017). For this reason, I tested the effect of the M1-R blocker pirenzepine (1µM) on Y1-R mediated MPP-dDG neurotransmission in high estrus females. The M1-R antagonist pirenzepine did not impact MPP-dDG neurotransmission (see appendix, Fig. A6). It also did not prevent the increase of MPP-dDG neurotransmission mediated by Y1-R blockade in young high estrus females ($t_{(24)}$=2.371, p=0.0261, unpaired t-test, two-tailed, *n*=11 (pirenzepine); *n*=15 (pirenzepine + BIBP3226); Fig. 18). These results demonstrate that increased MPP-dDG neurotransmission after Y1-R blockade in high estrus female mice is independent of M1-R activation.

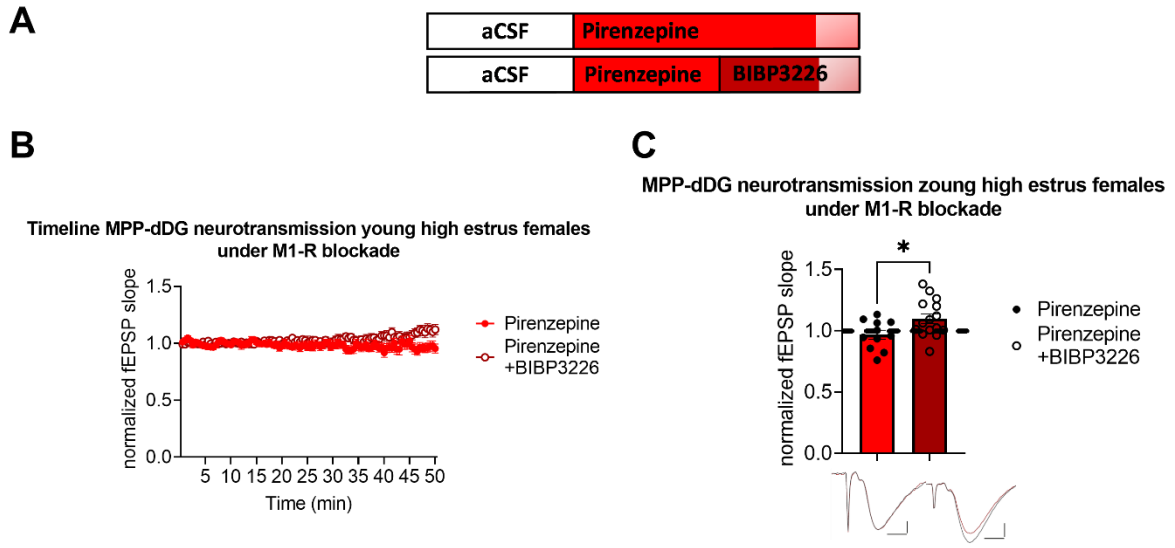

Figure 18: Increased MPP-dDG neurotransmission after Y1-R blockade is not mediated by M1-R in young high estrus females. A: Scheme of the experimental protocol for Y1-R blockade combined with M1-R blockade. The normalized data from the last 6 min, indicated by transparent sections in the columns, were used for statistical comparison shown in bar graphs. **B:** The plotted timeline of the MPP-dDG neurotransmission with the average fEPSP slopes of young high estrus females with M1-R blockade through pirenzepine (red) and with additional Y1-R blockade through BIBP3226 (white with dark red) starts with the last 10 min of baseline recordings (0-10 min) and finishes with a 40 min application of pirenzepine or an application of 20 min pirenzepine plus 20 min BIBP3226 application (10-50 min). **C:** The average of the last 6 min from the MPP-dDG neurotransmission with M1-R blockade (red) and the M1-R antagonist combined with the Y1-R blockade (dark red) plotted in the bar graph reveals an increase of the fEPSP slope after M1-R combined with Y1-R blockade. Below the graphs, representative fEPSP traces are plotted: before drug application (colored) and from the last 6 min of drug application (grey). Scale bar x-axis: 2 ms each and y-axis: 1 mV each. dDG = dorsal dentate gyrus, M1-R = Muscarinic receptor 1. And Y1-R = Neuropeptide Y 1 Receptor. fEPSP slope change (group comparison): *, $p < 0.05$

4.4.3. Application of β- estradiol and Y1-R agonist normalizes increase of MPP-dDG neurotransmission after Y1-R blockade in young high estrus female mice

The application of PHY combined with BIBP3226 failed to mediate the increase of MPP-dDG neurotransmission independent of age or cycle stage. Furthermore, Y1-R blockade mediated increase of MPP-dDG neurotransmission in young high estrus females was independent of M1-R activation. The studies mentioned above showed a direct modulation of NPY cell number, release, and mRNA in the DG by β-estradiol in ovariectomized rodents. To evaluate the effect of β-estradiol on Y1-R activation in the MPP-dDG neurotransmission of naturally cycling females, I applied β-estradiol with and without Y1-R blockade in young high and low estrus females. Exogenous estrogen application must be higher than the internal concentration (around 0.7 (diestrus) to 4.3 nM (proestrus) in the female brain (Hojo & Kawato, 2018) to affect synaptic transmission or plasticity, whereby the estrogen concentration decreases tremendously in slices (0.5 nM), and 1-10 nM exogenous β-estradiol should have

effects (Ooishi et al., 2012). Thus, a concentration of 10 nM was used. β-estradiol neither affects MPP-dDG neurotransmission in high estrus females nor low estrus females (see appendix, Fig. A7). However, 10 nM β-estradiol in high estrus females abolished the increased MPP-dDG neurotransmission mediated by Y1-R blockade under control conditions (1 µM) and did not affect the MPP-dDG neurotransmission in young low estrus females ($F_{(1, 30)}$=0.0005377, p=0.9817, two-way ANOVA, test, *n*=8 (young high estrus females with β-estradiol), *n*=10 (young high estrus females with β-estradiol + BIBP3226), *n*=8 (young low estrus females with β-estradiol), *n*=8 (young low estrus females with β-estradiol + BIBP3226); Fig. 19C). These experiments demonstrate that the modulation of Y1-R activation by estradiol is only possible in young high estrus stage females. The abolished increase after Y1-R blockade in young high estrus females might be mediated by increasing NPY-mediated Y1-R activation. This was tested in the next experiment, using the selective Y1-R agonist [Leu^{31}, Pro^{34}]-NPY (0.4 µM) in combination with Y1-R blockade through BIBP3226 (1 µM). The Y1-R agonist did not significantly change MPP-dDG neurotransmission in young high estrus females (see appendix, Fig. A8). Strikingly, the combination of Y1-R agonist and antagonist abolished the significant increase of MPP-dDG neurotransmission mediated by Y1-R blockade in young high estrus females ($t_{(12)}$=0.2689, p=0.7926, unpaired t-test, two-tailed, *n*=7 (Y1-R agonist), *n*=7 (Y1-R agonist + Y1-R antagonist); Fig. 19F).

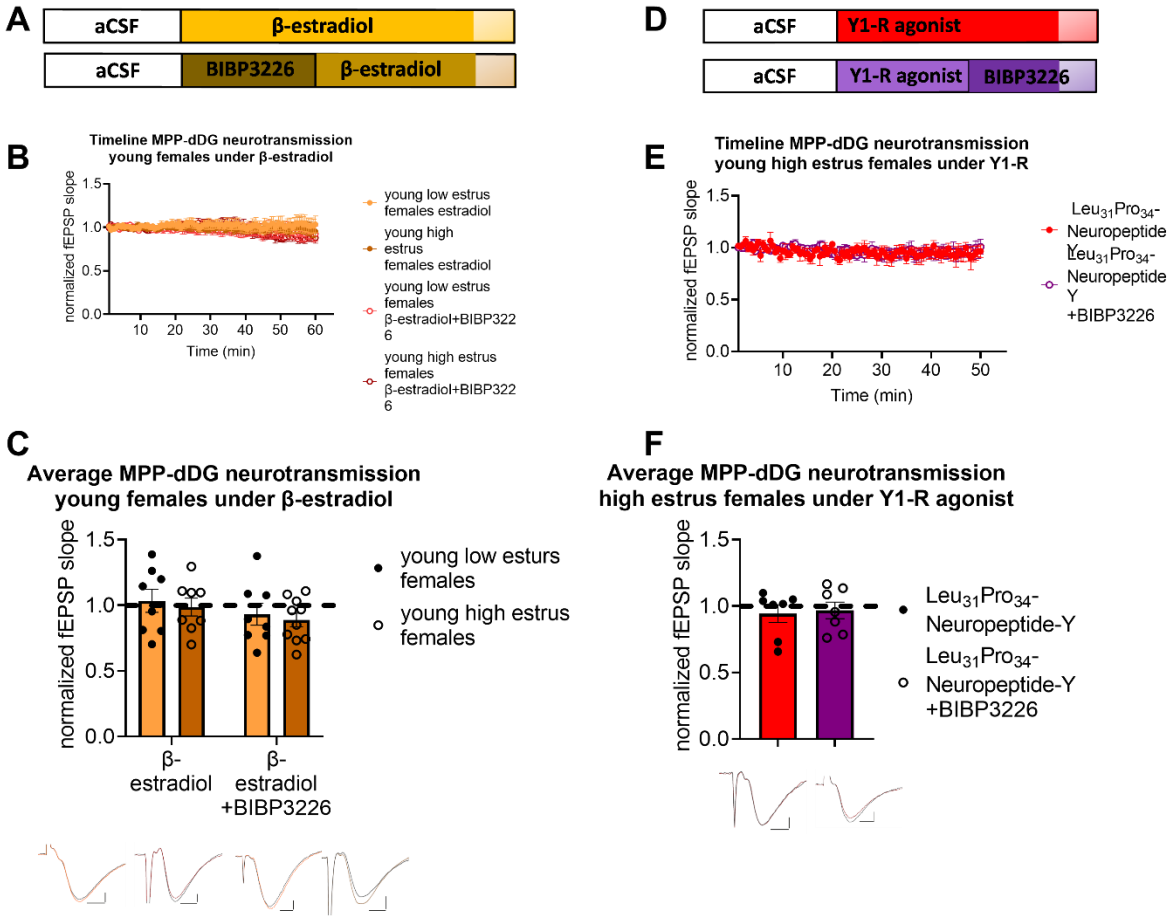

Figure 19: Increased MPP-dDG neurotransmission after Y1-R blockade is normalized through β-estradiol and Y1-R agonist application in young high estrus females. A: Scheme of the experimental protocol for Y1-R blockade under β-estradiol. The normalized data from the last 6 min, indicated by transparent sections in the columns, were used for statistical comparison shown in bar graphs. **B:** The plotted timeline of the MPP-dDG neurotransmission with the average fEPSP slope of young low estrus females with β-estradiol (orange), young high estrus females with β-estradiol (brown), young low estrus with β-estradiol + BIBP3226 (white with orange), and young high estrus females with β-estradiol + BIBP3226 (white with brown) starts with the last 10 min of baseline recordings (0-10 min) and finishes with a 50 min β-estradiol application or an application of a 20 min BIBP3226 plus 30 min β-estradiol (10-60 min). **C:** The average of the last 6 min from the MPP-dDG neurotransmission with β-estradiol and β-estradiol combined with the Y1-R blockade plotted in the bar graph reveals an unchanged fEPSP slope after β-estradiol with Y1-R blockade. Below the graphs, representative fEPSP traces are plotted. Scale bar x-axis: 2 ms each and y-axis: 1 mV each: before drug application (colored) and from the last 6 min of drug application (grey). **D:** Scheme of the experimental protocol for Y1-R blockade under exogenous Y1-R activation. In white, the baseline recording (20 min), colored the drug application (40 min), and transparent the time used (6 min) for the averaged fEPSP slope. **E:** The plotted timeline of the MPP-dDG neurotransmission with the average FEPSP slope of young high estrus females with the Y1-R agonist (red) and young high estrus females with the Y1-R agonist combined with Y1-R blockade (white with purple) starts with the last 10 min of baseline recordings (0-10 min) and finishes with a 40 min Y1-R agonist application or 20 min Y1-R agonist plus 20 min BIBP3226 application (10-50 min). **F:** The average of the last 6 min from the MPP-dDG neurotransmission with the Y1-R agonist and Y1-R agonist combined with the Y1-R blockade plotted in the bar graph reveals an unchanged fEPSP slope after the combined treatment. Below the graphs, representative fEPSP traces are plotted: before drug application (colored) and from the last 6 min of drug application (grey). Scale bar x-axis: 2 ms each and y-axis 1 mV each. dDG = dorsal dentate gyrus, Y1-R = Neuropeptide Y 1 Receptor.

4.5. Ovariectomy plus phyto-free food induces changes resembling MPP-dDG LTP in aged female mice

One of the main changes in human females during aging is entering menopause. The standard mouse model of menopause is OVX of young adult female mice. OVX female mice are used to mimic treatment after menopause (Høegh-Andersen et al., 2004) and to investigate the effect of sex-steroid therapies (e.g., Corvino et al., 2015; Koebele & Bimonte-Nelson, 2016; Ledoux et al., 2009; Velíšková et al., 2015; Velíšková & Velíšek, 2007). Regarding the enormous impact of menopause on human females during aging, I tested the OVX mouse model in relation to the changes observed in aged anestrus females. MPP-dDG LTP in females depended on ER activation through de novo synthesized estrogen in the CA1 (Vierk et al., 2012). The standard food in our animal facility contains phytoestrogens, and most phytoestrogens are metabolized to equol, which activates ERs, especially ER-β for S-equol and ER-α for R-equol (Muthyala et al., 2004). For this reason, I investigated two groups: one group of OVX females with standard food and one group of OVX females after six weeks of phytoestrogen-free (phyto-free) food, as before.

In aged anestrus female mice, MPP-dDG LTP could be induced in a Y1-R-dependent manner. To examine if the alteration of estrogen levels is the underlying reason, MPP-dDG LTP in young OVX female mice was investigated. The results revealed that OVX had no impact on MPP-dDG LTP in young females, as demonstrated by increased fEPSP slope after TBS under control conditions ($t_{(7)}$=2.770, p=0.0139, paired t-test, one-tailed, *n*=8; Fig. 20C) as well as with Y1-R blockade (BIBP3226 1 µM) ($t_{(7)}$=3.968, p=0.0027, paired t-test, one-tailed, *n*=8; Fig. 20C). Strikingly, the combination of phyto-free food and OVX (depleting all estrogen sources) led to a Y1-R dependence of MPP-dDG LTP in young OVX females (control: $t_{(7)}$=2.209, p=0.0315, paired t-test, one-tailed, *n*=8; BIBP3226: $t_{(7)}$=1.116, p=0.1507, paired t-test, one-tailed, *n*=8; Fig. 20C). MPP-dDG LTP strength did not differ between the groups ($F_{(1, 28)}$=1.868 p=0.1826, two-way ANOVA; Fig. 20C). Furthermore, the effect of PHY in OVX mice was tested to evaluate a possibly beneficial effect on MPP-dDG LTP in OVX phyto free female mice. MPP-dDG LTP was induced in a Y1-R independent manner in OVX female mice under moderate cholinergic activation (PHY 2 µM) ($t_{(7)}$=2.487, p=0.0209, paired t-test, one-tailed, *n*=8; Fig. 20F), shown by the existing MPP-dDG LTP under additional Y1-R blockade ($t_{(8)}$=4.536, p=0.0010, paired t-test, one-tailed, *n*=9; Fig. 20F). Indeed, in OVX phyto-free mice a Y1-R independent MPP-dDG LTP was achieved under moderate cholinergic activation (PHY: $t_{(7)}$=5.504, p=0.0005, paired t-test, one-tailed, *n*=8; BIBP3226: $t_{(7)}$=5.059, p=0.0007, paired t-test, one-tailed, *n*=8; Fig. 20F). As under control conditions MPP-dDG LTP strength

did also not differ between the groups ($F_{(1, 29)}$=0.2468, p=0.6231, two-way ANOVA; Fig. 20F). These experiments suggest that under moderate cholinergic activation, MPP-dDG LTP is also independent of NPY mediated Y1-R activation after total estrogen depletion. Notably, Y1-R blockade under control conditions and moderate cholinergic activation had no impact on MPP-dDG neurotransmission in young OVX female mice or OVX young female mice on phyto-free food (see appendix, Fig. A9). This experiment indicated that some electrophysiological MPP-dDG properties might be maintained through exogenous estrogen-like sources.

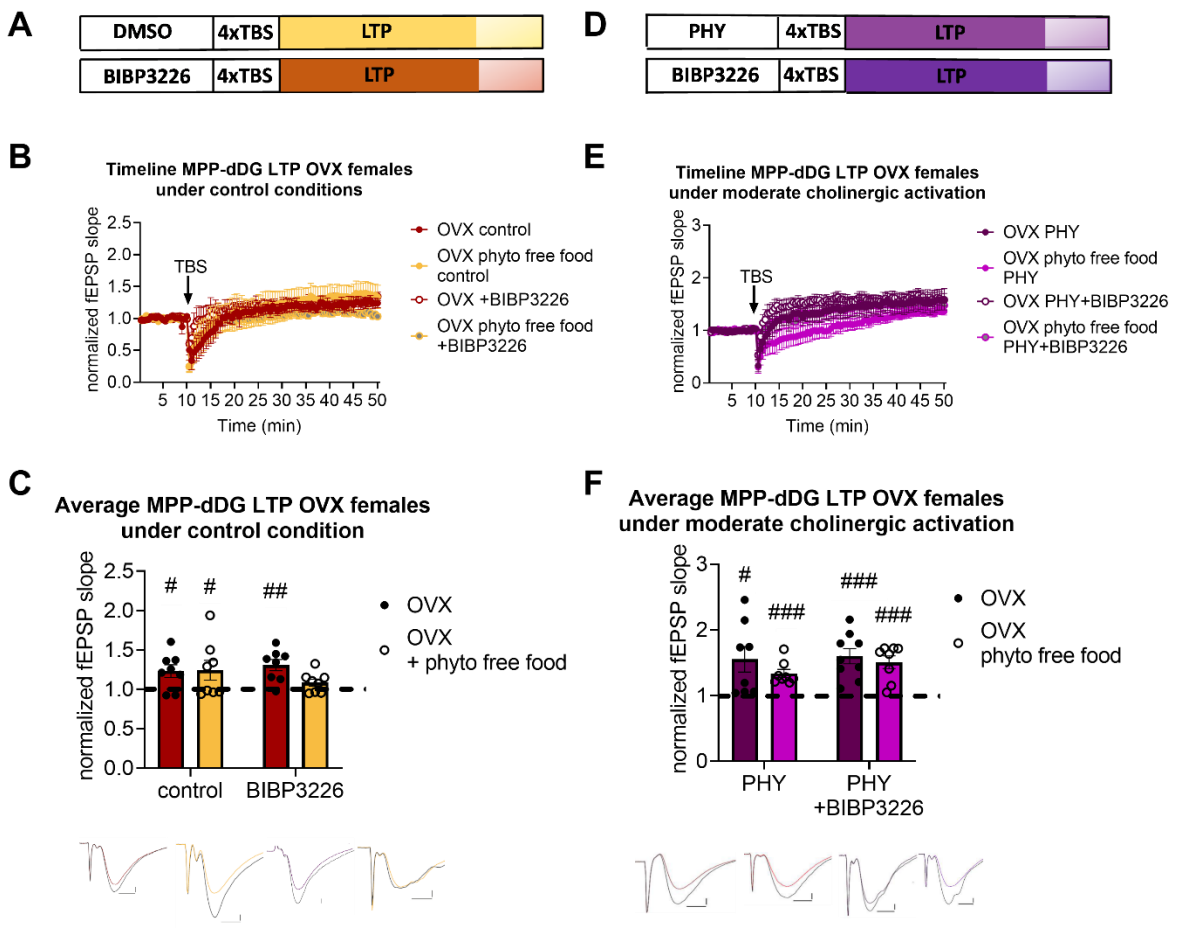

Figure 20: Complete depletion of estrogen source, not OVX alone, leads to Y1-R dependent MPP-dDG LTP, which is rescued by moderate cholinergic activation. A: Scheme of the experimental protocol for Y1-R blockade under control conditions. The normalized data from the last 10 min, indicated by transparent sections in the columns, were used for statistical comparison shown in bar graphs. **B:** The plotted timeline of MPP-dDG LTP with the average fEPSP slope of OVX female mice control (brown), OVX females on phyto-free food control (yellow), OVX females +BIBP3226 (white with brown), and OVX females on phyto-free food + BIBP3226 (grey with yellow) starts with the last 10 min of DMSO or selectively Y1-R blockade recording (0-10 min), followed by 4x TBS induction at 10 min, and finishes with 40 min of LTP recording (10-50 min). **C:** The average of the last 10 min from the MPP-dDG LTP recordings in the bar graph reveals successful MPP-dDG LTP in a Y1-R independent manner in OVX young female mice (brown). OVX young female mice on phyto-free food demonstrate a Y1-R dependent MPP-dDG LTP (yellow). Nevertheless, the strength of the signal after TBS does not differ between the groups. Below the graphs, representative fEPSP traces are plotted: before TBS (colored) and from the last 10 min of MPP-dDG LTP recording (grey). Scale bar x-axis: 2 ms each and y-axis: 1 mV each. **D:** Scheme of the experimental protocol for Y1-R blockade under moderate cholinergic activation. The normalized data from the last 10 min, indicated by transparent sections in the columns, were used for statistical comparison shown in bar graphs. **E:** The plotted timeline of MPP-dDG LTP with the average fEPSP slope of OVX female mice with PHY (dark purple), OVX females on phyto-free food with PHY (pink), OVX females with PHY + BIBP3226 (white with dark purple), and OVX females on phyto-free food with PHY + BIBP3226 (grey with pink) starts with the last 10 min of moderate cholinergic activation or moderate cholinergic activation with selectively Y1-R blockade (0-10 min), followed by 4x TBS induction at 10 min, and finishes with 40 min of LTP recording (10-50 min). **F:** The average of the last 10 min from the MPP-dDG LTP recordings in the bar graph reveals successful MPP-dDG LTP under both conditions in OVX and OVX young females on phyto-free food. Nevertheless, the strength of the signal after TBS does not differ between the groups. Below the graphs, representative fEPSP traces are plotted: before TBS (colored) and from the last 10 min of MPP-dDG LTP recording (grey). Scale bar x-axis: 2 ms each and y-axis: 1 mV each. dDG = dorsal dentate gyrus, LTP = Long-term potentiation, OVX = ovariectomy, TBS =theta-burst stimulation, and Y1-R = Neuropeptide Y 1 Receptor. LTP induction (in group comparison): #, $p < 0.05$, ##, $p < 0.01$, ###, $p < 0.001$

4.6. NPY concentration shows a sex- and age-dependent decrease

The electrophysiological recordings in this thesis and the literature pointed to an altered NPYergic system during aging. Therefore, to investigate age-mediated changes in NPY concentration and Y1-R expression, I collaborated with Miguel M. del Angel, MSc. He performed WB analysis and ELISA on the dDG tissue of young and aged male and female mice in a cycle stage-dependent manner. The ELISA data demonstrated that the NPY concentration in the dDG was lower in females than in males, as already shown (Nahvi and Sabban, 2020). This sex difference persisted through aging and was cycle stage independent ($F_{(4,24)}$=0.8873, p<0.0001, ordinary one-way ANOVA; post-hoc comparison young low estrus females vs. young males: p<0.0001, ordinary one-way ANOVA Fisher's LSD test; post-hoc comparison young high estrus females vs. young males: p<0.0001, ordinary one-way ANOVA Fisher's LSD test; post-hoc comparison aged anestrus females vs. young males: p<0.0001, ordinary one-way ANOVA Fisher's LSD test; post-hoc comparison young low estrus females vs. aged males: p=0.001, ordinary one-way ANOVA Fishers' LSD test; post-hoc comparison young high estrus females vs. aged males: p=0.006, ordinary one-way ANOVA Fishers' LSD test; post-hoc comparison aged anestrus females vs. aged males: p=0.001, ordinary one-way

ANOVA Fishers' LSD test; *n*=5 (young males), *n*=5 (aged males); *n*=6 (females low estrus); *n*=8 (females high estrus); *n*=5 (anestrus females); Fig. 21A). Strikingly, aged male mice showed reduced NPY levels in comparison to young male mice (post-hoc comparison p=0.0386, ordinary one-way ANOVA Fisher's LSD test, *n*=5 (young males); *n*=5 (aged males); Fig. 21A), while NPY concentration in females remained unchanged during aging (post-hoc comparison young low estrus vs. aged anestrus females: p=0.9612, ordinary one-way ANOVA Fishers' LSD test, *n*=6 (aged anestrus females); post-hoc comparison young high estrus vs. aged anestrus females: p=0.3971, ordinary one-way ANOVA Fishers' LSD test, *n*=6 (aged anestrus females); *n*=7 (young high estrus females); Fig. 21A) and between the analyzed estrus stages (post-hoc comparison young low vs. high estrus females : p=0.454, ordinary one-way ANOVA Fishers' LSD test, *n*=6 (young low estrus females); *n*=7 (young high estrus females); Fig. 21A). No age-dependent changes in Y1-R expression were evident ($F_{(4,25)}$=0.6889, p=0.6535, ordinary one-way ANOVA, *n*=5 (young males); *n*=5 (aged males); *n*=6 (females low estrus); *n*=8 (females high estrus); *n*=5 (anestrus females); Fig. 21B) in the dDG. To summarize, only male mice showed reduced NPY levels in the dDG during aging.

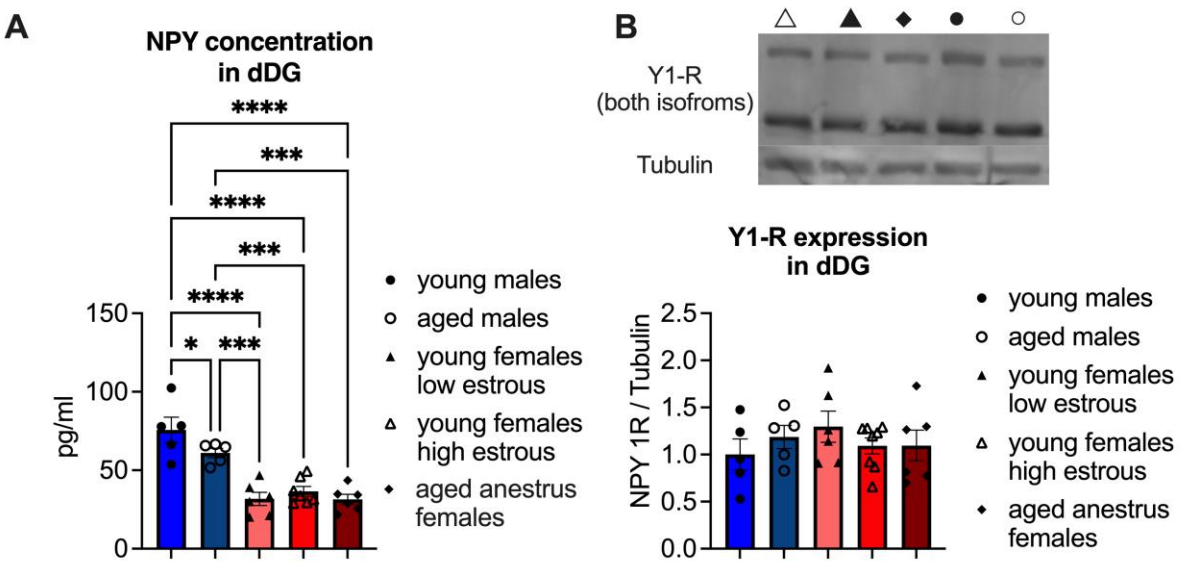

Figure 21: Aged male mice showed reduced NPY concentration in the dDG. A: NPY concentration from dDG measured by ELISA in pg/ml showed an apparent sex effect in NPY expression. Female mice expressed low but stable NPY expression through age and cycle. In contrast, young males showed higher NPY expression that decreased during aging. **B:** Y1-R expression measured by WB and normalized to tubulin stayed stable between sexes over lifetime and cycle stage. A representative WB membrane with one example of each sex, age, and cycle stage is presented. The symbols above the WB picture correspond to the legend of the bar graph. dDG = dorsal dentate gyrus, NPY = Neuropeptide Y, WB = western blot, and Y1-R = Neuropeptide Y receptor type 1. Changes in NPY concentration (group comparison): *, $p < 0.05$, ***, $p < 0.001$, ****, $p < 0.0001$

4.7. ERK1/2 phosphorylation increases during aging in a sex-dependent manner

ERK1/2, GluA1/GluR1 subunit of AMPA-R, and NR2B subunit of NMDA-R are crucial for LTP induction (Citri & Malenka, 2008; Coogan et al., 1996; Diering & Huganir, 2018; English & David Sweatt, 1997; Rosenblum et al., 1996; Thomas & Huganir, 2004). Moreover, age-dependent changes have been controversially shown for NR2B with either up- or down-regulation during aging (Clayton et al., 2002; Newton et al., 2008). In collaboration with Miguel M. del Angel, M.Sc., the phosphorylation at p42 and p44 for ERK1/2, Ser845 for GluA1, and Tyr1472 (main phosphorylation side of NR2B) (Chen & Roche, 2007) for NR2B were investigated by WB analysis in a sex and age-dependent manner. The cycle stage was left out in this experiment since NPY concentration did not reveal cycle-dependent changes. Preliminary data of GluR1 ($F_{(1, 8)}$=0.6933, p=0.4292, two-way ANOVA; *N*=3 (young males); *N*=3 (aged males); *N*=3 (young females); *N*=3 (aged females); Fig. 23A) and GluR1 phosphorylated at Ser845 ($F_{(1, 8)}$=2.437, p=0.1571, two-way ANOVA; *N*=3 (young males); *N*=3 (aged males); *N*=3 (young females); *N*=3 (aged females); Fig. 22A) revealed an unchanged expression independent of sex and age. In addition, the ratio for pGluR1/GluR1 was stable ($F_{(1, 8)}$=0.1042, p=0.7552, two-way ANOVA; *N*=3 (young males); *N*=3 (aged males); *N*=3 (young females); *N*=3 (aged females); Fig. 22A). Furthermore, phosphorylation of NR2B at Tyr1472 was unchanged over sex and age ($F_{(1, 20)}$=3.296, p=0.0845, two-way ANOVA; *N*=6 (young males); *N*=6 (aged males); *n*=6 (young females); *N*=6 (aged females); Fig. 22C). Neither NR2B ($F_{(1, 20)}$=0.03212, p=0.8596, two-way ANOVA; *N*=6 (young males); *n*=6 (aged males); *N*=6 (young females); *N*=6 (aged females); Fig. 22C) nor the ratio of pNR2B/NR2B was altered during aging or between sexes ($F_{(1, 20)}$=1.595, p=0.221, two-way ANOVA; *N*=6 (young males); *N*=6 (aged males); *N*=6 (young females); *N*=6 (aged females); Fig. 22C). Remarkably, the phosphorylation of ERK1/2 in the dDG revealed a sex- and age-dependent alteration ($F_{(1, 20)}$=7.590, p=0.0122, two-way ANOVA; Fig. 22B). ERK1/2 phosphorylation was increased in aged males compared to young males (post-hoc comparison: p=0.0147, two-way ANOVA Fisher's LSD test; *N*=6 (young males); *N*=6 (aged males); Fig. 22B). Furthermore, an age-dependent sex-difference was evident in ERK1/2 phosphorylation as pERK1/2 was lower in aged anestrus females compared to aged males (post-hoc comparison: p=0.0262, two-way ANOVA Fisher's LSD test; *N*=6 (aged males); *N*=6 (aged females); Fig. 22B), while ERK1/2 activation was stable between young and aged anestrus females (post-hoc comparison: p=0.2349, two-way ANOVA Fisher's LSD test; *N*=6 (young females); *N*=6 (aged females);

Fig. 22B). The ratio of pERK1/2 revealed a clear sex-differences independent of age and an age effect in male mice ($F_{(1, 20)}$=9.247, p=0.0065, two-way ANOVA; Fig. 22B). pERK1/2 ratio was significantly increased in aged males compared to young male mice (post-hoc comparison p=0.0183, two-way ANOVA Fisher's LSD test; *N*=6 (young males); *N*=6 (aged males); Fig. 22B) and to aged female mice (post-hoc comparison: p=0.0499, two-way ANOVA Fisher's LSD test; *N*=6 (aged males); *N*=6 (aged females); Fig. 22B). Moreover, pERK1/2 ratio is significantly higher in young females than in young males (post-hoc comparison: p=0.0386, two-way ANOVA Fisher's LSD test; *N*=6 (young males); *N*=6 (young females); Fig. 22C) while the ratio between young and aged females in unchanged (post-hoc comparison: p=0.0987, two-way ANOVA Fisher's LSD test; *N*=6 (young females); *N*=6 (aged females); Fig. 22B). Total ERK1/2 levels remaind unchanged ($F_{(1, 20)}$=0.007929, p=0.9299, two-way ANOVA; *N*=6 (young males); *N*=6 (aged males); *N*=6 (young females); *N*=6 (aged females); Fig. 22B). This study demonstrated an increased ERK1/2 phosphorylation in the dDG of aged males but not females compared to their young counterparts. Moreover, a sex difference in the pERK ratio could be detected, which persists in the opposite direction during aging.

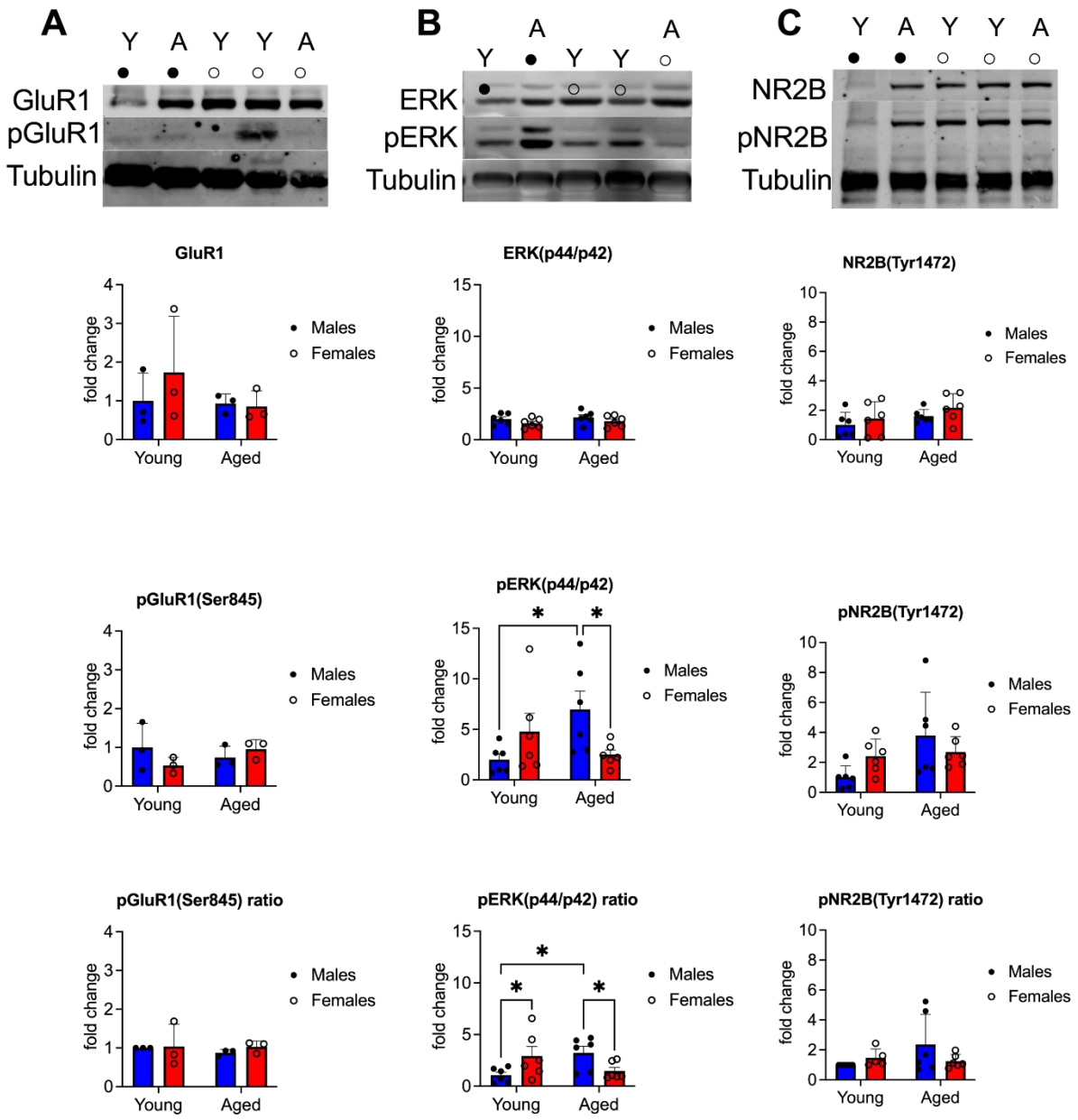

Figure 22: Aging caused increased ERK1/2 phosphorylation in male but not female mice. A: Protein expression of GluR1 and pGluR1(Ser845) measured by WB analysis in the dDG was unchanged for all groups. The calculated ratio reveals no change between the groups. **B:** Protein expression of ERK1/2 and pERK1/2(Thyr202/Thyr204) measured by WB analysis in the dDG of young and aged mice from both sexes reveals an age-dependent increase in male mice and a sex difference in pERK1/2(Thyr202/Thyr204) and pERK1/2(Thyr202/Thyr204) ratio. **C:** Protein expression of NR2B and pNR2B(Tyr1472) measured by WB analysis in the dDG demonstrated no difference between the groups. Moreover, the calculated ratio reveals no change either. Above the graphs, a representative picture of the protein expressions is plotted from one animal for each condition from young and aged mice of both sexes. The symbols correspond to legend in the bar graphs, while Y and A indicate young or aged, respectively. Group comparison: *, $p < 0.05$

5. Discussion

The dentate gyrus is the gate-keeper of the hippocampus, an area highly vulnerable to aging-related processes, and is of particular interest to investigate for age-related changes. The DG is a highly controlled area that reduces the neocortex's multi-informational signals in sparse information for the CA3 (Leutgeb et al., 2007; Treves & Rolls, 1994). Its physiological properties, especially excitability, transmission, and plasticity, provide relevant information on the cellular underpinnings of memory since synaptic plasticity has been extensively proven to be the cellular correlate of memory (Bliss & Collingridge, 1993). Any change in the excitability or plasticity of the dDG would have tremendous effects on proper episodic and spatial memory encoding, consolidation, or recall. Understanding aging-related changes in synaptic plasticity are assumed to be instrumental in identifying ways of supporting cognitive decline.

In this study, by inducing LTP at the MPP-dDG synapse in slice preparations under intact inhibition in both sexes (Fig. 11; 15), I investigated the local circuits mechanism of the dDG involved in the maintenance of plasticity during aging. I was able to demonstrate that cholinergic recovery of MPP-dDG LTP in aged male mice is dependent on the activation of Y1-R (Fig. 13) and that application of exogenous NPY can recover this form of plasticity (Fig. 14). Aged females in contrast to males, maintained MPP-dDG LTP even without cholinergic stimulation. Nevertheless, MPP-dDG LTP in aged anestrus female mice became dependent on Y1-R transmission (Fig. 15) – which was overcome by cholinergic stimulation (Fig. 16). These sex-specific alterations in plasticity were accompanied by alterations in neuronal excitability (Fig. 11; 15) as well as endogenous dDG NPY concentration (Fig. 21) and ERK1/2 phosphorylation (Fig. 22). These data demonstrate the sex-specific alteration of plasticity mechanisms in the dDG during aging and the critical involvement of local NPYergic transmission in the maintenance of plasticity. Moreover, my data demonstrated the potential of a nutritional estrogen replacement strategy to treat MPP-dDG LTP impairment in anestrus females (Fig. 20).

5.1. TBS induces MPP-dDG LTP under intact inhibition in young mice

An important technical aspect of this study is the successful LTP induction in the MPP-dDG synapse of both sexes under intact inhibition *in vitro* (Fig. 11; 15). The *(in vitro*) rarely used theta-burst stimulation achieved this by combining ortho- and antidromic stimulation. The protocol was established by Lopez-Roja (Lopez-Rojas et al., 2016) and, with this study, for the first time in our laboratory. The challenge was to establish suitable order and strength of ortho-

and antidromic stimulation in the dDG under intact inhibition (see appendix Fig. A1). With the established TBS protocol, this study showed successful MPP-dDG LTP induction in young male and female mice with 4x TBS, which was marked by an increase of at least 10% in the fEPSP slope (Fig. 11).

Historically, LTP induction *in vitro* has usually been performed using high-frequency stimulation under diminished inhibitory tonus in the MPP to dDG synapses (e.g., Hanse & Gustafsson, 1992; M. Zhang et al., 2021). However, LTP recordings under intact inhibition have also been performed in the DG *in vitro* (Arima-Yoshida et al., 2011; Corvino et al., 2014; Diana et al., 1994; Froc et al., 2003; Schreurs et al., 2017; Schurmans et al., 1997; Sha et al., 2016; Yun & Trommer, 2011; Chen et al., 2000; Wang et al., 2015). In the mentioned studies, the LTP induction at the PP-DG synapse has been shown to be successful, except for the analysis performed by Arima-Yoshida and colleagues (Arima-Yoshida et al., 2011). It is worth noting that Schreurs and colleagues (2017) mention specifically that LTP recording is performed at the MPP synapse in the dDG while investigating plasticity along the dorsoventral axis by performing multi-array recordings (MEA) in young and middle-aged male mice. The work demonstrates a more prominent LTP in the ventral pole than the dorsal, which decays during aging. Nevertheless, MPP-dDG LTP induction and maintenance has been demonstrated to persist also in middle-aged male mice (Schreurs et al., 2017). The other studies mentioned above do not specify if PP-DG LTP is recorded from the dorsal or ventral pole. Moreover, Chen and colleagues (2000), Wang and colleagues (2015), Yuan and Trommer (2011), Schreurs and colleagues (2017), as well as Arima-Yoshida and colleagues (2011) used young male rodents (Arima-Yoshida et al., 2011; Chen et al., 2000; Schreurs et al., 2017; Wang et al., 2016; Yun & Trommer, 2011). Corvino and colleagues (2014) reported from young female rats (Corvino et al., 2014); the other studies used young or aged rodents without reporting the sex or pooling the data from both sexes. Furthermore, LTP threshold differences between sexes have been shown by PP-DG LTP recordings from anesthetized rats (Maren, 1995; Maren et al., 1994), but this did not occur with 4x TBS. In these studies, HFS stimulation is used to induce PP-DG LTP. It thus appears that the 4x TBS protocol is strong enough to overcome sex differences in LTP induction in the dentate gyrus since MPP-dDG LTP can therefore be, in general, induced under intact GABAergic inhibition.

5.2. Deficit of MPP-dDG LTP without $GABA_A$ receptor blockade in aged male mice

Using the established TBS protocol, I was able to show that MPP-dDG LTP under intact inhibitory tonus *in vitro* is abolished in aged male mice (Fig. 11D). At the same time, increased baseline excitability could be observed during aging (Fig. 11A). By contrast, the pre-synaptic response was not altered compared to young males (Fig. 11B). These results are in line with several *in vivo studies*, showing that LTP induction, maintenance, and decay are impaired in the PP-DG synapse of aged male rodents (Barnes, 1979; Barnes & McNaughton, 1980, 1986; Geinisman et al., 1992; Geinisman et al., 1995). Rarely has this been shown *in vitro* for LTP induction under intact inhibition. Thus, Diana and colleagues (1994) successfully induced and maintained LTP (measured by the population spike) with 100Hz tetanus stimulation in the DG of aged rats from both sexes (Diana et al., 1994). On the other hand, impaired MPP-dDG LTP maintenance at the ventral pole induced with 4x HFS has been shown for middle-aged males *in vitro* (Schreurs et al., 2017). Furthermore, in aged mice (sex not mentioned), LTP can be rendered at the LPP-dDG synapse but not maintained under intact inhibitory tonus (Froc et al., 2003). A possible explanation for the abolished MPP-dDG LTP in aged male mice is a disturbance of the E-I balance (signal-to-noise-ratio), probably mediated by an increase of GC excitability resulting from interneuron loss in the dDG (Stanley & Shetty, 2004). Indeed, it has been shown that E-I balance is essential for spatial performance, signal-to-noise ratio, information capacity, and sparse GC activation in the DG (Coulter & Carlson, 2007; Marder & Buonomano, 2004; Shew et al., 2011).

Rubenstein and Merzenich described 2003 E-I as a possible cause for some forms of autism, which Sohal and Rubenstein further updated and proposed for other neuropsychiatric pathologies (Rubenstein & Merzenich, 2003; Sohal & Rubenstein, 2019). In aged rats, increased E-I balance after LPP stimulation correlates with reduced cognitive performance (Tran et al., 2019). In line, aged rat GCs displayed a higher population spike to a given PP stimulus and showed a reduced voltage threshold (Barnes & Mcnaughton, 1980). The increased post-synaptic excitability demonstrated in my study is in line with the mentioned observation and indicates reduced inhibitory tonus in the aged dDG. Enhanced post-synaptic inhibitory strength has previously also been found in cognitively unimpaired-aged rats (Tran et al., 2018). The unchanged pre-synaptic response in my study indicates that observed MPP-dDG LTP deficits resulted from local changes in the dDG during aging rather than alterations of baseline excitability or a non-functional input from the EC. The latter has been proposed in an entorhinal

lesion study (Scheff et al., 2006) in a survey of structural connectivity in elder humans (Scheff et al., 2006), and by a reduced number of PP synapses in the mid-ML (Detoledo-Morrell et al., 1988; Geinisman et al., 1992). The pre-synaptic response is measured in the FV, representing action potentials from the pre-synapse arising at the fEPSPs from the EC to the GCs (Sweatt, 2008). An unaltered FV in aged tissue may indicate that remaining MPP synapses are more efficient, which is underlined by former studies (reviewed in Geinisman et al., 1995). Besides the impact of the EC, a higher induction threshold (reviewed in Barnes et al., 2000; Geinisman et al., 1995) cannot be completely excluded as a possible reason for the abolished MPP-dDG LTP in aged male mice but is unlikely as a stimulation intensity was chosen that was well above threshold in control conditions.

In summary, the literature and my data strengthen a disrupted E-I balance as the possible reason for the abolished MPP-dDG LTP in aged male mice. A likely explanation for the increased E-I balance is the reduction of inhibitory interneurons. A possible candidate is NPYergic-containing HIPP cells since non-fast spiking interneurons (such as HIPP cells) are strongly recruited after strong PP activation to maintain the quiescence of GC (Liu et al., 2014). Furthermore, hilar interneurons containing NPY and NPYergic mRNA levels have been shown to decline during aging in males (Gavilán et al., 2007; Matsuoka et al., 1995; Vela et al., 2003). NPY is known to reduce glutamatergic transmission and the release of Ca^{2+} in GCs, leading to an inhibition (Sperk et al., 2007a), so a reduction of NPYergic cells and NPY release can be expected to lead to higher excitability. In fact, increased Ca^{2+} influx has been shown for the CA1 region and increased glutamate release for the DG in aged rodents (El-Hayek et al., 2013; Saransaari, 1995; Stephens et al., 2011). In contrast to this hypothesis, antagonizing the Y1-R had no impact on MPP-dDG LTP independent of age in the current study, leaving MPP-dDG LTP unaltered in young male mice and not affecting its abolition in the aged. Therefore, additional factors need to be considered. The cholinergic system is the major neuromodulatory system declining during aging, with a tremendous effect on plasticity. A decline of the projections from the MS to the DG has been described during aging (Ballinger et al., 2016; Lukoyanov et al., 1999; Schliebs & Arendt, 2011). In fact, cholinergic lesions are used to model aging-related changes in the hippocampus (Berger-Sweeney et al., 2001; Kesner et al., 1986; Nicolle et al., 1997), and acetylcholine esterase inhibitors are commonly used as a pharmacological treatment in AD (Yiannopoulou & Papageorgiou, 2020). Cholinergic projections from the MS targeting also inhibitory interneurons, including NPY-containing HIPP cells. These cells are especially vulnerable to a cholinergic decline (Matsuoka et al., 1995) and are involved in Y1-R activation through ACh during contextual fear learning (Raza

et al., 2017). On the other hand, the cholinergic decline could lead to a reduction of GC excitability since ACh mildly excites GC, reduces the spike threshold, and increases the propensity of action potential generation (Martinello et al., 2015; Prince et al., 2016; Raza et al., 2017). Nevertheless, a loss of excitability is in contrast to the increased post-synaptic excitability.

Therefore, two open questions were addressed in the following step: 1) Does moderate cholinergic activation induce Y1-R activation in aged male mice, as in young male mice? and 2) Does Y1-R inactivation impact MPP-dDG LTP under moderate cholinergic activation?

5.3. Increasing NPYergic MPP-dDG neurotransmission recovers deficit in MPP-dDG LTP in aged male mice

Y1-R blockade alone did not affect MPP-dDG neurotransmission or plasticity either in young or aged mice (Fig. 12C). However, it reversed the effect of moderate cholinergic activation (with PHY), which decreased MPP-dDG neurotransmission in the young (Fig. A2; 12F). Also, the recovery of MPP-dDG plasticity under moderate cholinergic activation could be blocked through the additional application of the Y1-R antagonist in aged but not young male mice (Fig. 13). Furthermore, NPYergic activity was not only necessary for the cholinergic stimulation of plasticity but sufficient to recover MPP-dDG LTP independently of it, as demonstrated by exogenous application of NPY in the perfusion solution (Fig. 14).

Previously we described with a pharmacological and chemogenetic approach that Y1-R stimulation in the dDG can be induced via cholinergic stimulation of HIPP cells (Raza et al., 2017). The current study proved in young male mice that moderate cholinergic activation (through PHY) mediates Y1-R activation (Fig. 12C/F). Similar to young males, aged mice depicted unchanged MPP-dDG neurotransmission after Y1-R blockade (Fig. 12C). In contrast to the young mice, reduced MPP-dDG neurotransmission upon moderate cholinergic activation was not reversed by Y1-R activation in the aged (Fig. 12F). The decrease of the fEPSP slope at the MPP-DG synapse through PHY has been previously shown to be mediated by the depression of glutamate release in young male rodents and proposed the involvement of endocannabinoids, specifically the endocannabinoid receptor 1 (Colgin et al., 2003). In this light, the reduced MPP-dDG neurotransmission in aged male mice can be interpreted as 1) an inability to mediate the effective difference in Y1-R activation due to a reduced NPYergic contribution mediated by a reduced NPY concentration (Fig. 21) and the loss of NPY containing interneurons in the dDG of aged males (Cadiacio et al., 2003; Hattiangady et al.,

2005; Stanley & Shetty, 2004) or 2) the involvement of endocannabinoids and not NPY-mediated Y1-R blockade, which is unlikely since endocannabinoids are not affecting the post-synapse (Castillo et al., 2011; Kirby et al., 1995). The impact of the reduced excitability in the dDG to enable MPP-dDG LTP recovery has been evaluated in the next step.

MPP-dDG LTP was successfully induced under moderate cholinergic activation and moderate cholinergic activation combined with Y1-R blockade in young male mice. (Fig. 12C). Previous studies show the facilitation of MPP-DG LTP through muscarinic agonists under a low tetanus protocol in anesthetized rats. Furthermore, muscarinic agonists facilitate GC response to MPP stimulation and increase the probability of eliciting MPP-DG LTP through disinhibition of PV+ interneurons via increased SST+ interneuron activation in young male mice. In both studies, PP-DG LTP was found to be facilitated by cholinergic activation but not dependent on it (Abe et al., 1994; Ogando et al., 2021).

The beneficial effect of acetylcholine esterase inhibitors, M-R agonists, and nicotine administration on CA1 LTP in aged rodents have been demonstrated (Fujii & Sumikawa, 2001; Hornick et al., 2011; Si et al., 2010). In line with these studies, in the current study, moderate cholinergic activation through PHY rescued the deficit of LTP at the MPP-dDG synapse in aged male mice (Fig. 13).

Strikingly, the beneficial effect of moderate cholinergic activation in this study was mediated by Y1-R activation, as indicated by re-occurring MPP-dDG LTP deficit after the combination of moderate cholinergic activation and Y1-R blockade (Fig. 13). These results suggest an important role of NPY-mediated Y1-R activation in the reduction of MPP-dDG neurotransmission and plasticity recovery in aged male mice. This interaction of ACh and NPY may be a more general feature relevant to aging, as indicated by the beneficial effect of nicotine treatment on MWM memory performance in a rat model of AD being Y1-R dependent (Rangani et al., 2012).

Besides this, the literature indicates a crucial role of NPY in spatial task learning, shown by impaired spatial learning in an NPY overexpressing rat model (Thorsell et al., 2000) that is reversed by age (Carvajal et al., 2004) and the beneficial effect of intracerebral NPY infusion prior to amyloid β peptides on some anxiety tasks and spatial memory in young mice (dos Santos et al., 2013). Moreover, intranasal co-administration of a Y1-R agonist and the neuropeptide Galanin 1 enhances spatial memory performance in young male mice, and intracerebroventricular injection of NPY or Y1-R agonist enhances spatial memory in an AD rat model (Borroto-Escuela et al., 2022; Rangani et al., 2012). Nevertheless, the only indication from the literature that NPY might benefit MPP-dDG LTP is given by Corvino and colleagues,

reporting a beneficial effect of exogenous NPY application on newly born neurons in the DG, which increases MPP-DG LTP in a TMT female rat model for hippocampal degeneration (Corvino et al., 2014). Notably, the TMT administration does not abolish MPP-dDG LTP. In line with the importance of NPY for plasticity, my data demonstrate that acute NPY application rescued the MPP-dDG LTP deficit in aged male mice *in vitro* (Fig. 14) without changing MPP-dDG neurotransmission (Fig. A4). The unchanged MPP-dDG neurotransmission has been demonstrated in previous studies showing no or minor effects of NPY on PP-evoked EPSPs in the ML (Sperk et al., 2007b).

At a cellular level, the Y1-R dependent MPP-dDG LTP rescue under moderate cholinergic activation might be explained by a reduction of GCs excitability through moderate cholinergic activation, possibly through mobilizing remaining NPY and mediating Y1-R activation. This is also indicated by the MPP-dDG neurotransmission reduction (Fig. 12, A3). Y1-R activation could reduce glutamate release and Ca^{2+} influx and, with that, reduce GC excitability (Sperk et al., 2007a). In young male mice, Y1-R blockade did not mediate MPP-dDG neurotransmission increase in the absence of cholinergic stimulation. Therefore, a Y1-R-dependent increase of MPP-dDG neurotransmission under moderate cholinergic activation in aged male mice would not be expected if GC excitability was reduced to normal excitability. An increase in Y1-R activation could increase the inhibitory strength on the GCs and reduce the heightened excitation in aged animals (Liu et al., 2014; Raza et al., 2017; Yuan et al., 2017). By that, E-I would be normalized and allows successful MPP-dDG LTP induction. This view is supported by the reported importance of E-I balance for spatial performance and proper DG output (Lee et al., 2016; Madar et al., 2019). Our laboratory findings have shown that, indeed, ACh-mediated Y1-R activation is incessant for proper contextual fear memory learning in young male mice (Raza et al., 2017). Moreover, the beneficial effects of nicotine treatment on memory performance in a rat model of AD have been shown to be Y1-R dependent (Rangani et al., 2012). As mentioned before, in young male mice, the disinhibition of PV+ interneurons facilitates MPP-DG LTP (Ogando et al., 2021). One could argue, therefore, that the effect in aged male mice may be mediated through a disinhibitory mechanism stimulated by increased NPYergic neurotransmission onto other interneurons. This study did not investigate the GABAergic tonus and PV+ interneurons. Nevertheless, due to the reported decline of GABAergic inhibition in the DG during aging and AD (Patrylo et al., 2007; Wu et al., 2014), the absence of LPP-DG LTP facilitation after $GABA_A$ blockade in aged mice, as well as the decline of PV+ interneurons during aging (Dugan et al., 2009; Froc et al., 2003; Shetty & Turner, 1999) an MPP-dDG LTP deficit due to the loss of disinhibition seems unlikely.

Together, my data reveal the importance of increasing NPYergic MPP-dDG neurotransmission in aged male mice to rescue the LTP deficit at the MPP-dDG synapse elicited by normalized E-I balance through increased Y1-R mediated inhibition.

5.4. TBS induces MPP-dDG LTP without $GABA_A$ receptor blockade in aged female mice

Using the same TBS protocol as in males, this study also demonstrates a Y1-R dependent MPP-dDG LTP in aged anestrus female mice (Fig. 15) - overcome by moderate cholinergic activation (Fig. 16). At the same time, postsynaptic excitability was increased in a cycle-dependent manner (Fig. 15A). The pre-synaptic excitability, by contrast, was only increased in aged anestrus female mice compared to young high estrus females, but not compared to young low estrus females (Fig. 15B).

MPP-dDG neurotransmission and plasticity are underinvestigated in natural cycling and aged females but have gained more interest over the last few years. Distinct changes in hippocampal plasticity, like a higher induction threshold of PP-DG LTP with HFS *in vivo,* have been shown (Maren, 1995; Maren et al., 1994). Furthermore, sex differences are known to appear in the NPYergic system, such as lower level of NPY in the hippocampus of young female mice compared to young male mice (reviewed in Nahvi & Sabban, 2020), and also in the cholinergic system, including lower spontaneous ACh release in young females (Masuda et al., 2005; Mitsushima et al., 2003, 2009a). The impact of estrogen on synaptic plasticity has been mostly studied in the CA1 subregion (reviewed in Hajszan et al., 2007). Furthermore, the known sex differences in neurodegenerative diseases, like steeper memory decline and controversial results of pharmacological treatment (Canevelli et al., 2017; Giacobini & Pepeu, 2018; Irvine et al., 2012; Mielke et al., 2014) the lower reduction of cholinergic projections from the MS to the DG in aged females compared to aged males (Lukoyanov et al., 1999) and the missing knowledge about LTP at the MPP-dDG synapse in aged anestrus females make it crucial to investigate the impact of aging in females.

The data from this study reveal increased post-synaptic excitability at the MPP-dDG synapse of young low estrus compared to high estrus females (Fig. 15A). This is contrary to the results of Maguire and colleagues, demonstrating reduced tonic inhibition and higher seizure susceptibility in estrus compared to young late diestrus females. Nevertheless, their study does not mention the pole of the DG recording and measured inhibitory currents by patch-clamp recordings (Maguire et al., 2005). Furthermore, in the current study, the high estrus

group contains young female mice of proestrus and estrus, while the low estrus groups contain diestrus and metestrus females. Progesterone levels start increasing in the late diestrus phase and are high in estrus, while estrogen is high in proestrus (Inoue, 2022). Progesterone is known to enhance tonic inhibition in cycling females, males, and OVX females (Maguire & Mody, 2007), while estradiol mediates NPY release and gene expression in the DG of ovariectomized rats and mice trough Erα and ERβ (Hilke et al., 2009; Ledoux et al., 2009; Velíšková et al., 2015; Velíšková & Velíšek, 2007). The NPYergic and GABAergic (tonic) inhibition might cause reduced post-synaptic excitability in young high estrus females compared to low estrus females. In contrast, low estrus females lack the increased NPY release and gene expression due to low estrogen levels. Notably, the low estrus group of the current study contained more females in metestrus than in the diestrus stage. Interestingly, post-synaptic excitability was not different between young low estrus and aged anestrus females, even though a tendency for an increase could be observed (Fig. 15A). Zhu and colleagues (2019) demonstrate that GC excitability is reduced in middle-aged (14-15-month-old) female Kumming mice, using patch-clamp recordings (Zhu et al., 2020). The pooled anestrus and permanent estrus females in the study may explain the contrary results. Anestrus females display low estradiol levels, while permanent estrus females show high levels of estrogen (Huang et al., 1978), which might lead to a higher inhibitory tonus, as explained above.

In the current study, pre-synaptic excitability was increased in aged anestrus females compared to young high estrus but not to young low estrus females and not between the cycle stages (Fig. 15B). This 1) indicates a local change in the excitability of GCs for young females during different cycle stages but 2) leaves the possibility of a non-local mediated increase of GC excitability in aged anestrus females. However, my data also demonstrate a Y1-R dependence of MPP-dDG LTP in aged anestrus female mice but not in the young ones (Fig. 15D), indicating an increased involvement of local NPYergic circuitry. Several reasons for the maintained but Y1-R-sensitive MPP-dDG LTP might apply in aged anestrus females. Female mice do not undergo the exact hormonal change during aging as humans do during menopause. Even though the estradiol levels are low in aged anestrus mice (Huang et al., 1978), they remain at detectable levels, which is not the case in humans. The remaining estradiol might protect against MPP-dDG LTP deficit, as it has been shown for estradiol application in a female-aged AD mouse model (22-24 months old) of MPP-DG LTP under $GABA_A$ blockade and in OVX-aged rats (15-18-month-old) for CA1 LTP (Inagaki et al., 2012; Sung et al., 2007). It has been shown that estradiol increases NPY release and gene expression in the DG of ovariectomized rodents directly through ERα and ERβ (Corvino et al., 2015; Ledoux et al., 2009; Velíšková et

al., 2015; Velíšková & Velíšek, 2007). Moreover, estradiol also modulates the cholinergic system, mainly through ERα (Gibbs, 2000, 2010; Luine, 1985), and thereby might also indirectly activate the Y1-R, as shown in young males (Raza et al., 2017). The current study confirmed ACh-mediated Y1-R activation also for aged males. Additionally, the smaller decline in cholinergic fibers in aged females compared to aged males could preserve the function of hilar interneurons, which are vulnerable to cholinergic decline, if the same mechanism as in males applies (Lukoyanov et al., 1999; Matsuoka et al., 1995). All these factors would increase inhibition in the dDG of aged anestrus female mice and might affect MPP-dDG LTP beneficial if retardation of the NPYergic system has already started. On the other hand, estradiol and ER modulators increase NMDA binding and phosphorylation of NR2B, which could induce higher excitability and facilitates LTP (Cyr et al., 2001; Nebieridze et al., 2012; Smith & McMahon, 2006) if a reduction of excitability occurs due to the loss of cycling hormones, as it has been shown for middle-aged female Kumming mice (cycle not investigated) (Zhu et al., 2020). Anyway, my data showed a tendentially increased and not reduced post-synaptic excitability of aged anestrus females compared to young females. This is also in line with the reported increase of post-synaptic excitability at the MPP-dDG pathway in ML of middle-aged female AD mice (Hazra et al., 2013).

Acetylcholine esterase treatment is widely used to treat cognitive decline, but its beneficial effect on women with AD has been discussed controversially (Canevelli et al., 2017; Giacobini & Pepeu, 2018; Irvine et al., 2012; Mielke et al., 2014). In the current study, moderate cholinergic activation led to a Y1-R independent MPP-dDG LTP. At the same time, the magnitude of LTP was unaffected (Fig. 16). Due to the lower decline of cholinergic projection to the dDG, moderate cholinergic activation might abolish the need for compensation by Y1-R activation. Another possibility might be if the same mechanism as in males applies, a less retarded NPYergic system. The Y1-R thus appears to be efficiently activated upon moderate cholinergic activation, leading to an MPP-dDG LTP as in young female mice (Fig. 15D, 16).

In sum, this indicates an essential role of Y1-R activation in MPP-dDG LTP maintenance during aging, per se. In contrast, the E-I balance seems less severely disrupted compared to aged male mice. This might be due to successful compensatory recruitment of the NPYergic system, which is unaltered during aging, as shown in the current study (Fig. 21A). This preservation may happen to a mildly declining cholinergic system (Ludovenkey, 1999) as indicated by the loss of this compensatory need upon moderate cholinergic stimulation. In this case, cholinergic activation might increase Y1-R activation, as it has been shown in young

males (Raza et al., 2017). Analog to the male dDG neurotransmission recording with Y1-R blockade under control conditions and moderate cholinergic activation should reveal the impact of the cholinergic system on Y1-R activation in females.

5.5. Y1-R activation possibly compensates for increased excitability

Young female mice displayed a measurable difference in Y1-R mediated MPP-dDG neurotransmission in a cycle-dependent manner (Fig. 17C). Further investigations revealed that Y1-R dependence was not mediated by acute stimulation of M1-R, which is known to be expressed on local NPYergic interneurons (Fig. 17F, 18). Still, the dependence of MPP-dDG neurotransmission on Y1-R was abolished by β-estradiol, Y1-R agonist application, and moderate cholinergic activation in high estrus females (Fig. 19). In contrast, β-estradiol combined or moderate cholinergic activation with Y1-R blockade had no impact on MPP-dDG neurotransmission in low estrus females (Fig. 19).

The current study provides evidence of Y1-R involvement in MPP-dDG neurotransmission, which was increased after Y1-R blockade in young high estrus females but not in young low estrus or aged anestrus females (Fig. 17C). The effect was not observed under moderate cholinergic stimulation and could not be blocked by application of an M1-R antagonist (Fig. 17F, 18). ACh mediates HIPP cell activation through M1-R in young male mice (Raza et al., 2017), but it cannot be excluded that nicotinic receptors influence Y1-R activation in the dDG of young high estrus females (Fraizer et al., 2003; Gahring and Rogers, 2008) since the beneficial effect of nicotine was Y1-R dependent in a male rat model of AD (Rangani et al., 2012).

The experiment of β-estradiol combined with the Y1-R antagonist application in high estrus female mice indicates a β-estradiol-mediated increase of Y1-R activation. Several studies have demonstrated the increase of NPY release through estrogen (Corvino et al., 2015; Ledoux et al., 2009; Velíšková et al., 2015; Velíšková & Velíšek, 2007). Smith and colleagues proposed a non-genomic mediation through membrane Erα in NPY/Agouit-related peptide neurons (Smith, 2013), while Titolo and colleagues (2008) presented a combination of genomic and non-genomic activation by showing that membrane ERα mediates phosphorylation of the ERK1/2 pathways in 5-30 min in the CA1, but also that estrogen acts on the promoter of NPY. They postulated that membrane ERα activation (non-genomic) is critical to induce long-lasting (genomic) changes in NPY gene expression in clonal immortalized neurons (Titolo et al.,

2008). However, I did not observe a significant difference in NPY concentration or Y1-R expression levels in the dDG between high estrus and low estrus females.
It needs to be considered that Y1-R dependence of MPP-dDG neurotransmission might result from a general change in the control of E-I balance in the dDG. Estrogen is known to stimulate the activity of the gad2 promoter (Hudgens et al., 2009), thus increasing GABA synthesis. Moreover, it also increases excitatory neurotransmission as estrogen activates metabotropic glutamate receptor (mGluR) group 1 and increases NMDA binding and NR2B phosphorylation. This facilitates LTP but does not impact neurotransmission at the MPP-DG synapse under $GABA_A$ blockade in young female rats (Cyr et al., 2001; Nebieridze et al., 2012). It is thus plausible that cycle stages differ in the network activity maintaining local E-I balance, and Y1-R dependent transmission gains importance when both excitation and inhibition are high. This effect might not be achieved in young low estrus stage females by application of β-estradiol due to the need for genomic changes, as Velísková and colleagues (2015) report that repetitive estrogen injections but not a single dose lead to increased NPY immunoreactivity in the DG of OVX females (Velíšková et al., 2015).

Aged anestrus females did not show a change in NPY or Y1-R levels but (tendentially) increased post-synaptic excitability and sensitivity of LTP to Y1-R blockage. In analogy to the above explanation and the observations made in aging males, a change in network configuration and the need of NPYergic transmission for compensation might explain this. This apparently is relieved by moderate cholinergic activation, which also reduces baseline MPP-dDG neurotransmission to comparable levels in all female groups. Cholinergic projections co-transmitting ACh and GABA mediated by M2-R activation in the DG of male rodents (Goral et al., 2022; Granger et al., 2016; Takács et al., 2018), due to the retardation of the cholinergic projections also GABA co-transmission is declining during aging which might lead to the compensatory increased recruitment of Y1-R activation. Thus, an increase of moderate cholinergic activation would also facilitate GABA co-transmission, decreasing MPP-dDG neurotransmission and abolishing the need to compensate for increased excitability by Y1-R activation. Adding to this activation of cholinergic projections leads to the activation of non-cholinergic projections from the MS, meditating together with cholinergic projections inhibition of neurotransmission in the CA3 of male rodents (Dannenberg et al., 2015).

In analogy to the explanation in aged male mice, the possibility of reduced disinhibition can be excluded. Nevertheless, the beneficial effect of PHY on MPP-dDG LTP in aged anestrus female mice needs to be further investigated. In sum, Y1-R is recruited in young females to

maintain MPP-dDG neurotransmission under physiological-like conditions while it compensates in aged anestrus females for slightly reduced inhibition.

5.6. Nutritional estrogen replacement as a possible treatment to preserve MPP-dDG LTP

The observed interaction of cycle stage, β-estradiol, and Y1-R on MPP-dDG LTP inspired me to investigate plasticity in a mouse model of chronic estrogen depletion, OVX, and the impact of nutritional estrogen supplementation. My data show that OVX females display Y1-R insensitive MPP-dDG LTP independent of moderate cholinergic activation (Fig. 20), thus resembling young low estrus females. Remarkably, OVX females kept on phyto-free food for six weeks (treatment, as described in Çalışkan et al., 2021), expressed a Y1-R sensitivity of MPP-dDG LTP (Fig. 20) that was overcome by moderate cholinergic activation (Fig. 20), hence resembling the observations in aged anestrus mice. In both groups, Y1-R blockade did not affect MPP-dDG neurotransmission with or without moderate cholinergic activation (see appendix, Fig. A9).

As discussed above, aged female mice do not resemble precisely the changes during menopause in humans, as they show follicular degradation instead of depletion and low but still measurable estrogen levels. By contrast, OVX, which has been used for decades as a model for menopause, causes the ablation of fluctuating estrogens. OVX female rodents show the first signs of retardation in step-through passive avoidance after four weeks of hormone deprivation. After eight weeks of OVX, hippocampus-dependent memory is impaired, depicted by deficits in the MWM and novel object recognition task (Tao et al., 2020). Accordingly, long-term OVX (19 months) but not short-term OVX (1 month) of rats of the same age has been shown to reduce CA1 LTP (Smith et al., 2010).

Until now, however, the effect of OVX on MPP-dDG LTP has not been investigated *in vitro* under intact inhibitory tonus. Strikingly, OVX for at least eight weeks could not mimic the age-related changes in MPP-dDG plasticity unless estrogen analogs were additionally depleted from the animal food. Standard housing food in our animal facility contains significant amounts of the phytoestrogens genistein and daidzein, as well as low levels of coumestrol, all derived from soy components. In mice, these phytoestrogens are almost entirely metabolized to equol, which activates ERs, especially ER-β for S-equol and ER-α for R-equol (Muthyala et al., 2004) and may thus substitute for the operationally induced ablation.

In fact, it has been demonstrated that soy-milk treatment directly after OVX can increase serum β- estradiol levels of neonatal OVX rats (serum levels measured at day 60) to levels observed in young gonadally intact rats of the same age (Abbasabadi et al., 2016). The recovery of CA1 LTP after β-estradiol treatment has been shown in OVX rats treated with aromatase inhibition (Vierk et al., 2012). Moreover, soy extract given i.p. prevented CA1 LTP decrease in anesthetized OVX females after seizure induction with kainic acid (Khodamoradi et al., 2017) and phytoestrogen applied orally to recover spatial working memory and dendritic spines in the CA1 of OVX females (Konuri et al., 2020). Furthermore, our laboratory showed that depletion of phytoestrogen leads to impaired ventral CA1 LTP, which can be rescued by equol, but not dorsal CA1 LTP accompanied by reduced stability of contextual fear memory but not novelty and spatial memory as well as a reduction of NR2B phosphorylation in the ventral and a tendentially decrease in the dorsal hippocampus of young male mice (Çalışkan et al., 2019). Moreover, low-phyto food decreases the mRNA of GAD67 and 65 as well as NPY mRNA in the amygdala of young male mice (Sandhu et al., 2015). At a cellular level, several possible mechanisms might account for the beneficial effect of nutritional estrogen replacement in the dDG. Estrogen derivates could increase NMDA binding in the DG, which is reduced in OVX females (Cyr et al., 2001). Furthermore, the recovery of adult neurogenesis through β-estradiol and soy extract in drinking water has been shown for 22-month-old rats (OVX at 12 months of age) (Perez-Martin et al., 2005). This has been proposed to benefit MPP-DG LTP in a TMT female rat model for hippocampal degeneration (Corvino et al., 2014). Moreover, a neuroprotective effect of phytoestrogens on neuronal loss in the hilus of the DG after kainic acid application in adult OVX females has been demonstrated (Azcoitia et al., 2006). Furthermore, the estrogen-mediated increase of the cholinergic release and maintenance of projections in the hippocampus (Gibbs, 2010; Gibbs & Aggarwal, 1998) could prevent an MPP-dDG LTP deficit due to ACh and GABA co-transmission (Goral et al., 2022; Granger et al., 2016; Takács et al., 2018b) or to a neuroprotective effect on NPYergic interneurons (Matsuoka et al., 1995). Moreover, repetitive estrogen injections lead to increased NPY immunoreactivity in the DG of OVX females (Velíšková et al., 2015), which might be resembled by continuous nutritional estrogen replacement.

OVX as an aging model should be further investigated, and data from aged OVX rodents must be handled with care regarding age-related changes.

Altogether these data indicate that nutritional estrogen replacement may be a suitable approach to slow down the estrogen deprivation-mediated decrease of MPP-dDG LTP. However, in aged anestrus females fed with standard housing food, it did not prevent age-

dependent alterations such as the Y1-R-dependent MPP-dDG. Aging-related changes might thus not be entirely counteracted by phytoestrogens. Similarly, it has been shown that short-term but not long-term estradiol treatment of long-term OVX rats is sufficient to prevent the loss of spine density of GCs (Miranda et al., 1999). It has been shown that the timepoint to start with estrogen therapy is crucial, as its beneficial effect on CA1 plasticity and spine density after OVX was observed for up to 15 months but not at OVX for 19 months in rats (Smith et al., 2010). In my experiments, therefore, OVX females and aged anestrus females were fed our standard housing food from their arrival (2 weeks after OVX), respectively, birth.

A possible explanation for the observed effects is that higher equol concentrations are needed to maintain MPP-dDG LTP fully due to aging and protracted hormone deprivation. Vedder and colleagues (2014) reported maintained responsiveness to acute estradiol treatment after OVX of 19 months when low estradiol doses are given from OVX on, displayed in maintained novel object recognition learning but not in the plasticity of the CA1 subregion (Vedder et al., 2014). Moreover, higher doses of phytoestrogens are able to restore reduced spine density in middle-aged and OVX females in the CA1 subregion, spatial memory in the OVX females, and adult hippocampal neurogenesis in middle-aged female mice (Luine et al., 2006; T. J. Wang et al., 2014; Yamada et al., 2016).

5.7. Age and sex-dependent decrease of NPY concentration in the dDG

This study proved that NPY concentration displayed substantial sex differences, with females having lower NPY levels which were stable over the cycle and lifespan in this study. Strikingly, NPY concentrations in the dDG declined in aged male mice but not aged female mice (Fig. 21A). Y-1R expression was unaltered during aging, independent of sex (Fig. 21B). The decline of NPY concentration during aging in males may be related to the loss of SST+ cells (Matsuoka et al., 1995; Stanley & Shetty, 2004) and mRNA loss starting at middle age in the DG (Hattiangady et al., 2005). Furthermore, the increased post-synaptic excitability can be explained due to a loss of NPYergic inhibition, which might increase Ca^{2+} and glutamate release. Moreover, the reduced NPY concentration strengthens the view that maintained (peptidergic) inhibition is necessary for successful MPP-dDG LTP induction.

The lower levels of NPY expression in young female mice compared to young male mice in the hippocampus have been shown previously (Nahvi & Sabban, 2020; Rugarn et al., 1999). Rugarn and colleagues (1999) showed stable NPY concentration in prepubertal and adult female rats, whereby NPY concentration was found to be lower in both cases than in

prepubertal and adult males in the hippocampus (Rugarn et al., 1999). Aged anestrus females, in my experiments, did not display a change in NPY concentration or Y1-R expression in the dDG compared to young females, independent of the cycle stage (Fig. 21A/ B). At the same time, they stayed lower compared to young and aged males. This is in line with the unchanged post-synaptic excitability compared to young, low estrus female mice and with the possibility to induce MPP-dDG LTP under control conditions. Nevertheless, since young high and low estrus females did not display alterations in NPY concentration either, altered NPY concentrations might hardly be the reason for cycle differences in young female mice. The Y1-R activity-dependent MPP-dDG LTP might occur from starting hyperexcitability of the dDG, which requires more inhibition and thus involves more Y1-R activation.

To my knowledge, no studies have yet investigated NPY+ cell number, protein, or mRNA in aged anestrus females. Results from human studies indicate an increase in NPY plasma level and plasma NPY-like immunoreactivity during aging (Khoury & Mathé, 2004; Kluess et al., 2019). Furthermore, Hilke and colleagues (2009) showed a non-significant trend to higher NPY-like immunoreactivity in the hippocampus of OVX mice which is reduced after β-estradiol treatment, but an increase in NPY mRNA after ovariectomy plus $\beta-$ estradiol in mice (Hilke et al., 2009). By contrast, Seo and colleagues (2018) depicted reduced NPY expression in the CA1 after ovariectomy (Seo et al., 2018). The outcomes of the OVX studies might result from different time windows of OVX duration until NPY measurements or from the measured area, CA1 (Seo et al., 2018), compared to the total hippocampal formation (Hilke et al., 2009). Importantly, the results of the rodent studies are contained in OVX animals and not in aged anestrus females, as in the current study.

The aged anestrus females of this study were fed with standard housing food containing phytoestrogen, as the aforementioned nutritional estrogen application leads to the preservation of MPP-dDG LTP properties; it also might lead to NPY concentration and Y1-R expression preservation.

In summary, a decay of NPY concentration in aging male mice may be involved in the observed changes in excitability and MPP-dDG plasticity, while the maintenance, albeit at low levels, in females may help to uphold a normal level of plasticity in aged anestrus females.

5.8. Aging in males mediates an increase in the phosphorylation of ERK1/2

This study showed increased pERK1/2 and pERK1/2 ratios in aged male mice compared to young male mice (Fig. 22B). In contrast, total ERK1/2, GluR1, pGluR1, NR2B, pNR2B, and their ratios were unchanged in comparison to young male mice (Fig. 22). Aged anestrus female mice, compared with young females, did not show any alteration in the investigated proteins and their phosphorylation (Fig. 22).

Increased free intracellular Ca^{2+} concentrations can mediate the activation of pERK through NMDA activation (Rosenblum et al., 2000b), and cytosolic Ca^{2+} has been shown to be high during aging in the hippocampus (Das & Ghosh, 1996; Satistegui et al., 1996). The observed increase of pERK1/2 in aged male mice thus is in line with the increased baseline excitability of aged animals in this study. The relationship between ERK phosphorylation and excitability may be bidirectional: on the one hand, increased activation of NMDAR mediates higher intracellular Ca^{2+}, which mediates ERK1/2 activation (Rosenblum et al., 2000). On the other hand, increased ERK1/2 activation leads to an increase of glutamate, shown by a MEK inhibitor, and might promote increased post-synaptic excitability (Mcgahon et al., 1999). Both explanations align with an E-I balance shifting towards higher excitation, which cannot or only partially be counterbalanced by available NPY. Zhang and colleagues (2015), as well as Ibrahim and colleagues (2020), state that the increase of ERK phosphorylation enhances cognition in models of AD (Ibrahim et al., 2020; Zhang et al., 2015), while defective LTP and impaired memory formation have been related to ERK1/2 inhibition (English & David Sweatt, 1997; Winder et al., 1999; Ying et al., 2002). Furthermore, the phosphorylation of ERK has been disrupted after intra-hippocampal injections of oligomeric amyloid β-peptide in the dDG of young male mice (Faucher et al., 2016) and was reduced in the DG of 22-month-old rats (Gooney et al., 2004). The contrary results of the current study to this literature might arise from different models, age or pole of the DG respectively undefined pole of the DG of the animals used in the aforementioned studies. In fact, inhibition of the ERK pathway leads to the recovery of Abeta-induced cellular changes and memory deficits in a mouse model of AD (Chang et al., 2020; Feld et al., 2014; Lee et al., 2009; Wang et al., 2019). Accordingly, a high basal ERK1/2 activation in aged male mice might prevent a further ERK1/2 activation through TBS and thus be involved in the observed MPP-dDG LTP deficit. Similarly, BDNF-induced LTP in the DG has been shown to promote pERK1/2 in young but not aged male rats (Gooney et al., 2004). Y1-R activation has been shown to activate ERK1/2 (Benarroch, 2009; Colmers

et al., 1988). As Y1-R activation became significant for LTP in aged males under moderate cholinergic activation, it may be speculated that in these animals, it compensates for the loss of other, e.g., BDNF-mediated, plasticity mechanisms. Moreover, NPY may inhibit Ca^{2+} influx through Y1-R activation to counterbalance the hyperactivity and reduce basal pERK1/2 before LTP induction, as it has been shown that Ca^{2+} blockade abolished NMDAR-dependent ERK1/2 activation in the PP-DG synapse (Rosenblum et al., 2000).

In aged anestrus females, these mechanisms do not seem to apply, in line with the MPP-dDG neurotransmission data and the maintained MPP-dDG LTP of aged anestrus females.

6. Conclusion

In this study, I demonstrated, by inducing LTP at the MPP-dDG synapse in slice preparations under intact inhibition, sex-specific alterations of MPP-dDG plasticity during healthy aging. I could show that MPP-dDG LTP maintenance, in both sexes, and recovery, in aged male mice, depends on the activation of the NPYergic system. These sex-specific alterations in plasticity were accompanied by sex-specific alterations in neuronal excitability as well as endogenous dDG NPY concentration and ERK1/2 phosphorylation. Nutritional estrogen replacement might play a crucial role in the observed sex differences. Moreover, I revealed sex-specific modulation of the NPYergic system by moderate cholinergic activation.

Episodic memory is impaired chiefly during healthy aging, and preserved hippocampal activity is correlated with maintaining episodic memory. Moreover, a common pharmacological treatment for AD is the application of an acetylcholine esterase inhibitor (Canevelli et al., 2017; Giacobini & Pepeu, 2018c; Light, 1991; Nyberg & Tulving, 1996; Tulving & Markowitsch, 1998). This doctoral thesis demonstrated that increased E-I balance mediated by increased basal ERK1/2 activation leads to MPP-dDG plasticity deficits. This plasticity deficit is rescued by increasing NPYergic transmission leading to normalization of the E-I balance through increased Y1-R mediated inhibition. These results open the door to a new therapeutical approach to cognitive decline: the application of NPY. NPY nose spray has been tested in post-traumatic stress disorder patients (Sayed et al., 2018) and could now be tested in healthy aged patients with cognitive decline. Since the beneficial effect of acetylcholine esterase inhibitor PHY is mediated by NPY, a direct therapeutical approach with NPY might gain more efficiency and less sight effect. Moreover, NPY has been demonstrated to increase longevity in animal aging models. This treatment might improve cognition, lifespan, and even more important live quality.

Different life expectancies, effects of pharmacological treatment, prevalence, and steepness in neurodegenerative diseases point to sex-specific aging processes. Indeed, I displayed a slower cognitive decline in aged anestrus females, accompanied by unchanged NPY concentration, Y1-R expression, NR2B, GluA1, and ERK. Nevertheless, MPP-dDG plasticity also depended on the activation of NPY without moderate cholinergic activation-overcome by moderate cholinergic activation. This strengthens, on the one hand, NPY as an essential factor during healthy aging and, on the other hand, sex-specific mechanistic changes during aging. In contrast to the reported higher prevalence of dementia in females, is has been proposed that the

decline of memory is steeper in AD females if affected (Irvine et al., 2012; Mielke et al., 2014; Nichols et al., 2019), indicating higher preservation of function until pathological changes occurring. The results of this thesis can also be interpreted in the light of the same mechanisms that are less retarded in aged anestrus females than in aged males. The cholinergic projections are less retarded in aged female rodents than in males (Lukoyanov et al., 1999). Moreover, this study depicted declining NPY concentrations in aged males but not females. In this case, NPY activation accounts as a compensatory mechanism for the declining cholinergic projections, which are co-transmitting GABA (Goral et al., 2022; Granger et al., 2016; Takács et al., 2018), until a certain grade of degradation of the cholinergic system (as seen in the aged anestrus females). When the retardation continues (as in aged males), a subpopulation of NPY cells is also declining, which is sensitive to cholinergic decline (Matsuoka et al., 1995). The additional decline of the NPYergic systems makes it impossible to counterbalance the increased excitation during aging, possibly occurring due to the reduction of co-transmitted GABA. This leads to a plasticity deficit in the dDG under physiological conditions. That can still be recovered by external activation or supplementation of NPY. A highly likely candidate to preserve cholinergic function are sex-steroids.

Testosterone declines in male rodents from 12 months, while estrogen declines in female mice from 16-20 months of age (Miller & Riegle, 1982; Nelson et al., 1981). The cholinergic system is sex-dependent mediated. In castrated males, the cholinergic function is restored by applying testosterone, while in OVX females, estrogen is needed (Mitsushima et al., 2009; Veng et al., 2003). In this view, starting retardation of the cholinergic system would be a marker for declining cognitive function, which advances with a declining NPYergic system. In this light, one could also argue for using a sex-steroid treatment as early as possible. Indeed, for aged females, the protective effect of estrogen has been shown in the literature, but severe side effects are also discussed (Lobo, 1995; Mehta et al., 2021). The current thesis depicted nutritional estrogen replacement as a possible treatment. This replacement could be performed in humans with a certain diet when the first sign of menopause occurs. Timepoint and concentrations could be easily adapted to the start and duration of menopause. This treatment might also have beneficial effects in males, as indicated by studies from our laboratory in young male mice (Çalışkan et al., 2019).

This study highlighted possible new treatment targets, possibly sex- or time-dependent. NPY can treat cognitive deficits in males or possibly deficits later in healthy aging, whereby nutritional estrogen replacement can treat cognitive deficits in females or possibly be used as an early intervention with the possibility as a medication slowing the cognitive decline.

Moreover, I proved that the natural estrus cycle impacts the NPYergic system and baseline excitability. Furthermore, the NPYergic system depicts sex-specific activation, and a common model for human menopause has to be handled with care using it for aging studies.

With this doctoral thesis a I added a puzzle piece to the understanding of healthy aging in a sex-dependent-manner. I highlighted that NPYergic inhibition is indispensable to maintain dDG plasticity in both sexes during healthy aging, even though this seems counterintuitive. Moreover, investigating mechanistic properties in both sexes separately is highly important. Even though the behavior or physiology is similar in both sexes, different mechanisms might account for the same outcome. Adding on the latter natural cycling impact the NPYergic system and might also impact other neuromodulatory systems as such it should be included as a biological variable when investigating females.

7. Future directions

This study gives a new insight into the mechanism of the beneficial effect of moderate cholinergic activation on MPP-dDG LTP in aged mice and the modulation of the NPYergic system in young female mice in a cycle-stage-dependent manner. Since the study reveals loss of NPY concentration in aged males but not females, fiber photometry could be used to investigate the NPY release in both sexes in object placement and location tasks, as these tasks are affected after chronic inactivation of SST+ hilar interneurons and intranasal delivery of Y1-agonist (Borroto-Escuela et al., 2022; Lyu et al., 2022). The measurement of NPY release could give insights into if and how much the release of NPY is reduced. The release probabilities could be correlated with behavioral performance. Adding MPP-dDG LTP measurements after the behavioral investigation would raise the possibility of relating MPP-dDG LTP to behavioral performance level. Furthermore, behavioral performance and NPY release could be measured after cholinergic treatment or intranasal delivery of NPY. This could allow for adjusting the NPY or cholinergic treatment *in vivo* and should be done for both sexes. Moreover, the beneficial effect of PHY on MPP-dDG LTP in aged anestrus females should be further investigated by altering the GABAergic tonus in combination with moderate cholinergic activation.

Regarding the MPP-dDG plasticity of aged male mice, testing the application of β-estradiol, equol or testosterone would give insights into the beneficial effect in hormone therapy and, in combination with a selective Y1-R antagonist, the possibility of estrogen to activate the NPYergic system in aged mice. Especially for aged anestrus females, a treatment with β-estradiol could be conducted in a food and time-dependent manner to test if the estrogen-window hypothesis (Bean et al., 2015) also accounts for aged anestrus females under defined food conditions. The electrophysiological properties at the MPP-dDG synapse would also be tested under phyto-free food. Additionally, comparing electrophysiological properties at the MPP-dDG synapse of the follicular depletion (VCD) model to OVX, OVX with phyto-free food and natural aging with phyto-free food, and natural aging would be fascinating since this study showed that OVX under phyto-free food but not OVX alone expresses the same electrophysiological properties as naturally aging females. The VCD model has been shown to develop sex-steroid levels similar to women after menopause. Investigating this model could give further insight into the effects of nutritional estrogen replacement on MPP-dDG plasticity and possible alterations due to low estrus levels in aged anestrus females. These experiments would further elucidate the shown sex differences in MPP-dDG plasticity and

neurotransmission of young and aged mice and give further insights into the possible protective effects of nutritional estrogen.

8. Appendix

8.1. Additional results

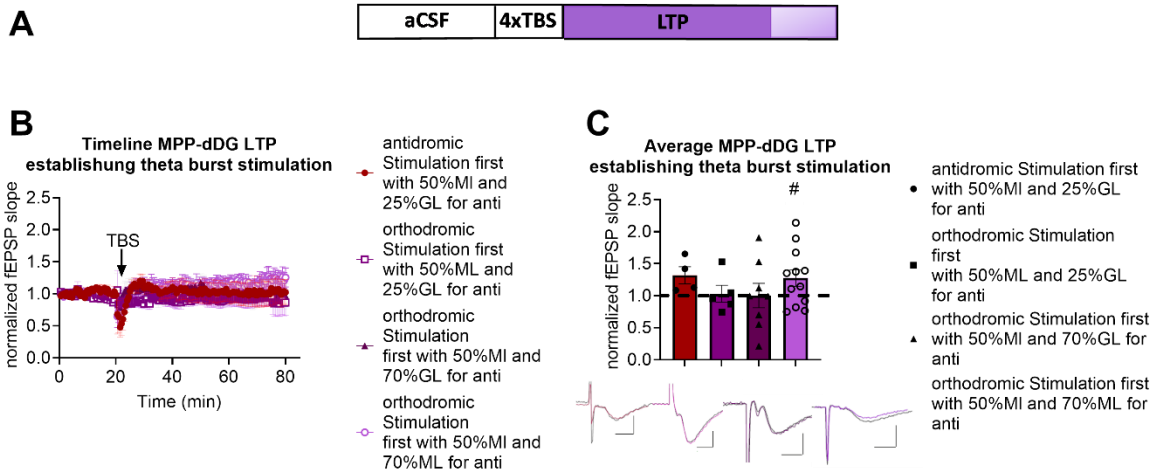

Figure A1: Orthodromic stimulation of the MPP pathway combined with antidromic stimulation in the hilus of the dDG induces reliable LTP at the MPP-dDG pathway. A: Scheme of the experimental protocol for MPP-dDG LTP. The normalized data from the last 10 min, indicated by transparent sections in the columns, were used for statistical comparison shown in bar graphs. **B:** Plotted timeline of the average fEPSP slope of different tests of TBS. Antidromic stimulation (activated during TBS) before orthodromic stimulation (dark red), orthodromic stimulation before antidromic stimulation (during TBS) with 25% of the max. GL fEPSP amplitude (purple), orthodromic stimulation before antidromic stimulation (during TBS) with 70% of the max. GL population spike amplitude (lilac) and orthodromic stimulation before antidromic stimulation (during TBS) with 70% of the max. ML fEPSP amplitude (light lilac) starts with the last 10 min of baseline recording (0-10 min), followed by TBS induction at 10 min, and finishes with 40 min of MPP-dDG LTP recording (10-50 min). **C:** The average of the last 10 min from the MPP-dDG LTP recordings in the bar graph reveals no change in fEPSP slope after TBS for antidromic stimulation with 25% of the population spike amplitude before orthodromic stimulation with 50% of ML fEPSP amplitude ($t_{(3)}$=2.705, p=0.0648, paired t-test, one-tailed, n=4; dark red), for orthodromic stimulation with 50% of ML fESPS amplitude followed by the antidromic stimulation with 25% of population spike amplitude ($t_{(4)}$=0.4817, p=0.3276, paired t-test, one-tailed, n=6; purple), and for orthodromic stimulation with 50% of ML fESPS amplitude followed by the antidromic stimulation with 70% of population spike amplitude ($t_{(7)}$=0.1582, p=0.4394, paired t-test, one-tailed, n=8; lilac). Nevertheless, a significant increase of fEPSP slope after TBS for orthodromic stimulation with 50% of the ML fEPSP amplitude before antidromic stimulation with 70% of ML fEPSP amplitude (during TBS) is demonstrated ($t_{(11)}$=0.1958, p=0.0380, paired t-test, one-tailed, n=12; light lilac). Below the graph, representative fEPSP traces are plotted. Scale bar x-axis: 2 ms each and y-axis: 1 mV each: before TBS (colored) and from the last 10 min of MPP-dDG LTP recording (grey). LTP = long-term potentiation, dDG = dorsal dentate gyrus, GL = granule layer, ML = molecular layer, MPP = medial perforant path, and TBS = theta-burst stimulation. LTP induction (in slice comparison): #, $p < 0.05$

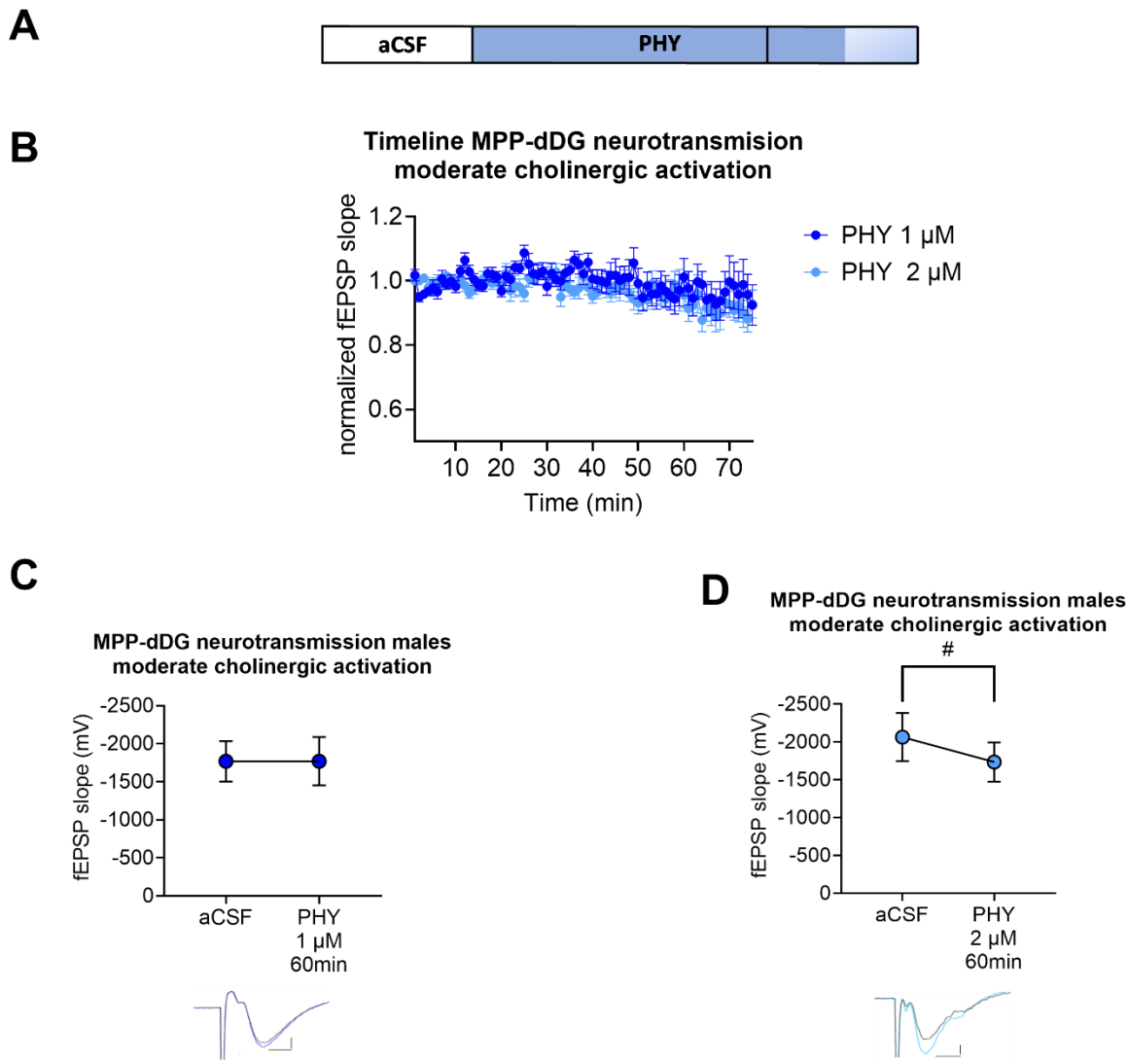

Figure A2: PHY (2 µM) is the lowest concentration to induce a reduction of MPP-dDG neurotransmission. A: Scheme of the experimental protocol of PHY application. The averaged raw data from the last 10 min, indicated by transparent sections in the columns, were used for statistical comparison shown in the line graphs. **B:** Plotted timeline of the average fEPSP slope of 1 µM PHY (blue) and 2 µM PHY (light blue) starts with the last 10 min of baseline recording with aCSF (0-10 min), followed by 60 min PHY application (10-70 min). **C:** The averaged raw data of the fEPSP slope from the MPP-dDG neurotransmission recording reveal a not significant decrease with one 1 µM PHY ($t_{(8)}$=0.01505, p=0.9884, paired t-test, two-tailed, n=9; blue). **D:** The averaged raw data of the fEPSP slope from the MPP-dDG neurotransmission recording reveal a significant decrease of the raw fEPSP slope with 2 µM PHY ($t_{(13)}$=2.877, p=0.0127, paired t-test, two-tailed, n=14; light blue). Below the graphs, representative signals are plotted. Scale bar x-axis: 2 ms each and y-axis: 0.4 mV each: before drug application (colored) and from the last 6 min of the drug application (grey). dDG = dorsal dentate gyrus, MPP = medial perforant path, and PHY = physostigmine. fEPSP slope change (in slice comparison): #, $p < 0.05$

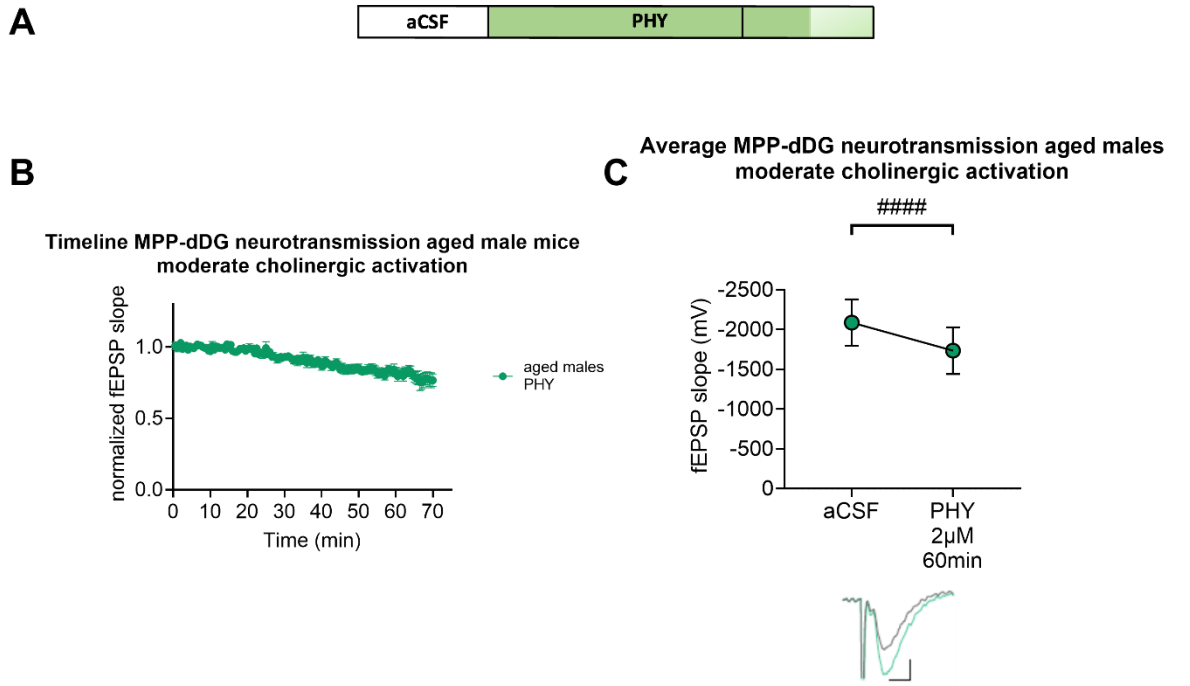

Figure A3: PHY (2 µM) reduces MPP-dDG neurotransmission in aged male mice. A: Scheme of the experimental protocol of PHY application. The averaged raw data from the last 10 min, indicated by transparent sections in the columns, were used for statistical comparison shown in the line graphs. **B:** Plotted timeline of the average fEPSP slope of aged male mice with PHY (green) starts with the last 10 min of baseline recording with aCSF (0-10 min), followed by 60 min PHY application (10-70 min). **C:** The averaged raw data of the fEPSP from the MPP-dDG neurotransmission recording reveals a significant decrease of the fEPSP slope with 2 µM PHY ($t_{(12)}$=5.732, p<0.0001, paired t-test, two-tailed, n=13; green). Below the graph, representative signals are plotted. Scale bar x-axis: 2 ms and y-axis: 0.4 mV each: before drug application (colored) and from the last 6 min of the drug application (grey). dDG = dorsal dentate gyrus, MPP = medial perforant path, and PHY = physostigmine. fEPSP slope change (in slice comparison): ####, p < 0.0001

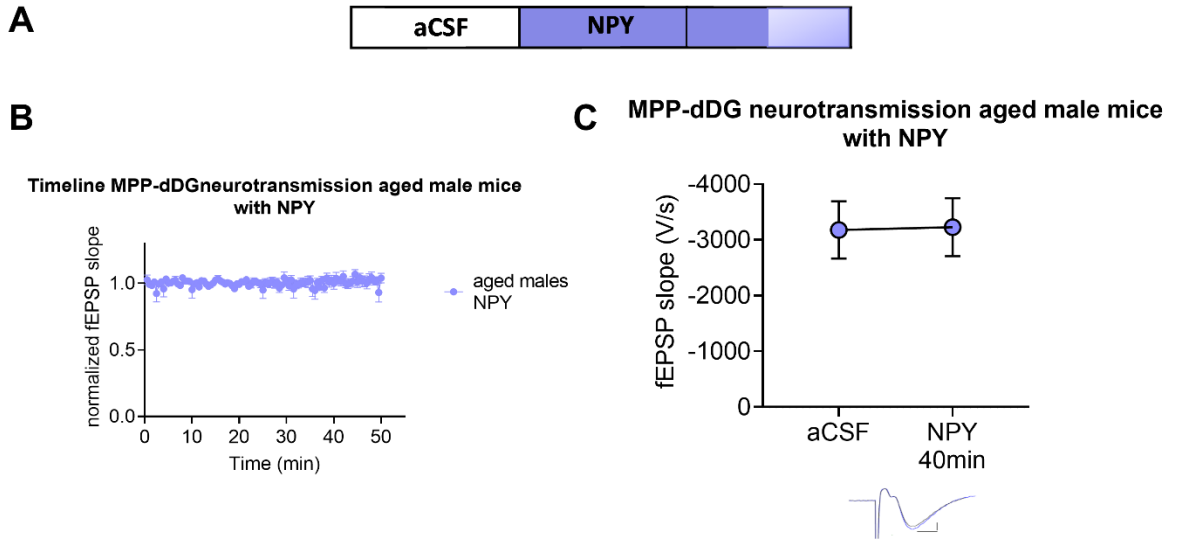

Figure A4: Exogenous NPY application has no impact on synaptic transmission of aged male mice. A: Scheme of the experimental protocol of NPY application. The averaged raw data from the last 10 min, indicated by transparent sections in the columns, were used for statistical comparison shown in the line graphs. **B:** Plotted timeline of the averaged fEPSP slope of NPY application in aged male mice starts with the last 10 min of baseline recording with aCSF (0-10 min), followed by 40 min NPY application (10-50 min). **C:** The averaged raw fEPSP slopes reveal unaltered MPP-dDG neurotransmission after NPY application ($t_{(10)}$=0.4604, p=0.6551, paired t-test, two-tailed, n=11). Below the graph, representative fEPSP traces are plotted. Scale bar x-axis: 2 ms and y-axis: 1 mV: before drug application (colored) and from the last 6 min of drug application (grey). dDG = dorsal dentet gyrus, MPP = medial perfornat path, and NPY = Neuropeptide Y.

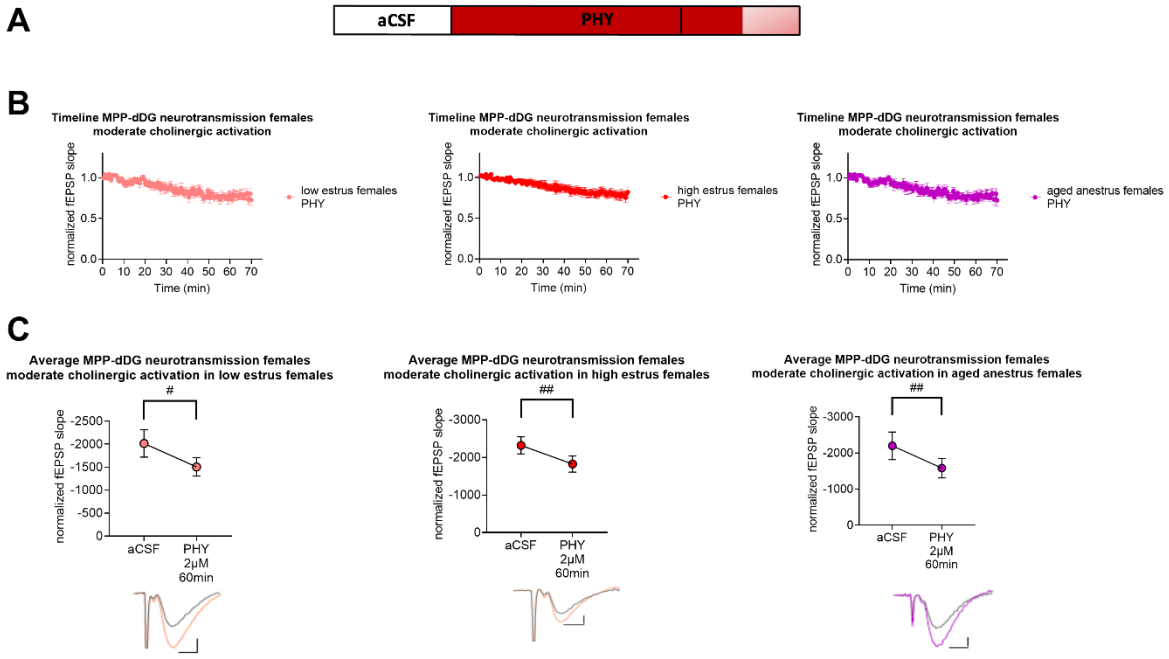

Figure A5: PHY (2 µM) reduces MPP-dDG neurotransmission in aged female mice. A: Scheme of the experimental protocol of PHY application. The averaged raw data from the last 6 min, indicated by transparent sections in the columns, were used for statistical comparison shown in the line graphs. **B:** Plotted timeline of the averaged fEPSP slope of 2 µM PHY in young low estrus females (light red), young high estrus females (red), and aged anestrus females (purple) start with the last 10 min of baseline recording with aCSF (0-10 min), followed by 60 min PHY application (10-70 min). **C:** The averaged raw data of the fEPSP from the MPP-dDG neurotransmission recording reveals a significant decrease of the fEPSP slope for low estrus females ($t_{(11)}$=3.041, p=0.012, paired t-test, two-tailed, n=12; light red), high estrus females ($t_{(15)}$=3.892, p=0.0014, paired t-test, two-tailed, n=16; red) and aged anestrus females ($t_{(6)}$=4.183, p=0.0058, paired t-test, two-tailed, n=7; purple). Below the graph, representative signals are plotted. Scale bar x-axis: 2 ms each and y-axis: 1 mV (for young low), 0.5 MV (for high estrus females), and 0.4 mV each (for aged anestrus females): before drug application (colored) and from the last 6 min of the drug application (grey). dDG = dorsal dentate gyrus, MPP = medial perforant path, and PHY = physostigmine. fEPSP slope change (in slice comparison): #, $p < 0.05$, ##, $p < 0.01$

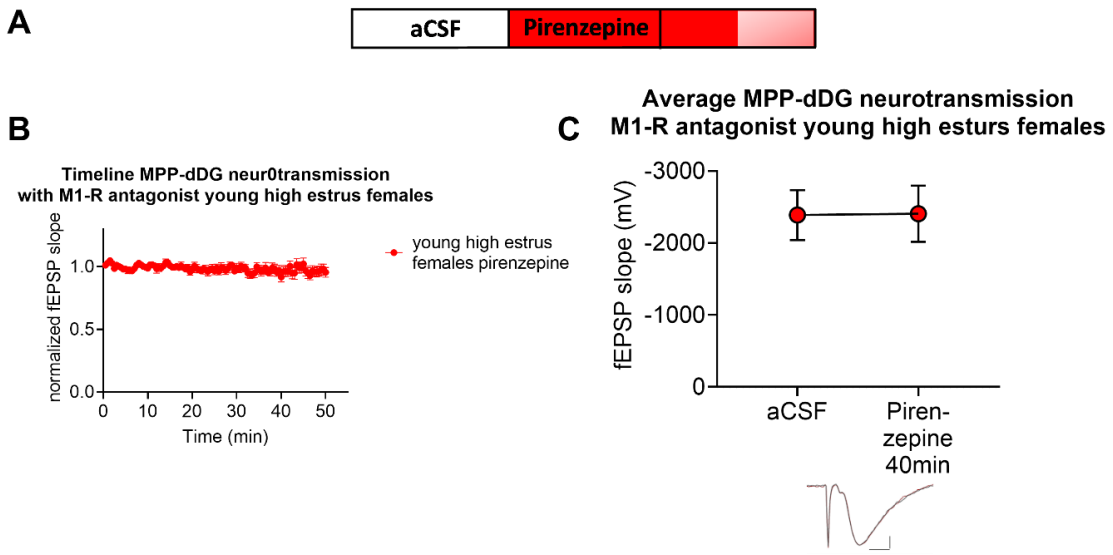

Figure A6: M1-R blockade does not change MPP-dDG neurotransmission. A: Scheme of the experimental protocol of M1-R blockade. The averaged raw data from the last 10 min, indicated by transparent sections in the columns, were used for statistical comparison shown in the line graphs. **B:** Plotted timeline of the averaged fEPSP slope of M1-R blockade in young high estrus females (red) starts with the last 10 min of baseline recording with aCSF (0-10 min), followed by 40 min pirenzepine application (10-50 min). **C:** The averaged raw fEPSP slopes reveal unaltered MPP-dDG neurotransmission after M1-R blockade ($t_{(10)}$=0.2235, p=0.8276, paired t-test, two-tailed, n=11). Below the graph, representative fEPSP traces are plotted. Scale bar x-axis: 2 ms and y-axis: 1 mV: before drug application (colored) and from the last 6 min of drug application (grey). dDG = dorsal dentet gyrus, M1-R = muscarinic receptor 1, and MPP = medial perfornat path.

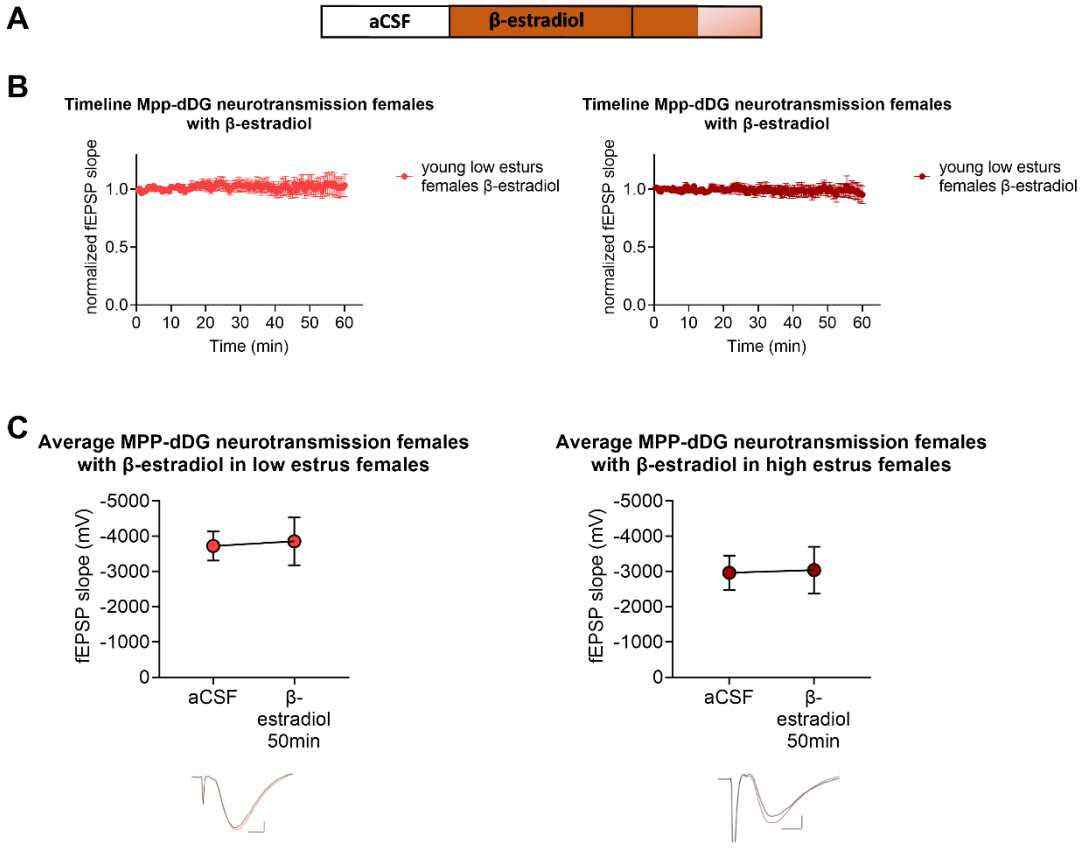

Figure A7: β-estradiol does not change dDG transmission in young females independent of the cycle stage. A: Scheme of the experimental protocol of β-estradiol application. The averaged raw data from the last 10 min, indicated by transparent sections in the columns, were used for statistical comparison shown in the line graphs. **B:** Plotted timeline of the averaged fEPSP slope of β-estradiol application in young low estrus females (red) and in young high estrus females (dark red) starts with the last 10 min of baseline recording with aCSF (0-10 min), followed by 50 min β-estradiol application (10-50 min). **C:** The averaged raw fEPSP slopes reveal unaltered MPP-dDG neurotransmission after β-estradiol application in young low estrus females ($t_{(8)}$=0.4164, p=0.6881, paired t-test, two-tailed, n=9) and young high estrus females ($t_{(7)}$=0.3522, p=0.7351, paired t-test, two-tailed, n=8). Below the graph, representative fEPSP traces are plotted. Scale bar x-axis: 2 ms each and y-axis: 1 mV each: before drug application (colored) and from the last 6 min of drug application (grey). dDG = dorsal dentet gyrus, and MPP = medial perfornat path.

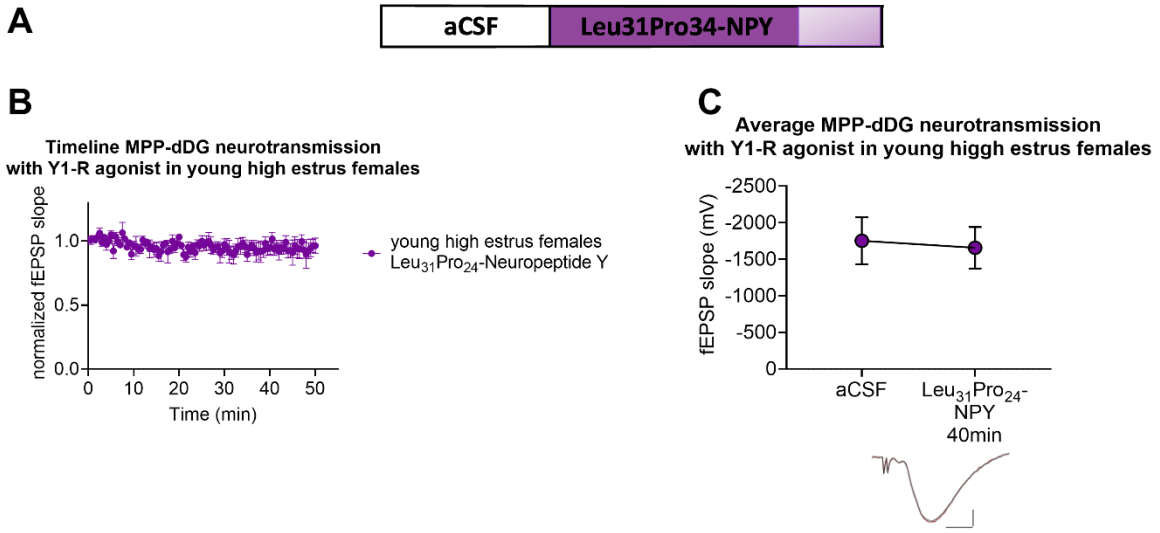

Figure A8: MPP-dDG neurotransmission with Y1-R agonist female. A: Scheme of the experimental protocol of Y1-R agonist application. The averaged raw data from the last 10 min, indicated by transparent sections in the columns, were used for statistical comparison shown in the line graphs. **B:** Plotted timeline of the averaged fEPSP slope of Y1-R agonist application in young high estrus females (purple) starts with the last 10 min of baseline recording with aCSF (0-10 min), followed by 40 min Y1-R agonist application (10-50 min). **C:** The averaged raw fEPSP slopes reveal unaltered MPP-dDG neurotransmission after Y1-R agonist application in young high estrus females ($t_{(6)}$=0.8068, p=0.4506, paired t-test, two-tailed, n=7). Below the graph, representative fEPSP traces are plotted. Scale bar x-axis: 2 ms and y-axis: 1 mV: before drug application (colored) and from the last 6 min of drug application (grey). dDG = dorsal dentet gyrus, MPP = medial perfornat path, and Y1-R = Neuropeptide receptor type 1.

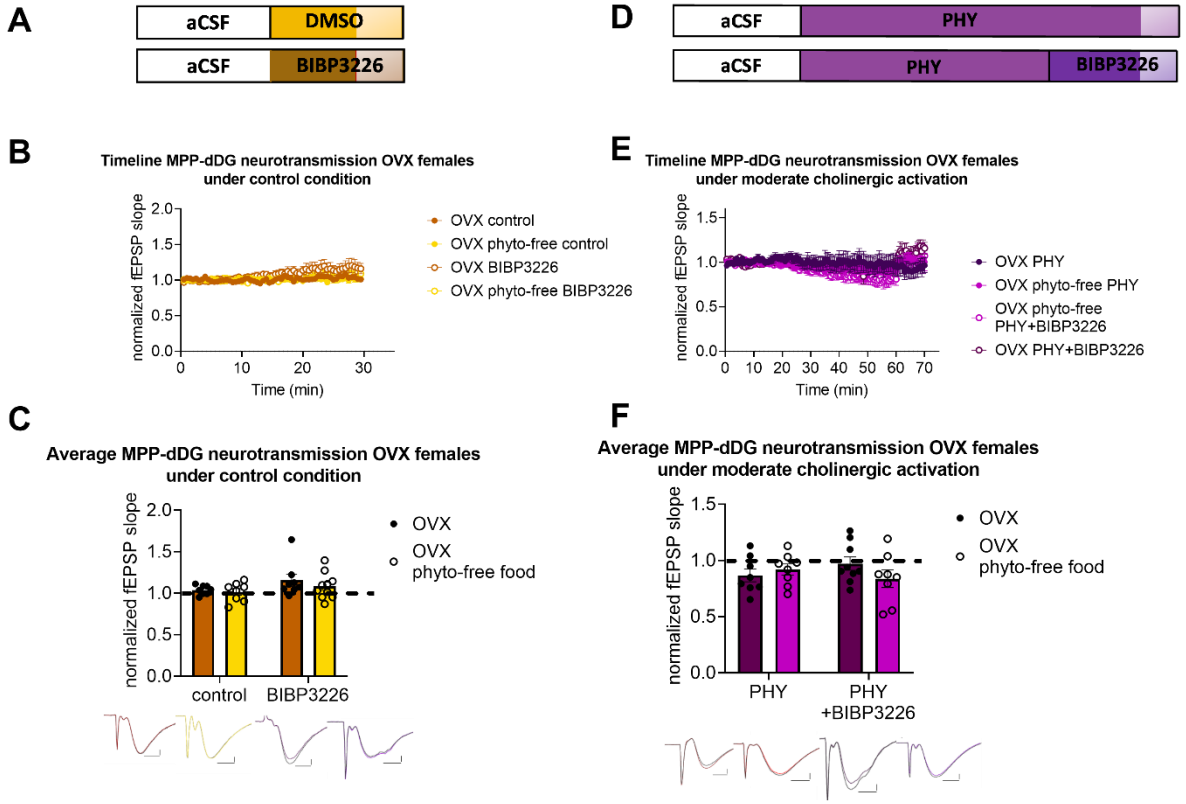

Figure A9: Blockade of Y1-R does not affect MPP-dDG neurotransmission under control conditions nor under moderate cholinergic activation in young OVX females, independent of food. A: Scheme of the experimental protocol for Y1-R blockade under control conditions. The averaged raw data from the last 6 min, indicated by transparent sections in the columns, were used for statistical comparison shown in the line graphs. **B:** The plotted timeline of MPP-dDG LTP with the average values of OVX female mice control (brown), OVX females on phyto-free food control (yellow), OVX females +BIBP3226 (white with brown), and OVX females on phyto-free food + BIBP3226 (white with yellow) starts with the last 10 min of baseline recording (0-10 min) and finishes with 20 min drug application (10-30 min). **C:** The average of the last 6 min from the MPP-dDG neurotransmission recordings in the bar graph reveals no change of fEPSP slope in OVX females control (brown), OVX females with BIBP3226 (white with brown), OVX phyto-free food (yellow), OVX phyto-free food with BIBP (white with yellow) ($F_{(1,\ 30)}$=0.2264, p=0.6377, two-way ANOVA, n=8 (OVX control); n=8 (OVX with BIBP3226); n=8 (OVX phyto-free food control); n=10 (OVX phyto-free food with BIBP3226). Below the graphs, representative fEPSP traces are plotted. Scale bar x-axis: 2 ms each and y-axis: 1 mV each: before drug application (colored) and from the last 6 min of MPP-dDG neurotransmission recording (grey). **D:** Scheme of the experimental protocol for Y1-R blockade under moderate cholinergic activation. In white, the baseline recording (20 min), colored the drug application (60 min), and transparent the time used for the averaged fEPSP slope (6 min). **E:** The plotted timeline of MPP-dDG neurotransmission with the average values of OVX female mice with PHY (dark purple), OVX females on phyto-free food with PHY (pink), OVX females with PHY + BIBP3226 (white with dark purple), and OVX females on phyto-free food with PHY + BIBP3226 (white with pink) starts with the last 10 min of baseline recording (0-10 min) and finishes with 60 min of drug application (10-70 min). **C:** The average of the last 6 min from the MPP-dDG neurotransmission recordings reveals an unchanged MPP-dDG neurotransmission after Y1-R blockade under moderate cholinergic activation in OVX females with PHY+ BIBP3226 (white with dark purple) and OVX on phyto-free food with PHY+BIBP3226 (white with pink) ($F_{(1,\ 29)}$=2.220, p=0.1470, two-way ANOVA, n=8 (OVX PHY); n=9 (OVX PHY + BIBP3226); n=8 (OVX phyto-free food PHY); n=8 (OVX phyto-free food PHY + BIBP3226). Below the graphs, representative fEPSP traces are plotted. Scale bar x-axis: 2 ms each and y-axis: 1 mV each: before TBS (colored) and from the last 6 min of drug application (grey). dDG = dorsal dentate gyrus, LTP = Long-term potentiation, OVX = ovariectomy, TBS =theta-burst stimulation, and Y1-R = Neuropeptide Y 1 Receptor.

8.2. Bibliography

Abe, K., Nakata, A., Mizutani, A., & Saito, H. (1994). Pergamon 0028-3908(94)EOO34-0 Facilitatory but Nonessential Role of the Muscarinic Cholinergic System in the Generation of Long-term Potentiation of Population Spikes in the Dentate Gyrus In Vivo. In *Neuropharmacology* (Vol. 33, Issue 7).

Abraham, W. C., & Bear, M. F. (1996). Metaplasticity: the plasticity of synaptic plasticity. In *Trends Ntwosc-i* (Vol. 19).

Abraham, W. C., Jones, O. D., & Glanzman, D. L. (2019). Is plasticity of synapses the mechanism of long-term memory storage? In *npj Science of Learning* (Vol. 4, Issue 1). Springer Nature. https://doi.org/10.1038/s41539-019-0048-y

Ackert-Bicknell, C. L., Anderson, L. C., Sheehan, S., Hill, W. G., Chang, B., Churchill, G. A., Chesler, E. J., Korstanje, R., & Peters, L. L. (2015). Aging Research Using Mouse Models. *Current Protocols in Mouse Biology*, *5*(2), 95–133. https://doi.org/10.1002/9780470942390.mo140195

Ackert-Bicknell, C. L., Karasik, D., Li, Q., Smith, R. v., Hsu, Y. H., Churchill, G. A., Paigen, B. J., & Tsaih, S. W. (2010). Mouse BMD quantitative trait loci show improved concordance with human genome-wide association loci when recalculated on a new, common mouse genetic map. *Journal of Bone and Mineral Research*, *25*(8), 1808–1820. https://doi.org/10.1002/jbmr.72

Aggleton, J. P., & Pearce, J. M. (2001). Neural systems underlying episodic memory: Insights from animal research. *Philosophical Transactions of the Royal Society B: Biological Sciences*, *356*(1413), 1467–1482. https://doi.org/10.1098/rstb.2001.0946

Allen, E. (1922). The oestrous cycle in the mouse. *American Journal of Anatomy*, *30*(3), 297–371. https://doi.org/10.1002/aja.1000300303

Amani, M., Lauterborn, J. C., Le, A. A., Cox, B. M., Wang, W., Quintanilla, J., Cox, C. D., Gall, C. M., & Lynch, G. (2021). Rapid aging in the perforant path projections to the rodent dentate gyrus. *Journal of Neuroscience*, *41*(10), 2301–2312. https://doi.org/10.1523/JNEUROSCI.2376-20.2021

Annamneedi, A., Caliskan, G., Müller, S., Montag, D., Budinger, E., Angenstein, F., Fejtova, A., Tischmeyer, W., Gundelfinger, E. D., & Stork, O. (2018). Ablation of the presynaptic organizer Bassoon in excitatory neurons retards dentate gyrus maturation and enhances learning performance. *Brain Structure and Function*, *223*(7), 3423–3445. https://doi.org/10.1007/s00429-018-1692-3

Arima-Yoshida, F., Watabe, A. M., & Manabe, T. (2011). The mechanisms of the strong inhibitory modulation of long-term potentiation in the rat dentate gyrus. *European Journal of Neuroscience*, *33*(9), 1637–1646. https://doi.org/10.1111/j.1460-9568.2011.07657.x

Armstrong, C. M. J., Conti, F., Defelice, . J, & Wanke, E. (1982). N europeptide Y-a novel brain peptide with structural similarities to peptide YY and pancreatic polypeptide. In *J. Physiol., Lond* (Vol. 296, Issue 9).

Azcoitia, I., Moreno, A., Carrero, P., Palacios, S., & Garcia-Segura, L. M. (2006). Neuroprotective effects of soy phytoestrogens in the rat brain. *Gynecological Endocrinology*, *22*(2), 63–69. https://doi.org/10.1080/09513590500519161

Azcoitia, I., Perez-Martin, M., Salazar, V., Castillo, C., Ariznavarreta, C., Garcia-Segura, L. M., & Tresguerres, J. A. F. (2005). Growth hormone prevents neuronal loss in the aged rat hippocampus. *Neurobiology of Aging*, *26*(5), 697–703. https://doi.org/10.1016/j.neurobiolaging.2004.06.007

Baeza, I., de Castro, N. M., Giménez-Llort, L., & de la Fuente, M. (2010). Ovariectomy, a model of menopause in rodents, causes a premature aging of the nervous and immune systems. *Journal of Neuroimmunology*, *219*(1–2), 90–99. https://doi.org/10.1016/j.jneuroim.2009.12.008

Ballinger, E. C., Ananth, M., Talmage, D. A., & Role, L. W. (2016). Basal Forebrain Cholinergic Circuits and Signaling in Cognition and Cognitive Decline. In *Neuron* (Vol. 91, Issue 6, pp. 1199–1218). Cell Press. https://doi.org/10.1016/j.neuron.2016.09.006

Baratta, M. v., Lamp, T., & Tallent, M. K. (2002). Somatostatin depresses long-term potentiation and Ca2+ signaling in mouse dentate gyrus. *Journal of Neurophysiology*, *88*(6), 3078–3086. https://doi.org/10.1152/jn.00398.2002

Barnes, C. A. (1979). Memory Deficits Associated With Senescence: A Neurophysiological and Behavioral Study in the Rat. In *Journal of Comparative and Physiological Psychology* (Vol. 93, Issue 1).

Barnes, C. A., & Mcnaughton, B. L. (1980). PHYSIOLOGICAL COMPENSATION FOR LOSS OF AFFERENT SYNAPSES IN RAT HIPPOCAMPAL GRANULE CELLS DURING SENESCENCE. In *J. Physiol* (Vol. 309).

Barnes, C. A., & Mcnaughton, B. L. (1986). An Age Comparison of the Rates of Acquisition and Forgetting of Spatial Information in Relation to Long-Term Enhancement of Hippocampal Synapses. In *Behavioral Neuroscience* (Vol. 99, Issue 6).

Barnes, C. A., Rao, G., & Houston, F. P. (2000). *LTP induction threshold change in old rats at the perforant path-granule cell synapse*. www.elsevier.com/locate/neuaging

Baudry, M., Bi, X., & Aguirre, C. (2013). Progesterone-estrogen interactions in synaptic plasticity and neuroprotection. In *Neuroscience* (Vol. 239, pp. 280–294). https://doi.org/10.1016/j.neuroscience.2012.10.051

Bean, L. A., Kumar, A., Rani, A., Guidi, M., Rosario, A. M., Cruz, P. E., Golde, T. E., & Foster, T. C. (2015). Re-opening the critical window for estrogen therapy. *Journal of Neuroscience*, *35*(49), 16077–16093. https://doi.org/10.1523/JNEUROSCI.1890-15.2015

Benarroch, E. E. (2009). Neuropeptide Y. *Neurology*, *72*(11), 1016. https://doi.org/10.1212/01.wnl.0000345258.18071.54

Berger-Sweeney, J., Stearns, N. A., Murg, S. L., Floerke-Nashner, L. R., Lappi, D. A., & Baxter, M. G. (2001). *Selective Immunolesions of Cholinergic Neurons in Mice: Effects on Neuroanatomy, Neurochemistry, and Behavior*.

Besnard, A., & Sahay, A. (2021). Enhancing adult neurogenesis promotes contextual fear memory discrimination and activation of hippocampal-dorsolateral septal circuits. *Behavioural Brain Research*, *399*. https://doi.org/10.1016/j.bbr.2020.112917

Bettio, L. E. B., Rajendran, L., & Gil-Mohapel, J. (2017). The effects of aging in the hippocampus and cognitive decline. In *Neuroscience and Biobehavioral Reviews* (Vol. 79, pp. 66–86). Elsevier Ltd. https://doi.org/10.1016/j.neubiorev.2017.04.030

Bi, R., Broutman, G., Foy, M. R., Thompson, R. F., & Baudry, M. (2000). *The tyrosine kinase and mitogen-activated protein kinase pathways mediate multiple effects of estrogen in hippocampus* (Vol. 97, Issue 7). PNAS. www.pnas.orgcgidoi10.1073pnas.060034497

Bimonte-Nelson, H. A., Bernaud, V. E., & Koebele, S. v. (2021). Menopause, hormone therapy and cognition: maximizing translation from preclinical research. In *Climacteric* (Vol. 24, Issue 4, pp. 373–381). Taylor and Francis Ltd. https://doi.org/10.1080/13697137.2021.1917538

Bliss, T. V. P., & Collingridge, G. L. (1993). *A synaptic model of memory: long-term potentiation in the hippocampus*.

Bliss, T. V. P., Collingridge, G. L., & Morris, R. G. M. (2014). Synaptic plasticity in health and disease: Introduction and overview. *Philosophical Transactions of the Royal Society B: Biological Sciences*, *369*(1633). https://doi.org/10.1098/rstb.2013.0129

Bliss, T. V. P., & L0mo, T. (1973). LONG-LASTING POTENTIATION OF SYNAPTIC TRANSMISSION IN THE DENTATE AREA OF THE ANAESTHETIZED RABBIT FOLLOWING STIMULATION OF THE PERFORANT PATH. In *J. Physiol* (Vol. 232).

Bliss, T.V.P. & Collingridge, G. L. (1993). A synaptic model of memory: LTP in the hippocampus. *Nature*, *361*, 31–39.

Borroto-Escuela, D. O., Fores, R., Pita, M., Barbancho, M. A., Zamorano-Gonzalez, P., Casares, N. G., Fuxe, K., & Narváez, M. (2022). Intranasal Delivery of Galanin 2 and Neuropeptide Y1 Agonists Enhanced Spatial Memory Performance and Neuronal Precursor Cells Proliferation in the Dorsal Hippocampus in Rats. *Frontiers in Pharmacology*, *13*. https://doi.org/10.3389/fphar.2022.820210

Botelho, M., & Cavadas, C. (2015). Neuropeptide Y: An Anti-Aging Player? In *Trends in Neurosciences* (Vol. 38, Issue 11, pp. 701–711). Elsevier Ltd. https://doi.org/10.1016/j.tins.2015.08.012

Broadbent, N. J., Squire, L. R., & Clark, R. E. (2006). Reversible hippocampal lesions disrupt water maze performance during both recent and remote memory tests. *Learning and Memory*, *13*(2), 187–191. https://doi.org/10.1101/lm.134706

Byers, S. L., Wiles, M. v., Dunn, S. L., & Taft, R. A. (2012). Mouse estrous cycle identification tool and images. *PLoS ONE*, *7*(4). https://doi.org/10.1371/journal.pone.0035538

Cadiacio, C. L., Milner, T. A., Gallagher, M., & Pierce, J. P. (2003). Hilar neuropeptide Y interneuron loss in the aged rat hippocampal formation. *Experimental Neurology*, *183*(1), 147–158. https://doi.org/10.1016/S0014-4886(03)00126-2

Çalışkan, G., Raza, S. A., Demiray, Y. E., Kul, E., Sandhu, K. v., & Stork, O. (2019). Depletion of dietary phytoestrogens reduces hippocampal plasticity and contextual fear memory stability in adult male mouse. *Nutritional Neuroscience*, *24*(12), 951–962. https://doi.org/10.1080/1028415X.2019.1698826

Canevelli, M., Quarata, F., Remiddi, F., Lucchini, F., Lacorte, E., Vanacore, N., Bruno, G., & Cesari, M. (2017). Sex and gender differences in the treatment of Alzheimer's disease: A systematic review of randomized controlled trials. In *Pharmacological Research* (Vol. 115, pp. 218–223). Academic Press. https://doi.org/10.1016/j.phrs.2016.11.035

Cardoso, A., Freitas-da-Costa, P., Carvalho, L. S., & Lukoyanov, N. v. (2010). Seizure-induced changes in neuropeptide Y-containing cortical neurons: Potential role for seizure threshold and epileptogenesis. *Epilepsy and Behavior*, *19*(4), 559–567. https://doi.org/10.1016/j.yebeh.2010.09.008

Carvajal, C. C. (2007). *Neuropeptide Y (NPY) as a modulator of neuroplasticity and emotional behavior in animal models.* Library and Archives Canada = Bibliothèque et Archives Canada.

Carvajal, C. C., Vercauteren, F., Dumont, Y., Michalkiewicz, M., & Quirion, R. (2004). Aged neuropeptide Y transgenic rats are resistant to acute stress but maintain spatial and non-spatial learning. *Behavioural Brain Research*, *153*(2), 471–480. https://doi.org/10.1016/j.bbr.2004.01.004

Castillo, P. E., Chiu, C. Q., & Carroll, R. C. (2011). Long-term plasticity at inhibitory synapses. *Current Opinion in Neurobiology*, *21*(2), 328–338. https://doi.org/10.1016/j.conb.2011.01.006

Chang, K. W., Zong, H. F., Rizvi, M. Y., Ma, K. G., Zhai, W., Wang, M., Yang, W. N., Ji, S. F., & Qian, Y. H. (2020). Modulation of the MAPKs pathways affects Aβ-induced cognitive deficits in Alzheimer's disease via activation of α7nAChR. *Neurobiology of Learning and Memory*, *168*. https://doi.org/10.1016/j.nlm.2019.107154

Chen, B.-S., & Roche, K. W. (2007). *Regulation of NMDA Receptors by Phosphorylation*.

Chen, L., Miyamoto, Y., Furuya, K., Mori, N., & Sokabe, M. (2007). PREGS induces LTP in the hippocampal dentate gyrus of adult rats via the tyrosine phosphorylation international cooperative research CREB signaling. *Journal of Neurophysiology*, *98*(3), 1538–1548. https://doi.org/10.1152/jn.01151.2006

Chen, Q. S., Kagan, B. L., Hirakura, Y., & Xie, C. W. (2000). Impairment of hippocampal long-term potentiation by Alzheimer amyloid β-peptides. *Journal of Neuroscience Research*, *60*(1), 65–72. https://doi.org/10.1002/(SICI)1097-4547(20000401)60:1<65::AID-JNR7>3.0.CO;2-Q

Citri, A., & Malenka, R. C. (2008). Synaptic plasticity: Multiple forms, functions, and mechanisms. In *Neuropsychopharmacology* (Vol. 33, Issue 1, pp. 18–41). https://doi.org/10.1038/sj.npp.1301559

Clayton, D. A., Mesches, M. H., Alvarez, E., Bickford, P. C., & Browning, M. D. (2002). *A Hippocampal NR2B Deficit Can Mimic Age-Related Changes in Long-Term Potentiation and Spatial Learning in the Fischer 344 Rat*.

Colgin, L. L., Kramár, E. A., Gall, C. M., & Lynch, G. (2003). Septal modulation of excitatory transmission in hippocampus. *Journal of Neurophysiology*, *90*(4), 2358–2366. https://doi.org/10.1152/jn.00262.2003

Colmers, W. F., Lukowiak, K., & Pittman, Q. J. (1988). Neuropeptide Y Action in the Rat Hippocampal Mechanism of Presynaptic Inhibition Slice: Site and. In *The Journal of Neuroscience*.

Coogan, A. N., O, D. M., & O, J. J. (1996). *P42/44 MAP Kinase Inhibitor PD98059 Attenuates Multiple Forms of Synaptic Plasticity in Rat Dentate Gyrus In Vitro* (Vol. 81).

Corvino, V., di Maria, V., Marchese, E., Lattanzi, W., Biamonte, F., Michetti, F., & Geloso, M. C. (2015). Estrogen administration modulates hippocampal gabaergic subpopulations in the hippocampus of trimethyltin-treated rats. *Frontiers in Cellular Neuroscience*, *9*(NOVEMBER). https://doi.org/10.3389/fncel.2015.00433

Corvino, V., Marchese, E., Podda, M. V., Lattanzi, W., Giannetti, S., di Maria, V., Cocco, S., Grassi, C., Michetti, F., & Geloso, M. C. (2014). The neurogenic effects of exogenous neuropeptide Y: Early molecular events and long-lasting effects in the hippocampus of trimethyltin-treated rats. *PLoS ONE*, *9*(2). https://doi.org/10.1371/journal.pone.0088294

Coulter, D. A., & Carlson, G. C. (2007). Functional regulation of the dentate gyrus by GABA-mediated inhibition. In *Progress in Brain Research* (Vol. 163). Elsevier. https://doi.org/10.1016/S0079-6123(07)63014-3

Curcio, C. A., Hinds, J. W., & HINDS Stability, J. W. (1983). Stability of Synaptic Density and Spine Volume in Dentate Gyrus of Aged Rats. In *Neurobiology of Aging* (Vol. 4).

Cyr, M., Thibault, C., Morissette, M., Landry, M., & Paolo, T. di. (2001). Estrogen-like Activity of Tamoxifen and Raloxifene on NMDA Receptor Binding and Expression of its Subunits in Rat Brain. In *Neuropsychopharmacology* (Vol. 25, Issue 2).

da Costa, J. P., Vitorino, R., Silva, G. M., Vogel, C., Duarte, A. C., & Rocha-Santos, T. (2016). A synopsis on aging—Theories, mechanisms and future prospects. In *Ageing Research Reviews* (Vol. 29, pp. 90–112). Elsevier Ireland Ltd. https://doi.org/10.1016/j.arr.2016.06.005

Danielson, N. B. B., Kaifosh, P., Zaremba, J. D. D., Lovett-Barron, M., Tsai, J., Denny, C. A. A., Balough, E. M. M., Goldberg, A. R. R., Drew, L. J. J., Hen, R., Losonczy, A., & Kheirbek, M. A. A. (2016). Distinct Contribution of Adult-Born Hippocampal Granule Cells to Context Encoding. *Neuron*, *90*(1), 101–112. https://doi.org/10.1016/j.neuron.2016.02.019

Dannenberg, H., Pabst, M., Braganza, O., Schoch, S., Niediek, J., Bayraktar, M., Mormann, F., & Beck, H. (2015). Synergy of direct and indirect cholinergic septo-hippocampal pathways coordinates firing in hippocampal networks. *Journal of Neuroscience*, *35*(22), 8394–8410. https://doi.org/10.1523/JNEUROSCI.4460-14.2015

Das, N., & Ghosh, S. (1996). *The effect of age on calcium dynamics in rat brain in vivo*.

Davis, K. E., Eacott, M. J., Easton, A., & Gigg, J. (2013). Episodic-like memory is sensitive to both Alzheimer's-like pathological accumulation and normal ageing processes in mice. *Behavioural Brain Research*, *254*, 73–82. https://doi.org/10.1016/j.bbr.2013.03.009

Denny, C. A., Kheirbek, M. A., Alba, E. L., Tanaka, K. F., Brachman, R. A., Laughman, K. B., Tomm, N. K., Turi, G. F., Losonczy, A., & Hen, R. (2015). *Hippocampal Memory Traces Are Differentially Modulated by Experience, Time, and Adult Neurogenesis*. https://doi.org/10.1016/j.neuron

Dere, E., Huston, J. P., & de Souza Silva, M. A. (2005). Episodic-like memory in mice: Simultaneous assessment of object, place and temporal order memory. *Brain Research Protocols*, *16*(1–3), 10–19. https://doi.org/10.1016/j.brainresprot.2005.08.001

Detoledo-Morrell, L., Geinisman$ And, Y., & Morrell, F. (1988). Age-Dependent Alterations in Hippocampal Synaptic Plasticity: Relation to Memory Disorders. In *Neurobiology of Aging* (Vol. 9).

Diana, G., Domenici, M. R., Loizzo, A., Scotti De Carolis, A., & Sagratella, S. (1994). NEURO$CI[NC[tETTERS Age and strain differences in rat place learning and hippocampal dentate gyrus frequency-potentiation. In *Neuroscience Letters* (Vol. 171).

Diering, G. H., & Huganir, R. L. (2018). The AMPA Receptor Code of Synaptic Plasticity. In *Neuron* (Vol. 100, Issue 2, pp. 314–329). Cell Press. https://doi.org/10.1016/j.neuron.2018.10.018

Dillon, G. M., Qu, X., Marcus, J. N., & Dodart, J. C. (2008). Excitotoxic lesions restricted to the dorsal CA1 field of the hippocampus impair spatial memory and extinction learning in C57BL/6 mice. *Neurobiology of Learning and Memory*, *90*(2), 426–433. https://doi.org/10.1016/j.nlm.2008.05.008

dos Santos, V. v., Santos, D. B., Lach, G., Rodrigues, A. L. S., Farina, M., de Lima, T. C. M., & Prediger, R. D. (2013). Neuropeptide Y (NPY) prevents depressive-like behavior, Spatial memory deficits and oxidative stress following amyloid-β (Aβ1-40) administration in mice. *Behavioural Brain Research*, *244*, 107–115. https://doi.org/10.1016/j.bbr.2013.01.039

Douglas, R. M., & Goddard, G. v. (1975). LONG-TERM POTENTIATION OF THE PERFORANT PATH-GRANULE CELL SYNAPSE IN THE RAT HIPPOCAMPUS. In *Brain Res.'.arch* (Vol. 86).

Driscoll, I., Hamilton, D. A., Petropoulos, H., Yeo, R. A., Brooks, W. M., Baumgartner, R. N., & Sutherland, R. J. (2003). The Aging Hippocampus: Cognitive, Biochemical and Structural Findings. *Cerebral Cortex*, *13*(12), 1344–1351. https://doi.org/10.1093/cercor/bhg081

Dugan, L. L., Ali, S. S., Shekhtman, G., Roberts, A. J., Lucero, J., Quick, K. L., & Behrens, M. M. (2009). IL-6 mediated degeneration of forebrain GABAergic interneurons and cognitive impairment in aged mice through activation of neuronal NADPH oxidase. *PLoS ONE*, *4*(5). https://doi.org/10.1371/journal.pone.0005518

Dumont, Y., Fournier, A., St-Pierre, S., & Quirion', R. (1993). Comparative Characterization and Autoradiographic Distribution of Neuropeptide Y Receptor Subtypes in the Rat Brain. In *The Journal of Neuroscience* (Vol. 73, Issue l).

Dumont, Y., Jacques, D., Bouchard, P., & Quirion, R. (1998). Species differences in the expression and distribution of the neuropeptide Y Y1, Y2, Y4, and Y5 receptors in rodents, guinea pig, and primates brains. *Journal of Comparative Neurology*, *402*(3), 372–384. https://doi.org/10.1002/(SICI)1096-9861(19981221)402:3<372::AID-CNE6>3.0.CO;2-2

El-Hayek, Y. H., Wu, C., Ye, H., Wang, J., Carlen, P. L., & Zhang, L. (2013). Hippocampal excitability is increased in aged mice. *Experimental Neurology*, *247*, 710–719. https://doi.org/10.1016/j.expneurol.2013.03.012

English, J. D., & David Sweatt, J. (1997). A Requirement for the Mitogen-activated Protein Kinase Cascade in Hippocampal Long Term Potentiation*. In *THE JOURNAL OF BIOLOGICAL CHEMISTRY* (Vol. 272, Issue 31). http://www.jbc.org

Errington, M. L., Galley, P. T., & Bliss, T. V. P. (2003). Long-term potentiation in the dentate gyrus of the anaesthetized rat is accompanied by an increase in extracellular glutamate: Real-time measurements using a novel dialysis electrode. *Philosophical Transactions of the Royal Society B: Biological Sciences*, *358*(1432), 675–687. https://doi.org/10.1098/rstb.2002.1251

Fanselow, M. S., & Dong, H. W. (2010). Are the Dorsal and Ventral Hippocampus Functionally Distinct Structures? In *Neuron* (Vol. 65, Issue 1, pp. 7–19). https://doi.org/10.1016/j.neuron.2009.11.031

Faucher, P., Mons, N., Micheau, J., Louis, C., & Beracochea, D. J. (2016). Hippocampal injections of oligomeric amyloid β-peptide (1-42) induce selective working memory deficits and long-lasting alterations of ERK signaling pathway. *Frontiers in Aging Neuroscience*, *7*(JAN). https://doi.org/10.3389/fnagi.2015.00245

Feld, M., Krawczyk, M. C., Fustiñana, M. S., Blake, M. G., Baratti, C. M., Romano, A., & Boccia, M. M. (2014). Decrease of ERK/MAPK overactivation in prefrontal cortex reverses early memory deficit in a mouse model of alzheimer's disease. *Journal of Alzheimer's Disease*, *40*(1), 69–82. https://doi.org/10.3233/JAD-131076

Fernandez, S. M., Lewis, M. C., Pechenino, A. S., Harburger, L. L., Orr, P. T., Gresack, J. E., Schafe, G. E., & Frick, K. M. (2008). Estradiol-induced enhancement of object memory consolidation involves hippocampal extracellular signal-regulated kinase activation and membrane-bound estrogen receptors. *Journal of Neuroscience*, *28*(35), 8660–8667. https://doi.org/10.1523/JNEUROSCI.1968-08.2008

Foster, T. C., Barnes, C. A., Rao, G., & Mcnaughton, B. L. (1991). Increase in Perforant Path Quantal Size in Aged F-344 Rats. In *Neurobiology of Aging* (Vol. 12).

Fraize, N., Hamieh, A. M., Joseph, M. A., Touret, M., Parmentier, R., Salin, P. A., & Malleret, G. (2017). Differential changes in hippocampal CaMKII and GluA1 activity after memory training involving different levels of adaptive forgetting. *Learning and Memory*, *24*(2), 86–94. https://doi.org/10.1101/lm.043505.116

Freund, T. F., & Buzsáki, G. (1996). Interneurons of the Hippocampus. *Hippocampus*, *6*(4), 347–470. https://doi.org/10.1002/(SICI)1098-1063(1996)6:43.0.CO;2-I

Friedman, D. (2003). Cognition and aging: A highly selective overview of event-related potential (ERP) data. In *Journal of Clinical and Experimental Neuropsychology* (Vol. 25, Issue 5, pp. 702–720). https://doi.org/10.1076/jcen.25.5.702.14578

Friedman, D. (2013). The cognitive aging of episodic memory: A view based on the event-related brain potential. In *Frontiers in Behavioral Neuroscience* (Issue AUG). https://doi.org/10.3389/fnbeh.2013.00111

Froc, D. J., Eadie, B., Li, A. M., Wodtke, K., Tse, M., & Christie, B. R. (2003). Reduced synaptic plasticity in the lateral perforant path input to the dentate gyrus of aged C57BL/6 mice. *Journal of Neurophysiology*, *90*(1), 32–38. https://doi.org/10.1152/jn.00105.2003

Fujii, S., & Sumikawa, K. (2001). Acute and chronic nicotine exposure reverse age-related declines in the induction of long-term potentiation in the rat hippocampus. In *Brain Research* (Vol. 894). www.elsevier.com/locate/bres

Gaffan, D. (1991). Spatial Organization of Episodic. In *HZPPOCAMPUS* (Vol. 1, Issue 3).

Gavilán, M. P., Revilla, E., Pintado, C., Castaño, A., Vizuete, M. L., Moreno-González, I., Baglietto-Vargas, D., Sánchez-Varo, R., Vitorica, J., Gutiérrez, A., & Ruano, D. (2007). Molecular and cellular characterization of the age-related neuroinflammatory processes occurring in normal rat hippocampus: Potential relation with the loss of somatostatin GABAergic neurons. *Journal of Neurochemistry*, *103*(3), 984–996. https://doi.org/10.1111/j.1471-4159.2007.04787.x

Geinisman, Y., Detoledo-Morrell, L., & Morrell, F. (1992). *Comparison of Structural Synaptic Modifications Induced by Long-Term Potentiation in the Hippocampal Dentate Gyrus of Young Adult and Aged Rats*.

Giacobini, E., & Pepeu, G. (2018). Sex and Gender Differences in the Brain Cholinergic System and in the Response to Therapy of Alzheimer Disease with Cholinesterase Inhibitors. *Current Alzheimer Research*, *15*(11), 1077–1084. https://doi.org/10.2174/1567205015666180613111504

Gibbs, R. B. (1998). *Impairment of Basal Forebrain Cholinergic Neurons Associated with Aging and Long-Term Loss of Ovarian Function*.

Gibbs, R. B. (2000). *EFFECTS OF GONADAL HORMONE REPLACEMENT ON MEASURES OF BASAL FOREBRAIN CHOLINERGIC FUNCTION*. www.elsevier.com/locate/neuroscience

Gibbs, R. B. (2010). Estrogen therapy and cognition: A review of the cholinergic hypothesis. In *Endocrine Reviews* (Vol. 31, Issue 2, pp. 224–253). https://doi.org/10.1210/er.2009-0036

Gibbs, R. B., & Aggarwal, P. (1998). *Estrogen and Basal Forebrain Cholinergic Neurons: Implications for Brain Aging and Alzheimer's Disease-Related Cognitive Decline*.

Gibbs, R. B., Nelson, D., & Hammond, R. (2014). Role of GPR30 in mediating estradiol effects on acetylcholine release in the hippocampus. *Hormones and Behavior*, *66*(2), 339–345. https://doi.org/10.1016/j.yhbeh.2014.06.002

Goldman, J. M., Murr, A. S., & Cooper, R. L. (2007). The rodent estrous cycle: Characterization of vaginal cytology and its utility in toxicological studies. In *Birth Defects Research Part B - Developmental and Reproductive Toxicology* (Vol. 80, Issue 2, pp. 84–97). https://doi.org/10.1002/bdrb.20106

Gooney, M., Messaoudi, E., Maher, F. O., Bramham, C. R., & Lynch, M. A. (2004). BDNF-induced LTP in dentate gyrus is impaired with age: Analysis of changes in cell signaling events. *Neurobiology of Aging*, *25*(10), 1323–1331. https://doi.org/10.1016/j.neurobiolaging.2004.01.003

Gooney, M., Shaw, K., Kelly, Á., O'Mara, S. M., & Lynch, M. A. (2002). Long-term potentiation and spatial learning are associated with increased phosphorylation of TrkB and extracellular signal-regulated kinase (ERK) in the dentate gyrus: Evidence for a role for brain-derived neurotrophic factor. *Behavioral Neuroscience*, *116*(3), 455–463. https://doi.org/10.1037/0735-7044.116.3.455

Goral, R. O., Harper, K. M., Bernstein, B. J., Fry, S. A., Lamb, P. W., Moy, S. S., Cushman, J. D., & Yakel, J. L. (2022). Loss of GABA co-transmission from cholinergic neurons impairs behaviors related to hippocampal, striatal, and medial prefrontal cortex functions. *Frontiers in Behavioral Neuroscience*, *16*. https://doi.org/10.3389/fnbeh.2022.1067409

Granger, A. J., Mulder, N., Saunders, A., & Sabatini, B. L. (2016). Cotransmission of acetylcholine and GABA. In *Neuropharmacology* (Vol. 100, pp. 40–46). Elsevier Ltd. https://doi.org/10.1016/j.neuropharm.2015.07.031

Granholm, A.-C. E., Ford, K. A., Hyde, L. A., Bimonte, H. A., Hunter, C. L., Nelson, M., Albeck, D., Sanders, L. A., Mufson, E. J., & Crnic, L. S. (2002). *Estrogen restores cognition and cholinergic phenotype in an animal model of Down syndrome*.

Gruenewald, D. A., Naai, M. A., Marck, B. T., & Matsumoto, A. M. (1994). Age-Related Decrease in Neuropeptide-Y Gene Expression in the Arcuate Nucleus of the Male Rat Brain Is Independent of Testicular Feedback*. In *Endocrinology* (Vol. 134). https://academic.oup.com/endo/article/134/6/2383/3035448

Hajszan, T., Milner, T. A., & Leranth, C. (n.d.). *Sex Steroids and the Dentate Gyrus NIH Public Access*.

Hanse, E., & Gustafsson, B. (1992). Postsynaptic, but Not Presynaptic, Activity Controls the Early Time Course of Long-term Potentiation in the Dentate Gyrus. In *The Journal of Neuroscience* (Vol. 12).

Hargreaves, E. L., Rao, G., Lee, I., & Knierim, J. J. (2005). Neuroscience: Major dissociation between medial and lateral entorhinal input to dorsal hippocampus. *Science*, *308*(5729), 1792–1794. https://doi.org/10.1126/science.1110449

Hasselmo, M. E. (2006). The role of acetylcholine in learning and memory. In *Current Opinion in Neurobiology* (Vol. 16, Issue 6, pp. 710–715). https://doi.org/10.1016/j.conb.2006.09.002

Hattiangady, B., Rao, M. S., Shetty, G. A., & Shetty, A. K. (2005). Brain-derived neurotrophic factor, phosphorylated cyclic AMP response element binding protein and neuropeptide Y decline as early as middle age in the dentate gyrus and CA1 and CA3 subfields of the hippocampus. *Experimental Neurology*, *195*(2), 353–371. https://doi.org/10.1016/j.expneurol.2005.05.014

Hayashi, Y. (2022). Molecular mechanism of hippocampal long-term potentiation – Towards multiscale understanding of learning and memory. In *Neuroscience Research* (Vol. 175, pp. 3–15). Elsevier Ireland Ltd. https://doi.org/10.1016/j.neures.2021.08.001

Hazra, A., Gu, F., Aulakh, A., Berridge, C., Eriksen, J. L., & Žiburkus, J. (2013). Inhibitory Neuron and Hippocampal Circuit Dysfunction in an Aged Mouse Model of Alzheimer's Disease. *PLoS ONE*, *8*(5). https://doi.org/10.1371/journal.pone.0064318

Hilke, S., Holm, L., Åman, K., Hökfelt, T., & Theodorsson, E. (2009). Rapid change of neuropeptide Y levels and gene-expression in the brain of ovariectomized mice after administration of 17β-estradiol. *Neuropeptides*, *43*(4), 327–332. https://doi.org/10.1016/j.npep.2009.04.005

Hintzman, D. L. (1986). 'Schema Abstraction" in a Multiple-Trace Memory Model. In *Psychological Review* (Vol. 93, Issue 4).

Hintzman, D. L., & Block, R. A. (1971). *REPETITION AND MEMORY: EVIDENCE FOR A MULTIPLE-TRACE HYPOTHESIS* ^.

Høegh-Andersen, P., Tankó, L. B., Andersen, T. L., Lundberg, C. v., Mo, J. A., Heegaard, A. M., Delaissé, J. M., & Christgau, S. (2004). Ovariectomized rats as a model of postmenopausal osteoarthritis: validation and application. *Arthritis Research & Therapy*, *6*(2). https://doi.org/10.1186/ar1152

Hojo, Y., & Kawato, S. (2018). Neurosteroids in adult hippocampus of male and female rodents: Biosynthesis and actions of sex steroids. In *Frontiers in Endocrinology* (Vol. 9, Issue APR). Frontiers Media S.A. https://doi.org/10.3389/fendo.2018.00183

Hornick, A., Lieb, A., Vo, N. P., Rollinger, J. M., Stuppner, H., & Prast, H. (2011). The coumarin scopoletin potentiates acetylcholine release from synaptosomes, amplifies hippocampal long-term potentiation and ameliorates anticholinergic- and age-impaired memory. *Neuroscience*, *197*, 280–292. https://doi.org/10.1016/j.neuroscience.2011.09.006

Houser, C. R. (2007). Interneurons of the dentate gyrus: an overview of cell types, terminal fields and neurochemical identity. In *Progress in Brain Research* (Vol. 163). Elsevier. https://doi.org/10.1016/S0079-6123(07)63013-1

Huang, G. Z., & Woolley, C. S. (2012). Estradiol Acutely Suppresses Inhibition in the Hippocampus through a Sex-Specific Endocannabinoid and mGluR-Dependent Mechanism. *Neuron*, *74*(5), 801–808. https://doi.org/10.1016/j.neuron.2012.03.035

Huang, H. H., Steger, R. W., Bruni, J. F., & Meites, J. (1978). *Patterns of Sex Steroid and Gonadotropin Secretion in Aging Female Rats** (Vol. 103, Issue 5).

Hudgens, E. D., Ji, L., Carpenter, C. D., & Petersen, S. L. (2009). The gad2 promoter is a transcriptional target of estrogen receptor (ER) α and ERβ: A unifying hypothesis to explain diverse effects of estradiol. *Journal of Neuroscience*, *29*(27), 8790–8797. https://doi.org/10.1523/JNEUROSCI.1289-09.2009

Hunsaker, M. R., Mooy, G. G., Swift, J. S., & Kesner, R. P. (2007). Dissociations of the Medial and Lateral Perforant Path Projections Into Dorsal DG, CA3, and CA1 for Spatial and Nonspatial (Visual Object) Information Processing. *Behavioral Neuroscience*, *121*(4), 742–750. https://doi.org/10.1037/0735-7044.121.4.742

Hyer, M. M., Phillips, L. L., & Neigh, G. N. (2018). Sex Differences in Synaptic Plasticity: Hormones and Beyond. *Frontiers in Molecular Neuroscience*, *11*. https://doi.org/10.3389/fnmol.2018.00266

Ibrahim, W. W., Ismail, H. M., Khattab, M. M., & Abdelkader, N. F. (2020). Cognitive enhancing effect of diapocynin in D-galactose-ovariectomy-induced Alzheimer's-like disease in rats: Role of ERK, GSK-3β, and JNK signaling. *Toxicology and Applied Pharmacology*, *398*. https://doi.org/10.1016/j.taap.2020.115028

Inagaki, T., Kaneko, N., Zukin, R. S., Castillo, P. E., & Etgen, A. M. (2012). Estradiol attenuates ischemia-induced death of hippocampal neurons and enhances synaptic transmission in aged, long-term hormone-deprived female rats. *PLoS ONE*, *7*(6). https://doi.org/10.1371/journal.pone.0038018

Inoue, S. (2022). Neural basis for estrous cycle-dependent control of female behaviors. In *Neuroscience Research* (Vol. 176, pp. 1–8). Elsevier Ireland Ltd. https://doi.org/10.1016/j.neures.2021.07.001

Iri Geinisman, Y. I., Detoledo-Morrell, L., Morrellt, F., & Heller, R. E. (1995). 0301-0082(94)00047-6 HIPPOCAMPAL MARKERS OF AGE-RELATED MEMORY DYSFUNCTION: BEHAVIORAL, ELECTROPHYSIOLOGICAL AND MORPHOLOGICAL PERSPECTIVES. In *Progress in Neurobiology* (Vol. 45).

Irvine, K., Laws, K. R., Gale, T. M., & Kondel, T. K. (2012). Greater cognitive deterioration in women than men with Alzheimer's disease: A meta analysis. *Journal of Clinical and Experimental Neuropsychology*, *34*(9), 989–998. https://doi.org/10.1080/13803395.2012.712676

Jeffery, K. J., & Morris, R. G. M. (1993). Cumulative long-term potentiation in the rat dentate gyrus correlates with, but does not modify, performance in the water maze. *Hippocampus*, *3*(2), 133–140. https://doi.org/10.1002/hipo.450030205

Jiang, X., Chai, G. S., Wang, Z. H., Hu, Y., Li, X. G., Ma, Z. W., Wang, Q., Wang, J. Z., & Liu, G. P. (2015). CaMKII-dependent dendrite ramification and spine generation promote spatial training-induced memory improvement in a rat model of sporadic Alzheimer's disease. *Neurobiology of Aging*, *36*(2), 867–876. https://doi.org/10.1016/j.neurobiolaging.2014.10.018

Jinno, S., & Kosaka, T. (2006). Cellular architecture of the mouse hippocampus: A quantitative aspect of chemically defined GABAergic neurons with stereology. In *Neuroscience Research* (Vol. 56, Issue 3, pp. 229–245). https://doi.org/10.1016/j.neures.2006.07.007

Kennard, J. A., & Woodruff-Pak, D. S. (2011). Age sensitivity of behavioral tests and brain substrates of normal aging in mice. *Frontiers in Aging Neuroscience*, *3*(MAY), 1–22. https://doi.org/10.3389/fnagi.2011.00009

Kesner, R. P., Crutcher, K. A., Measom, M. O., Kesner, R. P., Crutcher, K. A., & Medial, M. O. M. (1986). Medial Septal and Nucleus Basalis Magnocellularis Lesions Produce Order Memory Deficits in Rats Which Mimic Symptomatology of Alzheimer's Disease. In *Neurobiology of Aging* (Vol. 7).

Khodamoradi, M., Asadi-Shekaari, M., Esmaeili-Mahani, S., Sharififar, F., & Sheibani, V. (2017). Effects of hydroalcoholic extract of soy on learning, memory and synaptic plasticity deficits induced by seizure in ovariectomized rats. *Basic and Clinical Neuroscience*, *8*(5), 395–404. https://doi.org/10.18869/nirp.bcn.8.5.395

Khoury, A. el, & Mathé, A. A. (2004). Neuropeptide Y in euthymic lithium-treated women with bipolar disorder. *Neuropsychobiology*, *50*(3), 239–243. https://doi.org/10.1159/000079978

Kiihler, C., & Eriksson, L. G. (1984). Anatomy and Embryology An immunohistochemical study of somatostatin and neurotensin positive neurons in the septal nuclei of the rat brain. In *Anat Embryol* (Vol. 170).

Kirby, M. T., Hampson, R. E., & Deadwyler, S. A. (1995). Cannabinoids selectively decrease paired-pulse facilitation of perforant path synaptic potentials in the dentate gyrus in vitro. In *Brain Research* (Vol. 688).

Klapstein, G. J., & Colmers, W. F. (1993). On the sites of presynaptic inhibition by neuropeptide y in rat hippocampus in vitro. *Hippocampus*, *3*(1), 103–111. https://doi.org/10.1002/hipo.450030111

Kluess, H. A., Neidert, L. E., Sandage, M. J., & Plexico, L. W. (2019). Neuropeptide y and dipeptidyl peptidase IV in normally cycling and postmenopausal women A prospective pilot study. *Medicine (United States)*, *98*(13). https://doi.org/10.1097/MD.0000000000014982

Koebele, S. v., & Bimonte-Nelson, H. A. (2016). Modeling menopause: The utility of rodents in translational behavioral endocrinology research. In *Maturitas* (Vol. 87, pp. 5–17). Elsevier Ireland Ltd. https://doi.org/10.1016/j.maturitas.2016.01.015

Kullmann, D. M., Moreau, A. W., Bakiri, Y., & Nicholson, E. (2012). Plasticity of Inhibition. *Neuron*, *75*(6), 951–962. https://doi.org/10.1016/j.neuron.2012.07.030

Lacagnina, A. F., Brockway, E. T., Crovetti, C. R., Shue, F., McCarty, M. J., Sattler, K. P., Lim, S. C., Santos, S. L., Denny, C. A., & Drew, M. R. (2019). Distinct hippocampal engrams control extinction and relapse of fear memory. *Nature Neuroscience*, *22*(5), 753–761. https://doi.org/10.1038/s41593-019-0361-z

Ledoux, V. A., Smejkalova, T., May, R. M., Cooke, B. M., & Woolley, C. S. (2009). Estradiol facilitates the release of neuropeptide y to suppress hippocampus-dependent seizures. *Journal of Neuroscience*, *29*(5), 1457–1468. https://doi.org/10.1523/JNEUROSCI.4688-08.2009

Lee, C. T., Kao, M. H., Hou, W. H., Wei, Y. T., Chen, C. L., & Lien, C. C. (2016). Causal Evidence for the Role of Specific GABAergic Interneuron Types in Entorhinal Recruitment of Dentate Granule Cells. *Scientific Reports*, *6*. https://doi.org/10.1038/srep36885

Lee, H.-K., Takamiya, K., Han, J.-S., Man, H., Kim, C.-H., Rumbaugh, G., Yu, S., Ding, L., He, C., Petralia, R. S., Wenthold, R. J., Gallagher, M., & Huganir, R. L. (2003). Phosphorylation of the AMPA Receptor GluR1 Subunit Is Required for Synaptic Plasticity and Retention of Spatial Memory GluR1 subunit of AMPA receptors changes with LTP and LTD induction, consistent with a role for GluR1. In *Cell* (Vol. 112).

Lee, J. W., Lee, Y. K., Ban, J. O., Ha, T. Y., Yun, Y. P., Han, S. B., Oh, K. W., & Hong, J. T. (2009). Green tea (-)-epigallocatechin-3-gallate inhibits β-amyloid-induced cognitive dysfunction through modification of secretase activity via inhibition of ERK and NF-κB pathways in mice. *Journal of Nutrition*, *139*(10), 1987–1993. https://doi.org/10.3945/jn.109.109785

Lee, S. J. R., Escobedo-Lozoya, Y., Szatmari, E. M., & Yasuda, R. (2009). Activation of CaMKII in single dendritic spines during long-term potentiation. *Nature*, *458*(7236), 299–304. https://doi.org/10.1038/nature07842

Leutgeb, J. K., Leutgeb, S., Moser, M.-B., & Moser, E. I. (2007). *Pattern Separation in the Dentate Gyrus and CA3 of the Hippocampus*. www.sciencemag.org

Li, Y., Chen, Y., Gao, X., & Zhang, Z. (2017). The behavioral deficits and cognitive impairment are correlated with decreased IGF-II and ERK in depressed mice induced by chronic unpredictable stress. *International Journal of Neuroscience*, *127*(12), 1096–1103. https://doi.org/10.1080/00207454.2017.1337014

Light, L. L. (1991). *MEMORY AND AGING: FOUR HYPOTHESES IN SEARCH OF DATA*. www.annualreviews.org

Liguz-Lecznar, M., Dobrzanski, G., & Kossut, M. (2022). Somatostatin and Somatostatin-Containing Interneurons—From Plasticity to Pathology. In *Biomolecules* (Vol. 12, Issue 2). MDPI. https://doi.org/10.3390/biom12020312

Liu, S. bing, & Zhao, M. gao. (2013). Neuroprotective effect of estrogen: Role of nonsynaptic NR2B-containing NMDA receptors. In *Brain Research Bulletin* (Vol. 93, pp. 27–31). https://doi.org/10.1016/j.brainresbull.2012.10.004

Liu, X., Ramirez, S., Pang, P. T., Puryear, C. B., Govindarajan, A., Deisseroth, K., & Tonegawa, S. (2012). Optogenetic stimulation of a hippocampal engram activates fear memory recall. *Nature*, *484*(7394), 381–385. https://doi.org/10.1038/nature11028

Liu, Y. C., Cheng, J. K., & Lien, C. C. (2014). Rapid dynamic changes of dendritic inhibition in the dentate gyrus by presynaptic activity patterns. *Journal of Neuroscience*, *34*(4), 1344–1357. https://doi.org/10.1523/JNEUROSCI.2566-13.2014

Lobo, R. A. (1995). *Benefits and risks of estrogen replacement therapy*.

Lopez-Rojas, J., Heine, M., & Kreutz, M. R. (2016). Plasticity of intrinsic excitability in mature granule cells of the dentate gyrus. *Scientific Reports*, *6*, 1–12. https://doi.org/10.1038/srep21615

Luine, V., Attalla, S., Mohan, G., Costa, A., & Frankfurt, M. (2006). Dietary phytoestrogens enhance spatial memory and spine density in the hippocampus and prefrontal cortex of ovariectomized rats. *Brain Research*, *1126*(1), 183–187. https://doi.org/10.1016/j.brainres.2006.07.016

Luine, V. N. (1985). RESEARCH NOTE Estradiol Increases Choline Acetyltransferase Activity in Specific Basal Forebrain Nuclei and Projection Areas of Female Rats. In *EXPERIMENTAL NEUROLOGY* (Vol. 89).

Lukoyanov, N. v, Andrade, J. Â. P., Madeira, M. D., & Paula-Barbosa, M. M. (1999). *Effects of age and sex on the water maze performance and hippocampal cholinergic ®bers in rats*.

Lutz, C. M., & Osborne, M. A. (2014). Optimizing mouse models of neurodegenerative disorders: Are therapeutics in sight? In *Future Neurology* (Vol. 9, Issue 1, pp. 67–75). https://doi.org/10.2217/fnl.13.66

Lyu, J., Nagarajan, R., Kambali, M., Wang, M., & Rudolph, U. (2022). *Dissecting the cellular basis of age-related cognitive dysfunction: Chronic chemogenetic inhibition of somatostatin-positive interneurons in the dentate gyrus hilus induces memory impairments*. https://doi.org/10.1101/2022.10.05.511002

Madar, A. D., Ewell, L. A., & Jones, M. v. (2019). Pattern separation of spiketrains in hippocampal neurons. *Scientific Reports*, *9*(1). https://doi.org/10.1038/s41598-019-41503-8

Maguire, J. L., Stell, B. M., Rafizadeh, M., & Mody, I. (2005). Ovarian cycle-linked changes in GABAA receptors mediating tonic inhibition alter seizure susceptibility and anxiety. *Nature Neuroscience*, *8*(6), 797–804. https://doi.org/10.1038/nn1469

Maguire, J., & Mody, I. (2007). Neurosteroid synthesis-mediated regulation of GABAA receptors: Relevance to the ovarian cycle and stress. *Journal of Neuroscience*, *27*(9), 2155–2162. https://doi.org/10.1523/JNEUROSCI.4945-06.2007

Makino, Y., Johnson, R. C., Yu, Y., Takamiya, K., & Huganir, R. L. (2011). Enhanced synaptic plasticity in mice with phosphomimetic mutation of the GluA1 AMPA receptor. *Proceedings of the National Academy of Sciences of the United States of America*, *108*(20), 8450–8455. https://doi.org/10.1073/pnas.1105261108

Marder, C. P., & Buonomano, D. v. (2004). Timing and balance of inhibition enhance the effect of long-term potentiation on cell firing. *Journal of Neuroscience*, *24*(40), 8873–8884. https://doi.org/10.1523/JNEUROSCI.2661-04.2004

Maren, S. (1995). NEUROSCIENC[IEIT[RS Sexually dimorphic perforant path long-term potentiation (LTP) in urethane-anesthetized rats. In *Neuroscience Letters* (Vol. 196).

Maren, S., de Oca, B., & Fanselow, M. S. (1994). Sex differences in hippocampal long-term potentiation (LTP) and Pavlovian fear conditioning in rats: positive correlation between LTP and contextual learning. In *Brain Research* (Vol. 661). ELSEVIER.

Marriott, L. K., & Korol, D. L. (2003). Short-term estrogen treatment in ovariectomized rats augments hippocampal acetylcholine release during place learning. *Neurobiology of Learning and Memory*, *80*(3), 315–322. https://doi.org/10.1016/j.nlm.2003.08.003

Martinello, K., Huang, Z., Lujan, R., Tran, B., Watanabe, M., Cooper, E. C., Brown, D. A., & Shah, M. M. (2015). Cholinergic afferent stimulation induces axonal function plasticity in adult hippocampal granule cells. *Neuron*, *85*(2), 346–363. https://doi.org/10.1016/j.neuron.2014.12.030

Marzban Abbasabadi, B., Tadjalli, M., Marzban, B., & Dvm, A. (2016). Effect of soy milk on circulating 17-β estradiol, number of neurons in cerebral cortex and hippocampus and determination of their ratio in neonatal ovariectomized rats. In *Veterinary Research Forum* (Vol. 7, Issue 4).

Masuda, J., Mitsushima, D., Funabashi, T., & Kimura, F. (2005). Sex and housing conditions affect the 24-h acetylcholine release profile in the hippocampus in rats. *Neuroscience*, *132*(2), 537–542. https://doi.org/10.1016/j.neuroscience.2005.01.010

Matsuoka, N., Yamazaki, M., & Yamaguchi, I. (1995). Changes in brain somatostatin in memory-deficient rats: comparison with cholinergic markers. *Neuroscience*, *66*(3), 617–626. https://doi.org/10.1016/0306-4522(94)00628-I

McAvoy, K. M., Scobie, K. N., Berger, S., Russo, C., Guo, N., Decharatanachart, P., Vega-Ramirez, H., Miake-Lye, S., Whalen, M., Nelson, M., Bergami, M., Bartsch, D., Hen, R., Berninger, B., & Sahay, A. (2016). Modulating Neuronal Competition Dynamics in the Dentate Gyrus to Rejuvenate Aging Memory Circuits. *Neuron*, *91*(6), 1356–1373. https://doi.org/10.1016/j.neuron.2016.08.009

McEwen Harold, B. S., & Milliken, M. (1999). *Stress and the Aging Hippocampus*. http://www.idealibrary.com

McGahon, B., Maguire, C., Kelly, A., & Lynch, M. A. (1999). *ACTIVATION OF p42 MITOGEN-ACTIVATED PROTEIN KINASE BY ARACHIDONIC ACID AND TRANS-1-AMINO-CYCLOPENTYL-1,3-DICARBOXYLATE IMPACTS ON LONG-TERM POTENTIATION IN THE DENTATE GYRUS IN THE RAT: ANALYSIS OF AGE-RELATED CHANGES*.

McLean, A. C., Valenzuela, N., Fai, S., & Bennett, S. A. L. (2012). Performing vaginal lavage, crystal violet staining, and vaginal cytological evaluation for mouse estrous cycle staging identification. *Journal of Visualized Experiments*, *67*. https://doi.org/10.3791/4389

Mehta, J., Kling, J. M., & Manson, J. A. E. (2021). Risks, Benefits, and Treatment Modalities of Menopausal Hormone Therapy: Current Concepts. In *Frontiers in Endocrinology* (Vol. 12). Frontiers Media S.A. https://doi.org/10.3389/fendo.2021.564781

Mesulam, M. M., Mufson, E. J., Wainer, B. H., & Levey, A. I. (1983). Central cholinergic pathways in the rat: An overview based on an alternative nomenclature (Ch1-Ch6). *Neuroscience*, *10*(4), 1185–1201. https://doi.org/10.1016/0306-4522(83)90108-2

Michalkiewicz, M., Knestaut, K. M., Bytchkova, E. Y., & Michalkiewicz, T. (2003). Hypotension and reduced catecholamines in neuropeptide Y transgenic rats. *Hypertension*, *41*(5), 1056–1062. https://doi.org/10.1161/01.HYP.0000066623.64368.4E

Mielke, M. M., Vemuri, P., & Rocca, W. A. (2014). Clinical epidemiology of Alzheimer's disease: Assessing sex and gender differences. In *Clinical Epidemiology* (Vol. 6, Issue 1, pp. 37–48). https://doi.org/10.2147/CLEP.S37929

Miettinen, R. A., Kalesnykas, G., & Koivisto, E. H. (2002). Estimation of the Total Number of Cholinergic Neurons Containing Estrogen Receptor-in the Rat Basal Forebrain. In *The Journal of Histochemistry & Cytochemistry* (Vol. 50, Issue 7). http://www.jhc.org

Miller, A. E., & Riegle, G. D. (1982). Temporal Patterns of Serum Luteinizing Hormone and Testosterone and Endocrine Response to Luteinizing Hormone Releasing Hormone in Aging Male Rats 1. In *Journal of Gerontology* (Vol. 37, Issue 5).

Miranda, P., Williams, C. L., & Einstein, G. (1999). *Granule Cells in Aging Rats Are Sexually Dimorphic in Their Response to Estradiol*.

Mitchell, S. J., Scheibye-Knudsen, M., Longo, D. L., & de Cabo, R. (2015). Animal models of aging research: Implications for human aging and age-related diseases. *Annual Review of Animal Biosciences*, *3*, 283–303. https://doi.org/10.1146/annurev-animal-022114-110829

Mitsushima, D., Masuda, J., & Kimura, F. (2003). Sex differences in the stress-induced release of acetylcholine in the hippocampus and corticosterone from the adrenal cortex in rats. *Neuroendocrinology*, *78*(4), 234–240. https://doi.org/10.1159/000073707

Mitsushima, D., Takase, K., Takahashi, T., & Kimura, F. (2009). Activational and organisational effects of gonadal steroids on sex-specific acetylcholine release in the dorsal hippocampus. *Journal of Neuroendocrinology*, *21*(4), 400–405. https://doi.org/10.1111/j.1365-2826.2009.01848.x

Mo, L., Ren, Q., Duchemin, A. M., Neff, N. H., & Hadjiconstantinou, M. (2005). GM1 and ERK signaling in the aged brain. *Brain Research*, *1054*(2), 125–134. https://doi.org/10.1016/j.brainres.2005.06.068

Morris, A. M., Churchwell, J. C., Kesner, R. P., & Gilbert, P. E. (2012). Selective lesions of the dentate gyrus produce disruptions in place learning for adjacent spatial locations. *Neurobiology of Learning and Memory*, *97*(3), 326–331. https://doi.org/10.1016/j.nlm.2012.02.005

Morris, R. G. M. (1989). *Synaptic Plasticity and Learning: Selective Impairment of Learning in Rats and Blockade of Long-Term Potentiation in viva by the IV-Methyl-D-Aspartate Receptor Antagonist AP5*.

Moscovitch, M. (1995). Recovered Consciousness: A Hypothesis Concerning Modularity and Episodic Memory*. *Journal of Clinical and Experimental Neuropsychology*, *17*(2), 276–290. https://doi.org/10.1080/01688639508405123

Moser, I. K. K. M. M. M. R. (1998). science.281.5385.2038. *Science*.

Mufson, E. J., Cai, W. J., Jaffar, S., Chen, E.-Y., Stebbins, G., Sendera, T., & Kordower, J. H. (1999). Estrogen receptor immunoreactivity within subregions of the rat forebrain: neuronal distribution and association with perikarya containing choline acetyltransferase 1. In *Brain Research* (Vol. 849). www.elsevier.comrlocaterbres

Muthyala, R. S., Ju, Y. H., Sheng, S., Williams, L. D., Doerge, D. R., Katzenellenbogen, B. S., Helferich, W. G., & Katzenellenbogen, J. A. (2004). Equol, a natural estrogenic metabolite from soy isoflavones: Convenient preparation and resolution of R- and S-equols and their differing binding and biological activity through estrogen receptors alpha and beta. *Bioorganic and Medicinal Chemistry*, *12*(6), 1559–1567. https://doi.org/10.1016/j.bmc.2003.11.035

Nadel, L., & Moscovitcht, M. (1997). Memory consolidation, retrograde amnesia and the hippocampal complex. *Current Opinion in Neurobiology*, *7*, 217–227.

Nahvi, R. J., & Sabban, E. L. (2020). Sex differences in the neuropeptide Y system and implications for stress related disorders. In *Biomolecules* (Vol. 10, Issue 9, pp. 1–21). MDPI AG. https://doi.org/10.3390/biom10091248

Nakamura, N., Fujita, H., & Kawata, M. (2002). *EFFECTS OF GONADECTOMY ON IMMUNOREACTIVITY FOR CHOLINE ACETYLTRANSFERASE IN THE CORTEX, HIPPOCAMPUS, AND BASAL FOREBRAIN OF ADULT MALE RATS*. www.neuroscience-ibro.com

Nebieridze, N., Zhang, X. lei, Chachua, T., Velíšek, L., Stanton, P. K., & Velíšková, J. (2012). β-Estradiol unmasks metabotropic receptor-mediated metaplasticity of NMDA receptor transmission in the female rat dentate gyrus. *Psychoneuroendocrinology*, *37*(11), 1845–1854. https://doi.org/10.1016/j.psyneuen.2012.03.023

Nelson, J. F., Felicio, L. S., Osterburg, H. H., & Finch, C. E. (1981). *Altered Profiles of Estradiol and Progesterone Associated with Prolonged Estrous Cycles and Persistent Vaginal Cornification in Aging C578L/6J Mice1*. https://academic.oup.com/biolreprod/article/24/4/784/2766994

Nelson, J. F., S Felicio, L. da, Randall, P. K., Sims, C., & Finch, C. E. (1982). A Longitudinal Study of Estrous Cyclicity in Aging C57BL/6J Mice: I. Cycle Frequency, Length and Vaginal Cytology1. In *BIOLOGY OF REPRODUCTION* (Vol. 27). https://academic.oup.com/biolreprod/article/27/2/327/2767330

Newton, I. G., Forbes, M. E., Linville, M. C., Pang, H., Tucker, E. W., Riddle, D. R., & Brunso-Bechtold, J. K. (2008). Effects of aging and caloric restriction on dentate gyrus synapses and glutamate receptor subunits. *Neurobiology of Aging*, *29*(9), 1308–1318. https://doi.org/10.1016/j.neurobiolaging.2007.03.009

Nguyen, P. v, & Kandel, E. R. (1997). *Brief O-Burst Stimulation Induces a Transcription-Dependent Late Phase of LTP Requiring cAMP in Area CA I of the Mouse Hippocampus*.

Nichols, E., Szoeke, C. E. I., Vollset, S. E., Abbasi, N., Abd-Allah, F., Abdela, J., Aichour, M. T. E., Akinyemi, R. O., Alahdab, F., Asgedom, S. W., Awasthi, A., Barker-Collo, S. L., Baune, B. T., Béjot, Y., Belachew, A. B., Bennett, D. A., Biadgo, B., Bijani, A., bin Sayeed, M. S., … Murray, C. J. L. (2019). Global, regional, and national burden of Alzheimer's disease and other dementias, 1990–2016: a systematic analysis for the Global Burden of Disease Study 2016. *The Lancet Neurology*, *18*(1), 88–106. https://doi.org/10.1016/S1474-4422(18)30403-4

Nicoll, R. A. (2017). A Brief History of Long-Term Potentiation. In *Neuron* (Vol. 93, Issue 2, pp. 281–290). Cell Press. https://doi.org/10.1016/j.neuron.2016.12.015

Nicolle, M. M., Shivers, § A, Gill, T. M., & Gallagher, M. (1997). *HIPPOCAMPAL N-METHYL-□-ASPARTATE AND KAINATE BINDING IN RESPONSE TO ENTORHINAL CORTEX ASPIRATION OR 192 IgG-SAPORIN LESIONS OF THE BASAL FOREBRAIN*.

Nitz, D., & McNaughton, B. (2004). Differential Modulation of CA1 and Dentate Gyrus Interneurons during Exploration of Novel Environments. *Journal of Neurophysiology*, *91*(2), 863–872. https://doi.org/10.1152/jn.00614.2003

Nyberg, L., Lövdén, M., Riklund, K., Lindenberger, U., & Bäckman, L. (2012). Memory aging and brain maintenance. In *Trends in Cognitive Sciences* (Vol. 16, Issue 5, pp. 292–305). https://doi.org/10.1016/j.tics.2012.04.005

Nyberg, L., & Tulving, E. (1996). Classifying human long-term memory: Evidence from converging dissociations. *European Journal of Cognitive Psychology*, *8*(2), 163–184. https://doi.org/10.1080/095414496383130

Ogando, M. B., Pedroncini, O., Federman, N., Romano, S. A., Brum, L. A., Lanuza, G. M., Refojo, D., & Marin-Burgin, A. (2021). Cholinergic modulation of dentate gyrus processing through dynamic reconfiguration of inhibitory circuits. *Cell Reports*, *36*(8). https://doi.org/10.1016/j.celrep.2021.109572

Ooishi, Y., Kawato, S., Hojo, Y., Hatanaka, Y., Higo, S., Murakami, G., Komatsuzaki, Y., Ogiue-Ikeda, M., Kimoto, T., & Mukai, H. (2012). Modulation of synaptic plasticity in the hippocampus by hippocampus-derived estrogen and androgen. In *Journal of Steroid Biochemistry and Molecular Biology* (Vol. 131, Issues 1–2, pp. 37–51). https://doi.org/10.1016/j.jsbmb.2011.10.004

Palacios-Filardo, J., & Mellor, J. R. (2019). Neuromodulation of hippocampal long-term synaptic plasticity. *Current Opinion in Neurobiology*, *54*(September), 37–43. https://doi.org/10.1016/j.conb.2018.08.009

Pang, K., Williams, M. J., & Olton, D. S. (n.d.). *Activation of the medial septal area attenuates LTP of the lateral perforant path and enhances heterosynaptic LTD of the medial perforant path in aged rats*.

Park, P., Volianskis, A., Sanderson, T. M., Bortolotto, Z. A., Jane, D. E., Zhuo, M., Kaang, B. K., & Collingridge, G. L. (2014). NMDA receptor-dependent long-term potentiation comprises a family of temporally overlapping forms of synaptic plasticity that are induced by different patterns of stimulation. In *Philosophical Transactions of the Royal Society B: Biological Sciences* (Vol. 369, Issue 1633). Royal Society. https://doi.org/10.1098/rstb.2013.0131

Patrylo, P. R., Tyagi, I., Willingham, A. L., Lee, S., & Williamson, A. (2007). Dentate filter function is altered in a proepileptic fashion during aging. *Epilepsia*, *48*(10), 1964–1978. https://doi.org/10.1111/j.1528-1167.2007.01139.x

Pawluski, J. L., Brummelte, S., Barha, C. K., Crozier, T. M., & Galea, L. A. M. (2009). Effects of steroid hormones on neurogenesis in the hippocampus of the adult female rodent during the estrous cycle, pregnancy, lactation and aging. In *Frontiers in Neuroendocrinology* (Vol. 30, Issue 3, pp. 343–357). https://doi.org/10.1016/j.yfrne.2009.03.007

Pereda, D., Al-Osta, I., Okorocha, A. E., Easton, A., & Hartell, N. A. (2019). Changes in presynaptic calcium signalling accompany age-related deficits in hippocampal LTP and cognitive impairment. *Aging Cell*, *18*(5). https://doi.org/10.1111/acel.13008

Perez-Martin, M., Salazar, V., Castillo, C., Ariznavarreta, C., Azcoitia, I., Garcia-Segura, L. M., & Tresguerres, J. A. F. (2005). Estradiol and soy extract increase the production of new cells in the dentate gyrus of old rats. *Experimental Gerontology*, *40*(5), 450–453. https://doi.org/10.1016/j.exger.2005.03.003

Persson, J., Pudas, S., Lind, J., Kauppi, K., Nilsson, L. G., & Nyberg, L. (2012). Longitudinal structure-function correlates in elderly reveal MTL dysfunction with cognitive decline. *Cerebral Cortex*, *22*(10), 2297–2304. https://doi.org/10.1093/cercor/bhr306

Perusini, J. N., Cajigas, S. A., Cohensedgh, O., Lim, S. C., Pavlova, I. P., Donaldson, Z. R., & Denny, C. A. (2017). Optogenetic stimulation of dentate gyrus engrams restores memory in Alzheimer's disease mice. *Hippocampus*, *27*(10), 1110–1122. https://doi.org/10.1002/hipo.22756

Petrantonakis, P. C., & Poirazi, P. (2014). A compressed sensing perspective of hippocampal function. *Frontiers in Systems Neuroscience*, *8*(AUG). https://doi.org/10.3389/fnsys.2014.00141

Pilch, H., & Miiller, W. E. (1988). Chronic treatment with choline or scopolamine indicates the presence of muscarinic cholinergic receptor plasticity in the frontal cortex of young but not of aged mice. In *J Neural Transm* (Vol. 71).

Prince, L. Y., Bacon, T. J., Tigaret, C. M., & Mellor, J. R. (2016). Neuromodulation of the feedforward dentate gyrus-CA3 microcircuit. *Frontiers in Synaptic Neuroscience*, *8*(OCT). https://doi.org/10.3389/fnsyn.2016.00032

Racine, R. J., Milgram, N. W., & Hafner, S. (1983). Long-term Potentiation Phenomena in the Rat Limbic Forebrain. In *Brain Research* (Vol. 260).

Ramirez, S., Liu, X., Lin, P. A., Suh, J., Pignatelli, M., Redondo, R. L., Ryan, T. J., & Tonegawa, S. (2013). Creating a false memory in the hippocampus. *Science*, *341*(6144), 387–391. https://doi.org/10.1126/science.1239073

Ramos, B., Baglietto-Vargas, D., Rio, J. C. del, Moreno-Gonzalez, I., Santa-Maria, C., Jimenez, S., Caballero, C., Lopez-Tellez, J. F., Khan, Z. U., Ruano, D., Gutierrez, A., & Vitorica, J. (2006). Early neuropathology of somatostatin/NPY GABAergic cells in the hippocampus of a PS1 × APP transgenic model of Alzheimer's disease. *Neurobiology of Aging*, *27*(11), 1658–1672. https://doi.org/10.1016/j.neurobiolaging.2005.09.022

Rangani, R. J., Upadhya, M. A., Nakhate, K. T., Kokare, D. M., & Subhedar, N. K. (2012). Nicotine evoked improvement in learning and memory is mediated through NPY Y1 receptors in rat model of Alzheimer's disease. *Peptides*, *33*(2), 317–328. https://doi.org/10.1016/j.peptides.2012.01.004

Raymond, C. R. (2007). LTP forms 1, 2 and 3: different mechanisms for the “long” in long-term potentiation. In *Trends in Neurosciences* (Vol. 30, Issue 4, pp. 167–175). https://doi.org/10.1016/j.tins.2007.01.007

Raza, S. A., Albrecht, A., Çallşkan, G., Müller, B., Demiray, Y. E., Ludewig, S., Meis, S., Faber, N., Hartig, R., Schraven, B., Lessmann, V., Schwegler, H., & Stork, O. (2017). HIPP neurons in the dentate gyrus mediate the cholinergic modulation of background context memory salience. *Nature Communications*, *8*(1). https://doi.org/10.1038/s41467-017-00205-3

Redrobe, J. P., Dumont, Y., Herzog, H., & Quirion, R. (2004). *Characterization of Neuropeptide Y, Y 2 Receptor Knockout Mice in Two Animal Models of Learning and Memory Processing*.

Rosenblum, K., Dudai, Y., & Richter-Levint, G. (1996). Long-term potentiation increases tyrosine phosphorylation of the N-methyl-D-aspartate receptor subunit 2B in rat dentate gyrus in vivo. In *Neurobiology* (Vol. 93). https://www.pnas.org

Rosenblum, K., Futter, M., Jones, M., Hulme, E. C., & Bliss, T. V. P. (2000). *ERKI/II Regulation by the Muscarinic Acetylcholine Receptors in Neurons*.

Rot-Y Mcquiston, A., Petrozzino, J. J., Connor, J. A., Colmersl, W. F., & Roche, *. (1996). Neuropeptide Y, Receptors Inhibit N-Type Calcium Currents and Reduce Transient Calcium Increases in Rat Dentate Granule Cells. In *The Journal of Neuroscience* (Vol. 16, Issue 4).

Roy, D. S., Arons, A., Mitchell, T. I., Pignatelli, M., Ryan, T. J., & Tonegawa, S. (2016). Memory retrieval by activating engram cells in mouse models of early Alzheimer’s disease. *Nature*, *531*(7595), 508–512. https://doi.org/10.1038/nature17172

Rubenstein, J. L. R., & Merzenich, M. M. (2003). *Model of autism: increased ratio of excitation/inhibition in key neural systems*.

Rugarn, O., Hammar, M., Theodorsson, A., Theodorsson, E., & Stenfors, C. (1999). *Sex differences in neuropeptide distribution in the rat brain*.

Russell, J. K., Jones, C. K., & Newhouse, P. A. (2019). The Role of Estrogen in Brain and Cognitive Aging. In *Neurotherapeutics* (Vol. 16, Issue 3, pp. 649–665). Springer New York LLC. https://doi.org/10.1007/s13311-019-00766-9

Sambandan, S., Sauer, J. F., Vida, I., & Bartos, M. (2010). Associative plasticity at excitatory synapses facilitates recruitment of fast-spiking interneurons in the dentate gyrus. *Journal of Neuroscience*, *30*(35), 11826–11837. https://doi.org/10.1523/JNEUROSCI.2012-10.2010

Sandhu, K. v., Yanagawa, Y., & Stork, O. (2015). Transcriptional regulation of glutamic acid decarboxylase in the male mouse amygdala by dietary phyto-oestrogens. *Journal of Neuroendocrinology*, *27*(4), 285–292. https://doi.org/10.1111/jne.12262

Saransaari, P. (1995). ELSEVIER Mechanisms of Ageing and Development and dl?wloplIMt Age-related changes in the uptake and release of glutamate and aspartate in the mouse brain. In *Oja / Mechanisms of' Ageing and Deuelopntent* (Vol. 81).

Satistegui, J., Viilalba, M., Pexeira, R., Bog6nez, E., & Mardnez-Serrano, A. (1996). CYTOSOLIC AND MlTOCHONDRIAL CALCIUM IN SYNAPTOSOMES DURING AGING. In *Life seienecr* (Vol. 59, Issue 6). Facvier scieme Inc.

Savanthrapadian, S., Meyer, T., Elgueta, C., Booker, S. A., Vida, I., & Bartos, M. (2014). Synaptic properties of SOM-and CCK-expressing cells in dentate gyrus interneuron networks. *Journal of Neuroscience*, *34*(24), 8197–8209. https://doi.org/10.1523/JNEUROSCI.5433-13.2014

Sawano, E., Iwatani, K., Tominaga-Yoshino, K., Ogura, A., & Tashiro, T. (2015). Reduction in NPY-positive neurons and dysregulation of excitability in young senescence-accelerated mouse prone 8 (SAMP8) hippocampus precede the onset of cognitive impairment. *Journal of Neurochemistry*, *135*(2), 287–300. https://doi.org/10.1111/jnc.13274

Sayed, S., van Dam, N. T., Horn, S. R., Kautz, M. M., Parides, M., Costi, S., Collins, K. A., Iacoviello, B., Iosifescu, D. v., Mathé, A. A., Southwick, S. M., Feder, A., Charney, D. S., & Murrough, J. W. (2018). A Randomized Dose-Ranging Study of Neuropeptide y in Patients with Posttraumatic Stress Disorder. *International Journal of Neuropsychopharmacology*, *21*(1), 3–11. https://doi.org/10.1093/ijnp/pyx109

Scheff, S. W., Price, D. A., Schmitt, F. A., & Mufson, E. J. (2006). Hippocampal synaptic loss in early Alzheimer's disease and mild cognitive impairment. *Neurobiology of Aging*, *27*(10), 1372–1384. https://doi.org/10.1016/j.neurobiolaging.2005.09.012

Schliebs, R., & Arendt, T. (2011). The cholinergic system in aging and neuronal degeneration. *Behavioural Brain Research*, *221*(2), 555–563. https://doi.org/10.1016/j.bbr.2010.11.058

Schreurs, A., Sabanov, V., & Balschun, D. (2017). Distinct Properties of Long-Term Potentiation in the Dentate Gyrus along the Dorsoventral Axis: Influence of Age and Inhibition. *Scientific Reports*, *7*(1). https://doi.org/10.1038/s41598-017-05358-1

Schulz, S., Siemer, H., Krug, M., & Hö, V. (1999). *Direct Evidence for Biphasic cAMP Responsive Element-Binding Protein Phosphorylation during Long-Term Potentiation in the Rat Dentate Gyrus In Vivo*.

Schurmans, S., Schiffmann, S. N., Gurden, H., Lemaire, M., Lipp, H., Schwam, V., Pochet, R., Imperato, A., Andrees, G. B., & Parmentier, M. (1997). *Impaired long-term potentiation induction in dentate gyrus of calretinin-deficient mice* (Vol. 94). www.pnas.org.

Schwartzkroin, P. A., & Wester, K. (1975). H I P P O C A M P A L SLICE. In *Brain Research* (Vol. 89).

Seese, R. R., Maske, A. R., Lynch, G., & Gall, C. M. (2014). Long-term memory deficits are associated with elevated synaptic ERK1/2 activation and reversed by mGluR5 antagonism in an animal model of autism. *Neuropsychopharmacology*, *39*(7), 1664–1673. https://doi.org/10.1038/npp.2014.13

Seo, S. Y., Moon, J. Y., Kang, S. Y., Kwon, O. S., Kwon, S., Bang, S. K., Kim, S. P., Choi, K. H., & Ryu, Y. (2018). An estradiol-independent BDNF-NPY cascade is involved in the antidepressant effect of mechanical acupuncture instruments in ovariectomized rats. *Scientific Reports*, *8*(1). https://doi.org/10.1038/s41598-018-23824-2

Sha, S., Xu, J., Lu, Z. H., Hong, J., Qu, W. J., Zhou, J. W., & Chen, L. (2016). Lack of JWA Enhances Neurogenesis and Long-Term Potentiation in Hippocampal Dentate Gyrus Leading to Spatial Cognitive Potentiation. *Molecular Neurobiology*, *53*(1), 355–368. https://doi.org/10.1007/s12035-014-9010-4

Shapiro, M. (2001). Plasticity, Hippocampal Place Cells, and Cognitive Maps. In *BASIC SCIENCE SEMINARS IN NEUROLOGY (REPRINTED) ARCH NEUROL* (Vol. 58). https://jamanetwork.com/

Sheppard, P. A. S., Choleris, E., & Galea, L. A. M. (2019). Structural plasticity of the hippocampus in response to estrogens in female rodents. In *Molecular Brain* (Vol. 12, Issue 1). BioMed Central Ltd. https://doi.org/10.1186/s13041-019-0442-7

Shetty, A. K., & Turner, D. A. (1999). *Vulnerability of the Dentate Gyrus to Aging and Intracerebroventricular Administration of Kainic Acid*. http://www.idealibrary.com

Shew, W. L., Yang, H., Yu, S., Roy, R., & Plenz, D. (2011). Information capacity and transmission are maximized in balanced cortical networks with neuronal avalanches. *Journal of Neuroscience*, *31*(1), 55–63. https://doi.org/10.1523/JNEUROSCI.4637-10.2011

Si, W., Zhang, X., Niu, Y., Yu, H., Lei, X., Chen, H., & Cao, X. (2010). A novel derivative of xanomeline improves fear cognition in aged mice. *Neuroscience Letters*, *473*(2), 115–119. https://doi.org/10.1016/j.neulet.2010.02.031

Silva, A. P., Xapelli, S., Grouzmann, E., & Cavadas, C. (2005). The Putative Neuroprotective Role of Neuropeptide Y in the Central Nervous System. In *Current Drug Targets-CNS & Neurological Disorders* (Vol. 4).

A. W. Smith, M. A. B. E. J. W. O. K. R. and M. J. K. (2013). The membrane estrogen receptor ligand STX rapidly enhances GABAergic signaling in NPY/AgRP neurons: role in mediating the anorexigenic effects of 17β-estradiol. *Am J Physiol Endocrinol Metab*, *305*(5),E632–E640. ttps://www.ncbi.nlm.nih.gov/pmc/articles/PMC3761166/#__ffn_sectitle

Smith, C. C., & McMahon, L. L. (2006). Estradiol-induced increase in the magnitude of long-term potentiation is prevented by blocking NR2B-containing receptors. *Journal of Neuroscience*, *26*(33), 8517–8522. https://doi.org/10.1523/JNEUROSCI.5279-05.2006

Smith, C. C., Vedder, L. C., & McMahon, L. L. (2009). Estradiol and the relationship between dendritic spines, NR2B containing NMDA receptors, and the magnitude of long-term potentiation at hippocampal CA3-CA1 synapses. *Psychoneuroendocrinology*, *34*(SUPPL. 1). https://doi.org/10.1016/j.psyneuen.2009.06.003

Smith, C. C., Vedder, L. C., Nelson, A. R., Bredemann, T. M., & McMahon, L. L. (2010). Duration of estrogen deprivation, not chronological age, prevents estrogen's ability to enhance hippocampal synaptic physiology. *Proceedings of the National Academy of Sciences of the United States of America*, *107*(45), 19543–19548. https://doi.org/10.1073/pnas.1009307107

Sohal, V. S., & Rubenstein, J. L. R. (2019). Excitation-inhibition balance as a framework for investigating mechanisms in neuropsychiatric disorders. *Molecular Psychiatry*, *24*(9), 1248–1257. https://doi.org/10.1038/s41380-019-0426-0

Sperk, G., Hamilton, T., & Colmers, W. F. (2007). Neuropeptide Y in the dentate gyrus. In *Progress in Brain Research* (Vol. 163, pp. 285–297). https://doi.org/10.1016/S0079-6123(07)63017-9

Spiegel, A. M., Koh, M. T., Vogt, N. M., Rapp, P. R., & Gallagher, M. (2013). Hilar interneuron vulnerability distinguishes aged rats with memory impairment. *Journal of Comparative Neurology*, *521*(15), 3508–3523. https://doi.org/10.1002/cne.23367

Squire, L. R. (2009). Memory and brain systems: 1969-2009. In *Journal of Neuroscience* (Vol. 29, Issue 41, pp. 12711–12716). https://doi.org/10.1523/JNEUROSCI.3575-09.2009

Squire, L. R., & Zola, S. M. (1996). *Memory: Recording Experience in Cells and Circuits* (Vol. 93). https://www.pnas.org

Stanley, D. P., & Shetty, A. K. (2004). Aging in the rat hippocampus is associated with widespread reductions in the number of glutamate decarboxylase-67 positive interneurons but not interneuron degeneration. *Journal of Neurochemistry*, *89*(1), 204–216. https://doi.org/10.1111/j.1471-4159.2004.02318.x

Stephens, M. L., Quintero, J. E., Pomerleau, F., Huettl, P., & Gerhardt, G. A. (2011). Age-related changes in glutamate release in the CA3 and dentate gyrus of the rat hippocampus. *Neurobiology of Aging*, *32*(5), 811–820. https://doi.org/10.1016/j.neurobiolaging.2009.05.009

Sung, H. Y., Park, K. A., Kwon, S., Woolley, C. S., Sullivan, P. M., Pasternak, J. F., & Trommer, B. L. (2007). Estradiol enhances long term potentiation in hippocampal slices from aged ApoE4-TR mice. *Hippocampus*, *17*(12), 1153–1157. https://doi.org/10.1002/hipo.20357

Sweatt, J. D. (2008). *4.16 Long-Term Potentiation: A Candidate Cellular Mechanism for Information Storage in the CNS*.

Takács, V. T., Cserép, C., Schlingloff, D., Pósfai, B., Szőnyi, A., Sos, K. E., Környei, Z., Dénes, Á., Gulyás, A. I., Freund, T. F., & Nyiri, G. (2018). Co-transmission of acetylcholine and GABA regulates hippocampal states. *Nature Communications*, *9*(1). https://doi.org/10.1038/s41467-018-05136-1

Talpos, J. C., Dias, R., Bussey, T. J., & Saksida, L. M. (2008). Hippocampal lesions in rats impair learning and memory for locations on a touch-sensitive computer screen: The "ASAT" task. *Behavioural Brain Research*, *192*(2), 216–225. https://doi.org/10.1016/j.bbr.2008.04.008

Tao, X., Yan, M., Wang, L., Zhou, Y., Wang, Z., Xia, T., Liu, X., Pan, R., & Chang, Q. (2020). Effects of estrogen deprivation on memory and expression of related proteins in ovariectomized mice. *Annals of Translational Medicine*, *8*(6), 356–356. https://doi.org/10.21037/atm.2020.02.57

Tasan, R. O., Verma, D., Wood, J., Lach, G., Hörmer, B., de Lima, T. C. M., Herzog, H., & Sperk, G. (2016). The role of Neuropeptide Y in fear conditioning and extinction. In *Neuropeptides* (Vol. 55, pp. 111–126). Churchill Livingstone. https://doi.org/10.1016/j.npep.2015.09.007

Teles-Grilo Ruivo, L. M., Baker, K. L., Conway, M. W., Kinsley, P. J., Gilmour, G., Phillips, K. G., Isaac, J. T. R., Lowry, J. P., & Mellor, J. R. (2017). Coordinated Acetylcholine Release in Prefrontal Cortex and Hippocampus Is Associated with Arousal and Reward on Distinct Timescales. *Cell Reports*, *18*(4), 905–917. https://doi.org/10.1016/j.celrep.2016.12.085

Thomas, G. M., & Huganir, R. L. (2004). MAPK cascade signalling and synaptic plasticity. In *Nature Reviews Neuroscience* (Vol. 5, Issue 3, pp. 173–183). Nature Publishing Group. https://doi.org/10.1038/nrn1346

Thorsell, A., Michalkiewicz, M., Dumont, Y., Quirion, R., Caberlotto, L., Rimondini, R., Mathé, A. A., & Heilig, M. (2000). *Behavioral insensitivity to restraint stress, absent fear suppression of behavior and impaired spatial learning in transgenic rats with hippocampal neuropeptide Y overexpression*. www.pnas.orgcgidoi10.1073pnas.220232997

Tischmeyer, W., & Grimm, R. (1999). Activation of immediate early genes and memory formation. In *CMLS, Cell. Mol. Life Sci* (Vol. 55).

Titolo, D., Mayer, C. M., Dhillon, S. S., Cai, F., & Belsham, D. D. (2008). Estrogen facilitates both phosphatidylinositol 3-kinase/Akt and ERK1/2 mitogen-activated protein kinase membrane signaling required for long-term neuropeptide Y transcriptional regulation in clonal, immortalized neurons. *Journal of Neuroscience*, *28*(25), 6473–6482. https://doi.org/10.1523/JNEUROSCI.0514-08.2008

Tonegawa, S., & McHugh, T. J. (2007). Molecular and Circuit Mechanisms for Hippocampal Learning. *Retrotransposition, Diversity and the Brain*, 13–19. https://doi.org/10.1007/978-3-540-74966-0_2

Tran, T., Bridi, M., Koh, M. T., Gallagher, M., & Kirkwood, A. (2019). Reduced cognitive performance in aged rats correlates with increased excitation/inhibition ratio in the dentate gyrus in response to lateral entorhinal input. *Neurobiology of Aging*, *82*, 120–127. https://doi.org/10.1016/j.neurobiolaging.2019.07.010

Tran, T., Gallagher, M., & Kirkwood, A. (2018). Enhanced postsynaptic inhibitory strength in hippocampal principal cells in high-performing aged rats. *Neurobiology of Aging*, *70*, 92–101. https://doi.org/10.1016/j.neurobiolaging.2018.06.008

Treves, A., & Rolls, E. T. (1994). Computational analysis of the role of the hippocampus in memory. *Hippocampus*, *4*(3), 374–391. https://doi.org/10.1002/hipo.450040319

Tulving, E. (2001). *EPISODIC MEMORY: From Mind to Brain*. www.annualreviews.org

Tulving, E., & Markowitsch, H. J. (1998). Episodic and declarative memory: Role of the hippocampus. In *Hippocampus* (Vol. 8, Issue 3, pp. 198–204). https://doi.org/10.1002/(SICI)1098-1063(1998)8:3<198::AID-HIPO2>3.0.CO;2-G

Turrigiano, G. G., & Nelson, S. B. (2004). Homeostatic plasticity in the developing nervous system. In *Nature Reviews Neuroscience* (Vol. 5, Issue 2, pp. 97–107). European Association for Cardio-Thoracic Surgery. https://doi.org/10.1038/nrn1327

Unal, G., Joshi, A., Viney, T. J., Kis, V., & Somogyi, P. (2015). Synaptic targets of medial septal projections in the hippocampus and extrahippocampal cortices of the mouse. *Journal of Neuroscience*, *35*(48), 15812–15826. https://doi.org/10.1523/JNEUROSCI.2639-15.2015

Vedder, L. C., Bredemann, T. M., & McMahon, L. L. (2014). Estradiol replacement extends the window of opportunity forhippocampal function. *Neurobiology of Aging*, *35*(10), 2183–2192. https://doi.org/10.1016/j.neurobiolaging.2014.04.004

Vela, J., Gutierrez, A., Vitorica, J., & Ruano, D. (2003). Rat hippocampal GABAergic molecular markers are differentially affected by ageing. *Journal of Neurochemistry*, *85*(2), 368–377. https://doi.org/10.1046/j.1471-4159.2003.01681.x

Velíšková, J., Iacobas, D., Iacobas, S., Sidyelyeva, G., Chachua, T., & Velíšek, L. (2015). Oestradiol Regulates Neuropeptide Y Release and Gene Coupling with the GABAergic and Glutamatergic Synapses in the Adult Female Rat Dentate Gyrus. *Journal of Neuroendocrinology*, *27*(12), 911–920. https://doi.org/10.1111/jne.12332

Velíšková, J., & Velíšek, L. (2007). β-estradiol increases dentate gyrus inhibition in female rats via augmentation of hilar neuropeptide Y. *Journal of Neuroscience*, *27*(22), 6054–6063. https://doi.org/10.1523/JNEUROSCI.0366-07.2007

Veng, L. M., Granholm, A. C., & Rose, G. M. (2003). Age-related sex differences in spatial learning and basal forebrain cholinergic neurons in F344 rats. *Physiology and Behavior*, *80*(1), 27–36. https://doi.org/10.1016/S0031-9384(03)00219-1

Vezzani, A., & Sperk, G. (2004). Overexpression of NPY and Y2 receptors in epileptic brain tissue: An endogenous neuroprotective mechanism in temporal lobe epilepsy? In *Neuropeptides* (Vol. 38, Issue 4, pp. 245–252). https://doi.org/10.1016/j.npep.2004.05.004

Vierk, R., Glassmeier, G., Zhou, L., Brandt, N., Fester, L., Dudzinski, D., Wilkars, W., Bender, R. A., Lewerenz, M., Gloger, S., Graser, L., Schwarz, J., & Rune, G. M. (2012). Aromatase inhibition abolishes LTP generation in female but not in male mice. *Journal of Neuroscience*, *32*(24), 8116–8126. https://doi.org/10.1523/JNEUROSCI.5319-11.2012

Wang, H., Ardiles, A. O., Yang, S., Tran, T., Posada-Duque, R., Valdivia, G., Baek, M., Chuang, Y. A., Palacios, A. G., Gallagher, M., Worley, P., & Kirkwood, A. (2016). Metabotropic glutamate receptors induce a form of LTP controlled by translation and arc signaling in the hippocampus. *Journal of Neuroscience*, *36*(5), 1723–1729. https://doi.org/10.1523/JNEUROSCI.0878-15.2016

Wang, T. J., Chen, J. R., Wang, W. J., Wang, Y. J., & Tseng, G. F. (2014). Genistein partly eases aging and estropause-induced primary cortical neuronal changes in rats. *PLoS ONE*, *9*(2). https://doi.org/10.1371/journal.pone.0089819

Wang, W., Le, A. A., Hou, B., Lauterborn, J. C., Cox, C. D., Levin, E. R., Lynch, G., & Gall, C. M. (2018). Memory-related synaptic plasticity is sexually dimorphic in rodent hippocampus. *Journal of Neuroscience*, *38*(37), 7935–7951. https://doi.org/10.1523/JNEUROSCI.0801-18.2018

Wang, X., Wang, Y., Zhu, Y., Yan, L., & Zhao, L. (2019). Neuroprotective effect of S-trans, transfarnesylthiosalicylic acid via inhibition of RAS/ERK pathway for the treatment of Alzheimer's disease. *Drug Design, Development and Therapy*, *13*, 4053–4063. https://doi.org/10.2147/DDDT.S233283

Warren, S. G., Humphreys, A. G., Juraska, J. M., & Greenough, W. T. (1995). *LTP varies across the estrous cycle: enhanced synaptic plasticity in proestrus rats*.

Waters, E. M., Mazid, S., Dodos, M., Puri, R., Janssen, W. G., Morrison, J. H., McEwen, B. S., & Milner, T. A. (2019). Effects of estrogen and aging on synaptic morphology and distribution of phosphorylated Tyr1472 NR2B in the female rat hippocampus. *Neurobiology of Aging*, *73*, 200–210. https://doi.org/10.1016/j.neurobiolaging.2018.09.025

Wigström, H., & Gustafsson, B. (1983). Large long-lasting potentiation in the dentate gyrus in vitro during blockade of inhibition. *Brain Research*, *275*(1), 153–158. https://doi.org/10.1016/0006-8993(83)90428-6

Willner, P. (1966). VALIDATION CRITERIA FOR ANIMAL MODELS OF HUMAN MENTAL DISORDERS: LEARNED HELPLESSNESS AS A PARADIGM CASE. In *Neuro-Psychophormacol. b Biol. Psychiat* (Vol. 10).

Winder, D. G., Martin, K. C., Muzzio, I. A., Rohrer, D., Chruscinski, A., Kobilka, B., Kandel, E. R., & Hughes, H. (1999). ERK Plays a Regulatory Role in Induction of LTP by Theta Frequency Stimulation and Its Modulation by-Adrenergic Receptors dependent form of long-term potentiation (LTP). Inhibi-tors of ERK signaling reduce LTP evoked by

repeated high-frequency tetani (English and Sweatt In addition to the roles of ERK in persistent cellular. In *Neuron* (Vol. 24).

Witter, M. (2012). Hippocampus. In *The Mouse Nervous System*. Elsevier Inc. https://doi.org/10.1016/B978-0-12-369497-3.10005-6

Wu, Z., Asokan, A., & Samulski, R. J. (2006). Adeno-associated Virus Serotypes: Vector Toolkit for Human Gene Therapy. In *Molecular Therapy* (Vol. 14, Issue 3, pp. 316–327). https://doi.org/10.1016/j.ymthe.2006.05.009

Wu, Z., Guo, Z., Gearing, M., & Chen, G. (2014). Tonic inhibition in dentate gyrus impairs long-term potentiation and memory in an Alzhiemer' s disease model. *Nature Communications*, *5*. https://doi.org/10.1038/ncomms5159

Yagi, S., & Galea, L. A. M. (2019). Sex differences in hippocampal cognition and neurogenesis. *Neuropsychopharmacology*, *44*(1), 200–213. https://doi.org/10.1038/s41386-018-0208-4

Yamada, J., Hatabe, J., Tankyo, K., & Jinno, S. (2016). Cell type- and region-specific enhancement of adult hippocampal neurogenesis by daidzein in middle-aged female mice. *Neuropharmacology*, *111*, 92–106. https://doi.org/10.1016/j.neuropharm.2016.08.036

Yang, D. W., Pan, B., Han, T. Z., & Xie, W. (2004). Sexual dimorphism in the induction of LTP: Critical role of tetanizing stimulation. *Life Sciences*, *75*(1), 119–127. https://doi.org/10.1016/j.lfs.2003.12.004

Yiannopoulou, K. G., & Papageorgiou, S. G. (2020). Current and Future Treatments in Alzheimer Disease: An Update. *Journal of Central Nervous System Disease*, *12*, 117957352090739. https://doi.org/10.1177/1179573520907397

Ying, S.-W., Futter, M., Rosenblum, K., Webber, M. J., Hunt, S. P., Bliss, T. V. P., & Bramham, C. R. (2002). *Brain-Derived Neurotrophic Factor Induces Long-Term Potentiation in Intact Adult Hippocampus: Requirement for ERK Activation Coupled to CREB and Upregulation of Arc Synthesis*.

Ypsilanti, A. R., Girão da Cruz, M. T., Burgess, A., & Aubert, I. (2008). The length of hippocampal cholinergic fibers is reduced in the aging brain. *Neurobiology of Aging*, *29*(11), 1666–1679. https://doi.org/10.1016/j.neurobiolaging.2007.04.001

Yuan, M., Meyer, T., Benkowitz, C., Savanthrapadian, S., Ansel-Bollepalli, L., Foggetti, A., Wulff, P., Alcami, P., Elgueta, C., & Bartos, M. (2017). Somatostatin-positive interneurons in the dentate gyrus of mice provide local-and long-range septal synaptic inhibition. *ELife*, *6*. https://doi.org/10.7554/eLife.21105.001

Yuan, R., Peters, L. L., & Paigen, B. (2011). *Mice as a Mammalian Model for Research on the Genetics of Aging*. www.nia.nih.gov/researchinformation/scientificresources/interventionstestingprogram.htm

Yun, S. H., & Trommer, B. L. (2011). Fragile X mice: Reduced long-term potentiation and N-Methyl-D-Aspartate receptor-mediated neurotransmission in dentate gyrus. *Journal of Neuroscience Research*, *89*(2), 176–182. https://doi.org/10.1002/jnr.22546

Zaborszky, L., van den Pol, A. N., & Gyengesi, E. (2012). The Basal Forebrain Cholinergic Projection System in Mice. In *The Mouse Nervous System* (pp. 684–718). Elsevier Inc. https://doi.org/10.1016/B978-0-12-369497-3.10028-7

Zhang, L., Fang, Y., Xu, Y., Lian, Y., Xie, N., Wu, T., Zhang, H., Sun, L., Zhang, R., & Wang, Z. (2015). Curcumin improves amyloid β-peptide (1-42) induced spatial memory deficits through BDNF-ERK signaling pathway. *PLoS ONE*, *10*(6). https://doi.org/10.1371/journal.pone.0131525

Zhang, M., Weiland, H., Schöfbänker, M., & Zhang, W. (2021). Estrogen receptors alpha and beta mediate synaptic transmission in the pfc and hippocampus of mice. *International Journal of Molecular Sciences*, *22*(3), 1–15. https://doi.org/10.3390/ijms22031485

Zhang, W., Tan, Y. F., Atwood, H. L., & Martin Wojtowicz, J. (2010). Biphasic effects of the cholinergic agonist carbachol on long-term potentiation in the dentate gyrus of the mammalian hippocampus. *Neuroscience Letters*, *479*(2), 157–160. https://doi.org/10.1016/j.neulet.2010.05.056

Zhou, S., & Yu, Y. (2018). Synaptic E-I balance underlies efficient neural coding. In *Frontiers in Neuroscience* (Vol. 12, Issue FEB). Frontiers Media S.A. https://doi.org/10.3389/fnins.2018.00046

Zhu, H., Xu, G., Fu, L., Li, Y., Fu, R., Zhao, D., & Ding, C. (2020). The effects of repetitive transcranial magnetic stimulation on the cognition and neuronal excitability of mice. *Electromagnetic Biology and Medicine*, *39*(1), 9–19. https://doi.org/10.1080/15368378.2019.1696358

Zlotnik, G., & Vansintjan, A. (2019). Memory: An Extended Definition. *Frontiers in Psychology*, *10*. https://doi.org/10.3389/fpsyg.2019.02523

Zola-Morgan, S. (1996). Human amnesia and the medial temporal region: enduring memory impairment following a bilateral lesion limited to field CA1 of the hippocampus. *Neurocase*, *2*(4), 259aw–25298. https://doi.org/10.1093/neucas/2.4.259-aw

Zucker, R. S., & Regehr, W. G. (2002). Short-term synaptic plasticity. In *Annual Review of Physiology* (Vol. 64, pp. 355–405). https://doi.org/10.1146/annurev.physiol.64.092501.114547

Webpages

https://www.who.int/news-room/fact-sheets/detail/ageing-and-health

www.jax.org

https://www.nia.nih.gov/health/how-alzheimers-disease-treated

8.3. List of abbreviations

AC	=	adenylyl cyclase
ACh	=	acetylcholine
ANOVA	=	analysis of variance
aCSF	=	artificial cerebrospinal fluid
AD	=	Alzheimer's disease
AMPA-R	=	α-amino-3-hydroxy-5-methyl-4-isoxazole propionic acid receptor
BDNF	=	brain-derived neurotrophic factor
BM	=	Barnes Maze
bp	=	base pairs
CA	=	cornu ammonis
CaMKII	=	Ca2+/calmodulin-dependent protein kinase-II
cAMP	=	3',5'-cyclic adenosine monophosphate
CCK	=	cholecystokinin
CNS	=	central nervous system
CREB	=	cAMP response element-binding protein
DG	=	dentate gyrus
dDG	=	dorsal dentate gyrus
dH	=	dorsal hippocampus
DMSO	=	Dimethylsulfoxide
EC	=	entorhinal cortex
EEG	=	electroencepahlogram
E-I	=	excitation-inhibition
ELISA	=	Enzyme-linked Immunosorbent Assay
e-LTP	=	early long-term potentiation
EPSP	=	excitatory post-synaptic potential
ER	=	estrogen receptor
ERK	=	extracellular-signal regulated kinase
ERP	=	event-related brain potential
fEPSP	=	field excitatory post-synaptic potential
GABA	=	gamma-amino-butyric-acid
$GABA_A$-R	=	gamma-amino-butric-acid A receptor

GAD	=	glutamate decarboxylase
GC	=	granule cell
GIRK	=	G-protein-coupled, inwardly rectifying potassium currents
GL	=	granule layer
GluA1	=	c
GPCR	=	G-protein-coupled- receptors
GPR30	=	G-protein coupled receptor for estrogen
HFS	=	high-frequency stimulation
HICAP	=	hilar commissural associational path interneurons
HIL	=	hilus-associated interneurons
HIPP	=	hilar-perforant-path-associated interneurons
hSyn	=	human synapsin 1
I-O	=	Input-output curve
LPP	=	lateral perforant path
LSD	=	least significant difference
LTD	=	long-term depression
LTP	=	long-term potentiation
MAPK	=	mitogen-activated protein kinase
MCI	=	mild cognitive impairment
MF	=	mossy fiber
ML	=	molecular layer
MPP	=	medial perforant path
mRNA	=	messenger ribonucleic acid
M1-R	=	muscarinic receptor type 1
M2-R	=	muscarinic receptor type 2
M4-R	=	muscarinic receptor type 4
MS	=	medial septum
MWM	=	Morris Water Maze
ND	=	numerical density
NIH	=	national institutes of health
NMDA	=	N-methyl-D-aspartate
NMDA-R	=	N-methyl-D-aspartate receptor
NOS	=	nitric oxide synthase
NPY	=	Neuropeptide Y

NR2B	=	D-aspartate receptor subtype 2B
OVX	=	ovariectomy
PC	=	pyramidal cell
PHY	=	physostigmine
phyto-free food	=	phytoestrogen-free food
PI_3K	=	phosphoinositide 3-kinase
PKA	=	protein kinase A
PLC	=	phospholipase C
PP	=	perforant path
PV	=	parvalbumin
SC	=	Schaffer collaterals
SL	=	stratum lucidum
SST	=	somatostatin
STDP	=	spike-time dependent plasticity
TBS	=	theta-burst stimulation
VDCC	=	voltage-gated calcium channels
WHO	=	World Health Organization
WB	=	Western Blot
Y1-R	=	Neuropeptide Y receptor type 1
Y2-R	=	Neuropeptide Y receptor type 2
Y5-R	=	Neuropeptide Y receptor type 5
zif268	=	Egr1 (Early Growth Response Protein 1)

8.4. Table of Figures

8.5. Table of Tables

8.6. Chemicals

Acrylamide 30%, A124.1	Carl Roth, Karlsruhe, Germany
β-estradiol	Santa Cruz Biotechnology/CehmCruz Inc., Heidelberg, Germany
BIBP 3226	Tocris, Ellisville, Missouri, USA
CaCl	Carl Roth, Karlsruhe, Germany
Dimethylsulfoxid (DMSO)	Carl Roth, Karlsruhe, Germany
Ethidium bromid	Carl Roth, Karlsruhe, Germany
Glucose	Carl Roth, Karlsruhe, Germany
KCL	Carl Roth, Karlsruhe, Germany
Ketamin/Xylacine	Sigma-Aldrich, Seelze, Germany
(Leu_{31}, Pro_{34})_Neuropeptide Y (human, rat)	Tocris, Ellisville, Missouri, USA
Methylbutane	Carl Roth, Karlsruhe, Germany
Methylenblue	Sigma-Aldrich, Seelze, Germany
$MgSO_4$ x H_2O	Carl Roth, Karlsruhe, Germany
NaCl	Carl Roth, Karlsruhe, Germany
NaH_2PO_4	Carl Roth, Karlsruhe, Germany
NaH_2PO_4 x H_2O	Carl Roth, Karlsruhe, Germany
Na_3VO_4	Carl Roth, Karlsruhe, Germany
Neuropeptide Y	Cayman chemical company, Ann Arbor, Michigan, USA
Paraformaldehyde	Carl Roth, Karlsruhe, Germany
Physostigmine hemisfulfate	Santa Cruz Biotechnology/CehmCruz Inc., Heidelberg
Poly-L-Lysine 1%	Sigma-Aldrich, Seelze, Germany
Protease & phosphatase inhibitor 13393126	Thermo Scientific, St. Leon-Rot, Germany
Protein Assay 5000001	BIO-RAD Labortaories Inc., Kalifornien, USA
PVDF membranes IPFL000010	Thermo Scientific, St. Leon-Rot, Germany
Sucrose	Carl Roth, Karlsruhe, Germany
0.3% Triton-X, X100	Sigma-Aldrich, Seelze, Germany

Tween 20, 9127.1	Carl Roth, Karlsruhe, Germany

Solutions and buffers

aCSF (10x Stock 1)	129 mM NaCL
	1.25 mM NaH_2PO_4 x H_2O
	10 mM Glucose
	1.8 mM $MgSO_4$
	1.6 mM CaCl
	3 mM KCl
aCSF (10x Stock 2)	21 mM $NaHCO_3$
aCSF for 1L	100 ml Stock 1
	add a bit of Aqua dest.
	100 ml Stock 2
	Fill up with Aqua dest. Until 1 L
DNA loading buffer	0.25 % bromophenol blue
	0.25 % xylene cyanol FF
	15 % Ficoll in H_2O
Intercept blocking buffer	Li-Cor, 927-700001

1x Running buffer	25mM Tris 25 M glycine 1% SDS
10x Phosphatebuffered saline (PBS)	solve 11.5 g $Na_2HPO \times H_2O$ 2.0 g KH_2PO_4 80.0 g NaCl 2.0 g KCl in ca. 900 ml double-destilled water adjust pH to 7.4
4 % Paraformaldehyde	solve 40 g PFA in ca. 700 ml double-destilled water, stir on a heating plate at 70 °C until solution is clear add 500 µl NaOH (5 M) for better solving let cool down on ice (ca. 1 h) filtrate cooled PFA add 100 ml 10x PBS adjust pH to 7.4 fill up volume to 1 l with double-destilled water

LM Buffer	1% Laurymaltoside
	1% NP-40
	1 mM Na_3VO_4
	2 mM EDTA
	50 mM Tris-HCl pH 8.0
	150 mM NaCl
	0.5% DOC
	1 mM AEBSF
	1 µM Pepstatin A
	1 mM NaF
	1 Tablet of Pierce protease inhibitor
30 % Sucrose	solve 30 g sucrose in in 100ml 1xPBS
50x TAEBuffer	242 g Tris base
	57.1 ml acetic acid
	100 ml 0.5 M EDTA pH 8
1x TEBuffer	1 mM EDTA pH 8
	10 mM Tris/HCl pH 7.4

Transfern buffer	25 mM Tris
	0.192 M glycine
	20% methanol
	10% SDS

DNA length standard

GeneRulerTM 1kb DNA ladder	Thermo Scientific, St. Leon-Rot, Germany
GeneRulerTM 100bp DNA ladder	Thermo Scientific, St. Leon-Rot, Germany

ELISA Kit

ELISA kit NPY (PCEA879Hu; UOM: 96T)	Cloude-Clone Corp., Texas, USA

Instruments and consumables

Generally used instruments and consumables

animal care

Macrolon standard cages	Ebeco, Castrop-Rauxel, Germany
Ssniff R/M-H V-1534	Ssniff Spezialdiäten, Soest, Germany
ssniff R/M-H-V1554	Ssniff Spezialdiäten, Soest, Germany
Lignocel BK 8/15	J. Rettenmaier & Söhne, Rosenberg, Germany

Plastic ware

Safe lock tubes (1.5 ml)	Eppendorf, Hamburg, Germany
Falcon tube 50 ml	Greiner Bio-one, Frickenhausen, Germany

Glassware

glass bottles	Carl Roth, Karlsruhe, Germany
Erlenmeyer flasks	Carl Roth, Karlsruhe, Germany
Beaker	Carl Roth, Karlsruhe, Germany
graduated cylinders	Carl Roth, Karlsruhe, Germany

Pipettes

Pipettes	Brand, Wertheim, Germany
Pipette tipps	Brand, Wertheim, Germany
Pipette tips with filter	Brand, Wertheim, Germany

Freezers & Fridges

Liebherr KU 2407	Liebherr Hausgeräte, Ochsenhausen, Germany
Liebherr GU 4506	Liebherr Hausgeräte, Ochsenhausen, Germany

Sanyo Ultra Low	Ewald Innovationstechnik, Bad Nenndorf, Germany

Scales

Sartorius TE 1535	Sartorius AG, Göttingen, Germany
Sartorius TE 212	Sartorius AG, Göttingen, Germany
Sartorius TE 2101	Sartorius AG, Göttingen, Germany

Centrifuges

Centrifuge 5424	Eppendorf, Hamburg, Germany
Centrifuge 5430	Eppendorf, Hamburg, Germany
VWR Galaxy Mini	VWR International, Darmstadt, Germany

pH meter

inoLab pH720	WTW, Weilheim, Germany

Magnetic Stirrer

IKA RET basic	IKA-Werke, Staufen, Germany
magnetic stir bar	Brand, Wertheim, Germany

Rockers & vortexer

ProBlot 25 Economy Rocker	Labnet, Woodbridge, NJ, USA
IKA HS 260 basic	KA-Werke, Staufen, Germany
VWR Lab dancer S40	VWR International, Darmstadt, Germany

Rotor incubator

Hybrid 2000	H. Saur Laborbedarf, Reutlingen, Germany

Pumps

REGLO peristaltic pump	ISMATEC, Wertheim-Mondfeld, Germany

Autoclave

Systec DB-23	Systec Labortechnik, Wettenberg, Germany

Oven

Binder FP53	Binder, Tuttlingen, Germany

Others

Lab clock	Carl Roth, Karlsruhe, Germany
Aluminum foil	Carl Roth, Karlsruhe, Germany
Dewar transport flask Typ B	KGW Isotherm, Karlsruhe, Germany

Plastic ware

MicroAmp Fast Reaction Tubes	Applied Biosystems, Darmstadt, Germany
MicroAmp 8-cap strip	Applied Biosystems, Darmstadt, Germany
MicroAmp Fast Optical 96-Well plate	Applied Biosystems, Darmstadt, Germany
MicroAmp Optical Adhesive Film	Applied Biosystems, Darmstadt, Germany

Thermocycler

Veriti Thermal Cycler	Applied Biosystems, Darmstadt, Germany

Microwave

Clatronic MWG 746 H	Clatronic International, Kempen, Germany

Gel electrophoresis system

AGT3 & Maxi-VG	VWR International, Darmstadt, Germany

Gel documentation system

InGenius LHR	Syngene, Cambridge, UK

ELISA

Tecan Infinit M200 Pro	Tecan Group, Männedorf, Schweiz

Glassware

Slice holder	
Menzel Gläser Superfrost	Gerhard Menzel GmbH, Braunschweig, Germany

Microscopes

Lieca DMi8	Leica Microsystems, Wetzlar, Germany
Nicon Eclipse E200	Nicon Instruments Europe, Amsterdam, Netherlands
Zoom-Stereomicroscope SMZ168	MoticEurope, S.L.U., Barcelona, Spain
Stereomicroscope Stemi2000	Zeiss, Oberkochen, Germany

Material for electrophysiology

Amplifier EXT-20F npi	npi electronic GmbH, Tamm, Germany
Blades 752/1/SS	Campden Instruments Ltd, Loughborough, UK
Glass pipettesGB150F-8P	Science Products, Hofheim am Taunus, Germany
Glass pipettes puller P-87	Sutter instruments, California, USA
Interface chamber	built by the workshop
Stimulator	Digitimer Ltd., Welweyn Garden City, UK

Surgical instruments	VWR, Darmstadt, Germany
Tungston stimulation electrode	World precision instruments, Berlin, Germany
Vibratom Campden HA752-201	Campden Instruments Ltd, Loughborough, UK
Waterbath	VWR, Darmstadt, Germany
Stimulation electrode Tungsten Stereotrods WE3ST30.1B3	WPI, Florida, USA
Vibration table 9211-02-12	Kinetic Systems, California, USA
Lens cleaning paper	Tiffen, New York, USA
CED 1401	Cambridge Electronic Design, Cambridge, UK
Light source KL1500LCD	Schott, Mainz, Germany
Micromanipulators 00-42-101-0000	Märzhäuser Wetzlar GmbH, Wetzlar, Germany
Power supply BT-305	BASETech, Gleichen, Germany

Software

Microsoft Office Excel	Microsoft, Washington, USA
GraphPad prism	Dotmatics, Bishops Stortford, UK
Matlab	MathWorks, Inc., Massachusetts, USA
Mendeley Ltd.	Elsevier, Amsterdam, Netherlands
CED Spike2	Cambridge Electronic Design Limited, Cambridge, UK

Original provider of mouse lines used

Mouse line	**Strain name**	**Provider**
C57BL/6	C57BL/6BomTac	M&B Taconic, Berlin, Germany
C57BL/6	C57BL/6JRj	Janvier Labs, Le Genest-Saint-Isle, France
C57BL/6	C57BL/6J	Charles River, Wilmington, Massachusetts, USA

Declaration of Honour

“I hereby declare that I prepared this thesis without the impermissible help of third parties and that none other than the aids indicated have been used; all sources of information are clearly marked, including my own publications.

In particular I have not consciously:

- fabricated data or rejected undesirable results,
- misused statistical methods with the aim of drawing other conclusions than those warranted by the available data,
- plagiarized external data or publications,
- presented the results of other researchers in a distorted way.

I am aware that violations of copyright may lead to injunction and damage claims by the author and also to prosecution by the law enforcement authorities. I hereby agree that the thesis may be electronically reviewed with the aim of identifying plagiarism.

This work has not yet been submitted as a doctoral thesis in the same or a similar form in Germany, nor in any other country. It has not yet been published as a whole.”

Magdeburg, den 18-01-2023

(Katharina Klinger)